RESONANCES*)

Donald H. Miller

Department of Physics and Lawrence Radiation Laboratory,
University of California, Berkeley

Since the extensive subject of meson and baryon resonances is to be covered in three lectures, it will clearly not be possible to explore in detail the variety of techniques used in discovering and analysing these systems. We shall limit the content of the lectures to recent advances, stressing those areas where our knowledge is limited and further experimental and theoretical analysis is necessary.

1. THE BARYON RESONANCES

During the past few years remarkable progress has occurred in the clarification of the properties of the S = 0 (non-strange) and S = -1 baryon systems. Precision measurements of total cross-sections in the $\pi^- p$, $\pi^+ p$, $K^- p$, and $K^- d$ systems have suggested a large number of centre-of-mass (c.m.) energies at which resonances most likely occur. In the analysis it is usually assumed that the total cross-section consists of a smooth background with Breit-Wigner resonances superimposed. It is apparent that these observations only initiate the experimental programme. Angular distributions and polarizations in elastic channels must be measured, and then fitted in detailed phase-shift analyses to fix the parameters of the resonance; in many cases the analysis is complicated by the (accidental?) superposition of two or more resonances; at higher energies branching ratios must be determined through study of inelastic channels. As seen from the Lawrence Radiation Laboratory this work has recently been carefully and extensively summarized by Dr. Barbaro-Galtieri[1]; there is little point in reproducing the identical material in these brief notes. However, it is useful to devote a few paragraphs to putting the baryon resonances into some perspective. Let us start with an interesting recent development.

Not long ago Heinz and Ross[2] suggested that backward $\pi^+ p$ scattering would provide a useful region in which to determine the positions and spin-parity (J^P) assignments of the $I = 3/2$ resonances. They argued that since the non-resonant backward-scattering amplitudes tend to be small at higher energies, the presence of a resonance may result in a readily observable interference pattern. Since the background amplitude varies slowly with energy, a resonance with a particular parity will produce either a constructive or destructive interference; a comparison of patterns for known and unknown states should permit unique parity assignments. For explicit calculation of expected patterns they assumed that the background amplitude was dominated by nucleon-exchange.

Kormanyos et al.[3] have studied the structure in backwards $\pi^- p$ scattering with the dramatic result shown in Fig. 1. Nucleon-exchange does not contribute to $\pi^- p$ backward scattering; to fit the data Barger and Cline[4] have used a simple Regge-pole model as an alternative. They observe that with few exceptions the known S = 0 baryon resonances can be interpreted as recurrences of the three Regge trajectories.

---

*) Revised notes received for publication 6 June 1967.

I	P	Signature	Lowest state	Symbol
3/2	+1	-1	$N^*(1238)$ $J^P = 3/2^+$	Δ_δ
1/2	+1	+1	$N(938)$ $J^P = 1/2^+$	N_α
1/2	-1	-1	$N^*(1512)$ $J^P = 3/2^-$	N_γ

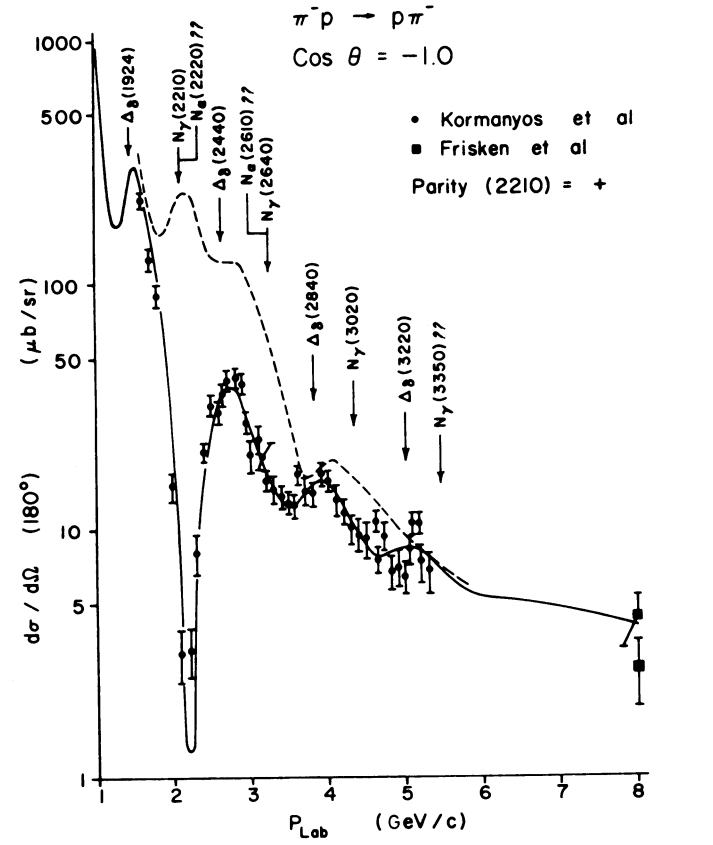

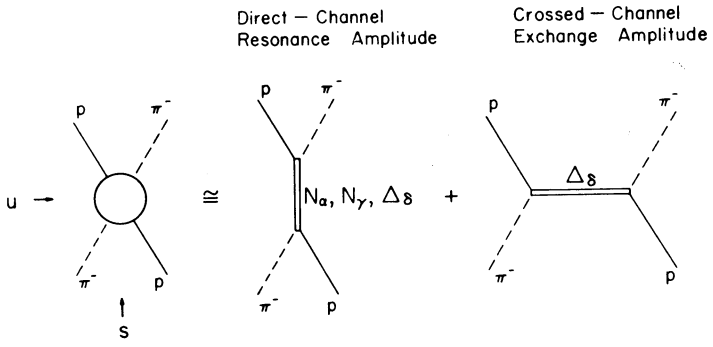

Figure 1 - Data of Kormanyos et al. [Ref. 3)] for backwards π^-p scattering. Solid curve is fit by Barger and Cline [Ref. 4)] using direct-channel resonance amplitude with Reggeized cross-channel exchange amplitude. Dashed curve shows effect of reversing the parity assignment for N(2190).

TABLE 1

The Regge-exchange model of Barger and Cline[4] was calculated using the values which are not underlined (where more than one value is given, the parenthetical value was used). The pure resonance fit by Dickmen[5] was calculated with the same parameters except that underlined values were used where indicated.

Resonance (mass in MeV)	Spin-parity (J^P)	Width (GeV)		(X_I)	
$\Delta_\delta(1236)$	$3/2^+$	0.12		1.0	1.0
$\Delta_\delta(1929)$	$7/2^+$	0.17		0.35 - 0.50(0.46)	0.46
$\Delta_\delta(2452)$ 2410	$11/2^+$	0.28	0.35	0.12	0.163
$\Delta_\delta(2840)$	$15/2^+$	0.40		0.05	0.061
$\Delta_\delta(3220)$	$19/2^+$	0.44		0.01 - 0.02(0.017)	0.025
$N_\gamma(1512)$	$3/2^-$	0.12		0.60	0.60
$N_\gamma(2190)$	$7/2^-$	0.24		0.20	0.20
$N_\gamma(2640)$	$11/2^-$	0.42	0.35	0.05	0.040
$N_\gamma(3020)$	$15/2^-$	0.40		0.015	0.002
$N_\gamma(3350)$	$19/2^-$	0.10		0.003-0.01(0.003)	0.003
$N_\alpha(938)$	$1/2^+$	...		...	
$N_\alpha(1688)$	$5/2^+$	0.10		0.60	0.60
$N_\alpha(2200)$	$9/2^+$	0.24		0.07	0.083
$N_\alpha(2610)$	$13/2^+$	0.42	0.32	0.02	0.035
$N_\alpha(2970)$	$17/2^+$	...		...	...

The known resonances are classified in Table 1; the recurrences are shown schematically in Fig. 2. Barger and Cline then assume that the backward-scattering amplitude can be approximated by the sum of the amplitudes for Regge recurrences in the direct s-channel ($\pi^- p \to \pi^- p$) and the exchange of the $I = 3/2$ Regge trajectory in the crossed u-channel ($\pi^+ p \to \pi^+ p$). The solid curve in Fig. 1 illustrates their fit to the data. Several highly inelastic resonances have not been included in the calculation; since these occur in regions dominated by stronger elastic resonances it is likely that the excellent fit achieved will not be seriously modified when they are included.

Barger and Cline point out that if the classification scheme is valid, the higher mass $I = 1/2$ resonances occur approximately as parity doublets. This is apparent in Fig. 2 where states with $E_r \gtrsim 2200$ MeV occur in pairs separated by one unit in J. The experimental determination of the spins and parities for these states will be particularly difficult.

Although Barger and Cline have shown that the backward-scattering data are consistent with the Regge-pole model, Dickmen[5] has emphasized the limitations of the model. In particular, available data on angular distributions slightly away from $\cos\vartheta = -1$ are in

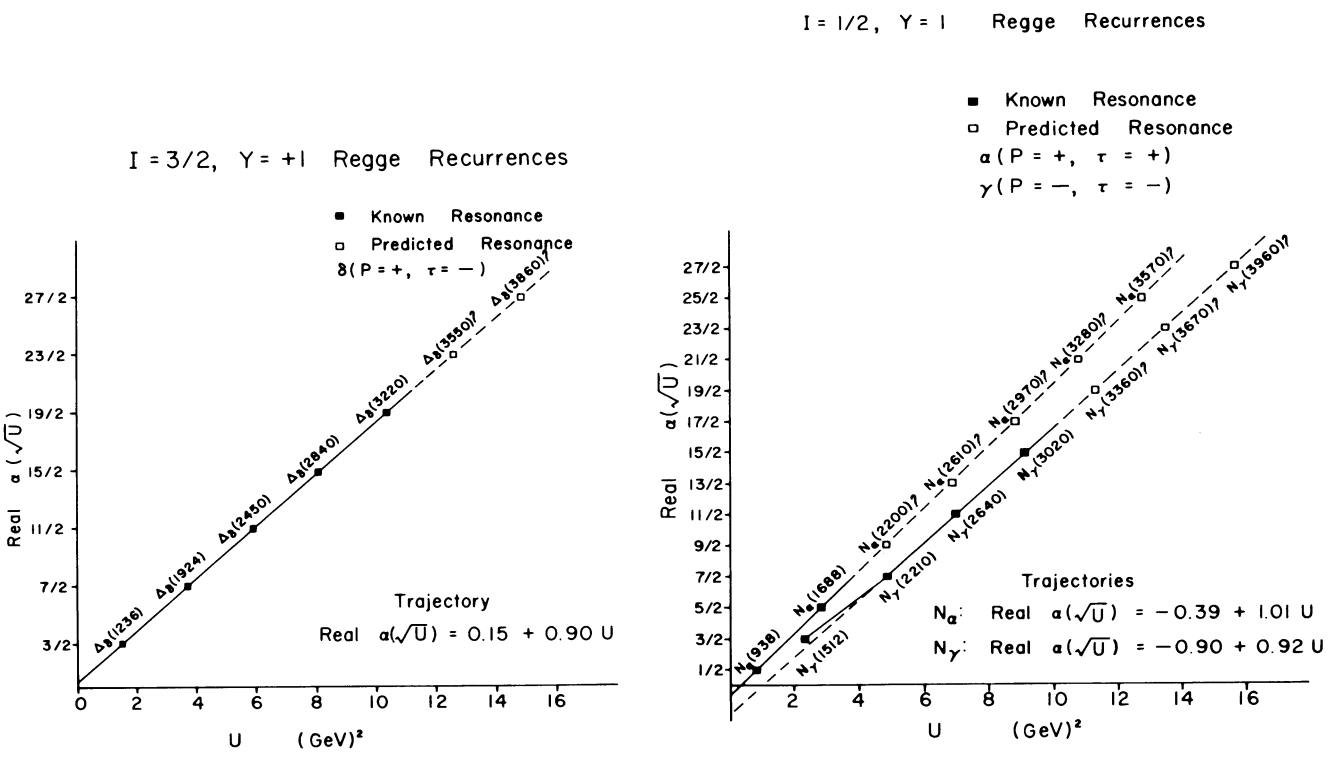

Figure 2 - Nucleon Regge trajectory assignments proposed by Barger and Cline [Ref. 5)] and used in their fit to the data of Kormanyos et al. The dashed portions of the curves correspond to predicted resonances.

poor agreement with the model; if the parameters are modified to give a reasonable fit at a single energy, the fit is poor at other energies. To illustrate the arbitrariness of the model, Dickmen attempted to fit the backward-scattering data with no exchange amplitude whatsoever. When the elasticities of the higher resonances are slightly increased an excellent fit is obtained. With this result Dickmen concludes that neither the parameters of the Regge-exchange amplitude nor its existence as distinct from the direct channel resonance amplitude can be considered established at present. It is apparent that we shall see a great increase in measurement and analysis of backward-scattering cross-sections in the near future!

There are several items which illustrate recent progress in understanding the S = -1 baryon systems. The remarkably accurate and detailed measurements by Cool et al.[6] of K^-p and K^-d total cross-sections have yielded precise I = 0 and I = 1 cross-sections to 3.4 GeV/c using

$$\sigma_p = (1/2)(\sigma_0 + \sigma_1) \tag{1}$$

and

$$\sigma_d = (1/2)(\sigma_0 + 3\sigma_1) - \sigma_g \tag{2}$$

where

$$\sigma_g = (1/4\pi) < r^{-2} > \sigma_p \sigma_n \tag{3}$$

is the Glauber correction for the screening of one nucleon by another in the deuteron; $< r^{-2} >$ is the average inverse-square separation of the nucleons. To use Eqs. (1) and (2) it is necessary that σ_p first be averaged over the Fermi momentum distribution of the deuteron; after the appropriate subtractions the Fermi momentum distribution must be unfolded.

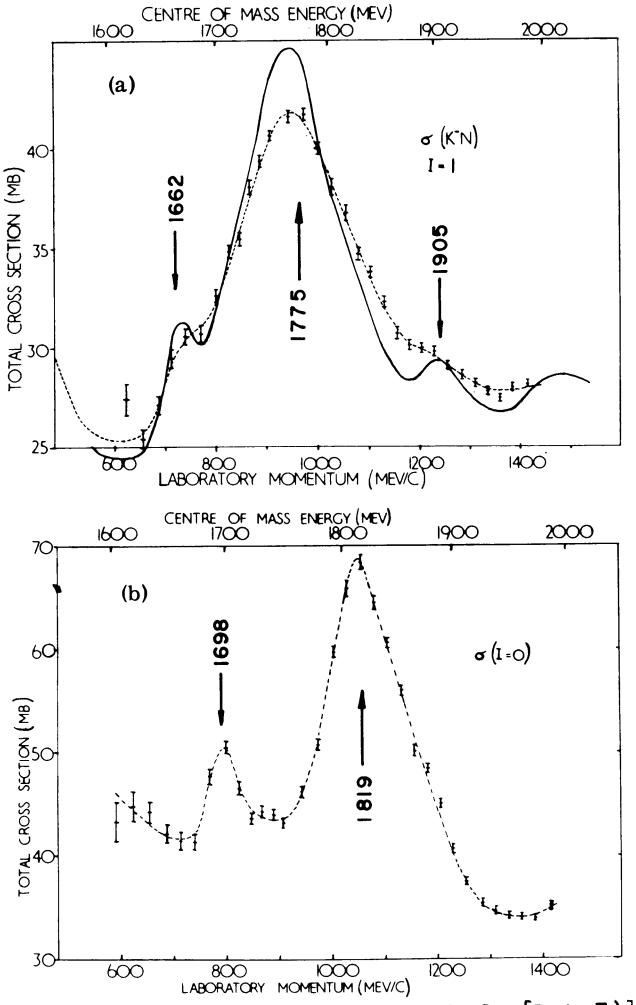

Figure 3 - $\bar{K}N$ total cross-section measurements of Davies et al. [Ref. 7)]. (a) experimental points represent K^-n cross-section before unfolding Fermi momentum. Solid curve is result of unfolding. (b) $\sigma(I = 0) = 2\sigma(K^-p) - \sigma(K^-n)$, where $\sigma(K^-n)$ is the unfolded cross-section. Errors are purely statistical.

The extension of detailed analyses of elastic and inelastic channels to well above 1.2 GeV/c during the past year has been particularly impressive. These analyses have been complicated by the presence of at least five distinct resonances in the interval P_K = 600 to 1400 MeV/c; they can be clearly seen in the recent data of Davies et al.[7] shown in Fig. 3. The separate I = 0 and I = 1 cross-sections were obtained from their K^-p and K^-d measurements using Eqs. (1) and (2). Despite the complexity of the partial-wave analyses through this region, convincing J^P assignments have been deduced for these resonances; details and references are given in the review by Dr. Barbaro-Galtieri[1].

The properties of the S = -2 Ξ^* systems remain obscure; despite their intrinsic interest there has been no report of progress in the past year. The Ω^- remains the only known S = -3 system.

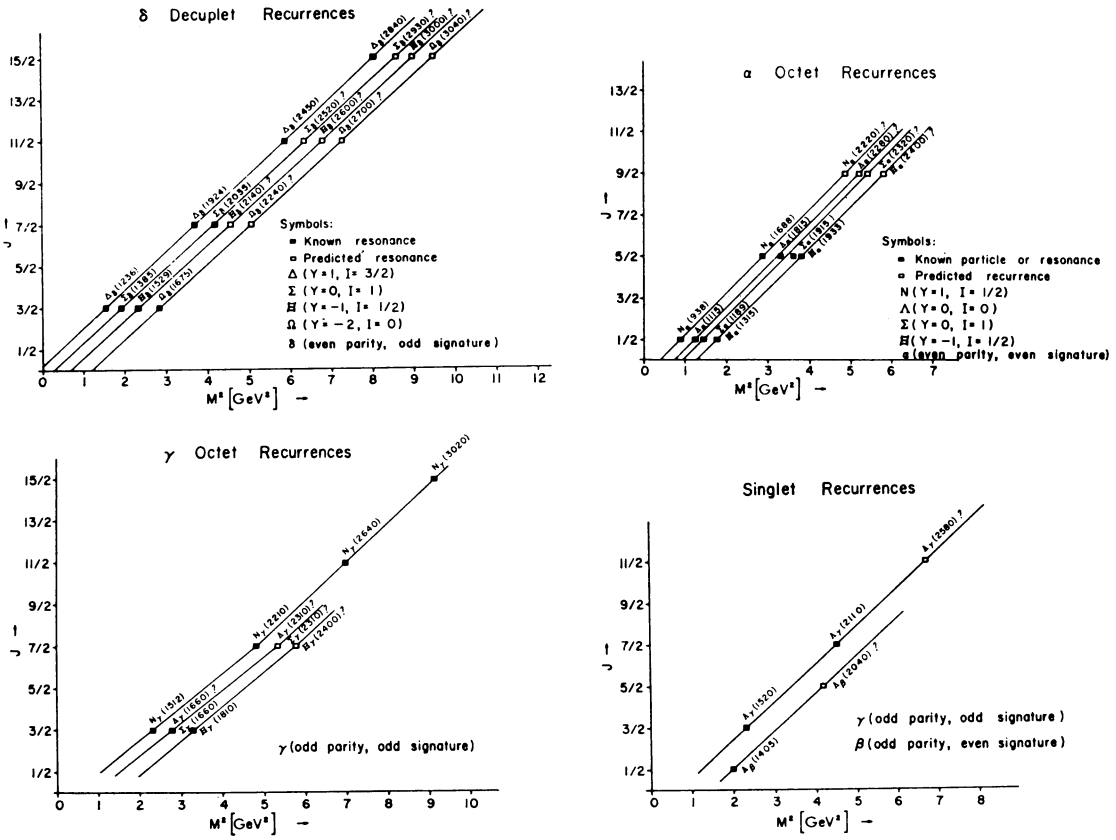

Figure 4 - Proposed classification of known baryon resonances within SU(3) and Regge models by Barger and Cline [Ref. 4)]

Barger and Cline[4] have proposed a classification of the known baryon states within the frameworks provided by SU(3) symmetry and the Regge-pole model. Although certainly subject to change with improved experimental data, their classification, shown in Fig. 4, provides a compact and plausible summary of our knowledge. In addition, the assumption of straight-line Regge trajectories through this mass region leads to predictions for c.m. energies and J^P assignments for new baryon resonances. We may hope that when the proper entries on this figure have been deduced from experiment the basic pattern of the baryon resonances will have been established.

2. OTHER BARYON RESONANCES ??

Thus far, our discussion has been limited to the baryon systems with S = 0, -1, -2, and -3 where our prejudices, based partly on the simplest representations of SU(3), have led us to anticipate resonances. However, let us look at the available S = +1 K^+p total cross-section data to 20 GeV shown in Fig. 5. The precision measurements by Cool et al.[8] demonstrate that near 1 GeV/c the cross-section in the K^+p system rises sharply from a plateau of 12 mb to a peak of almost 19 mb at 1.2 GeV/c; at higher momenta the cross-section drops to an apparently constant value of about 17.5 mb. Actually, the recent measurements of Abrams et al.[9], shown in Fig. 6, indicate that significant structure persists even above the large peak at 1.2 GeV/c. The K^+d measurements imply a very similar structure for the I = 0 KN system except that the low mass peak is larger and sharper. We shall consider only the region of the lowest mass peaks in the I = 0 and I = 1 systems, which, if interpreted as resonances, suggest the parameters

	E_r(MeV)	Γ(MeV)	P_K(GeV/c)	$(J_r + \frac{1}{2})x$
Z_o^* (I = 0)	1836	150	1.15	0.55
Z_1^* (I = 1)	1910	180	1.25	0.31

The Z_o^* would require the $\overline{10}$ representation of SU(3), while the Z_1^* would require the 27.

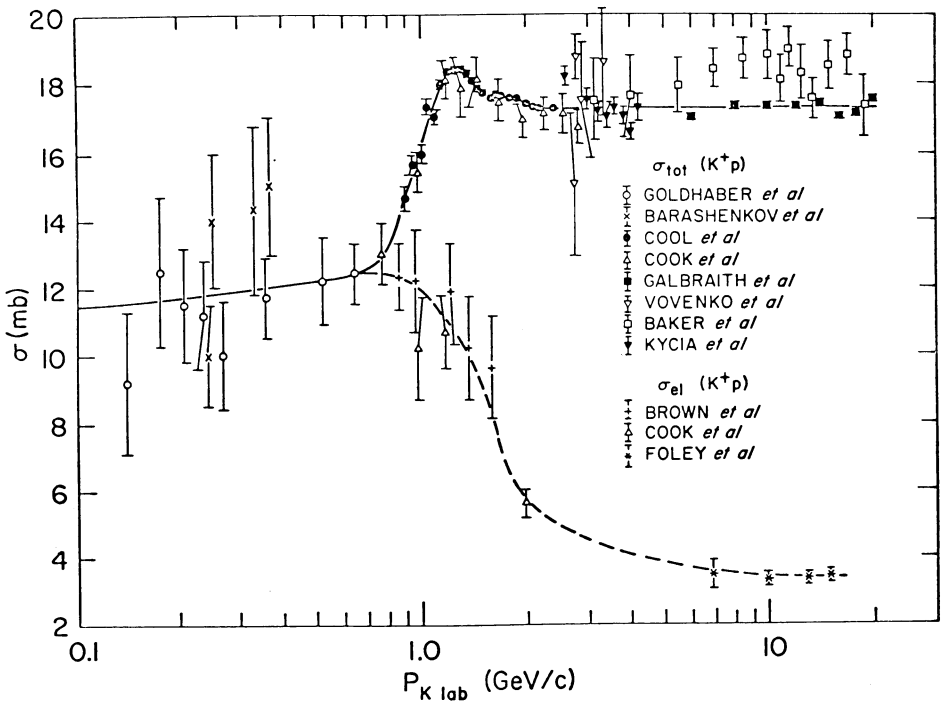

Figure 5 - Solid curve representstotal K^+p cross-sections from 0.1 to 20.0 GeV/c. The precision measurements of Cool et al. [Ref. 8)] indicate a peak at P_K = 1.25 GeV/c, possibly associated with an S = +1 baryon resonance (Z_1^*).

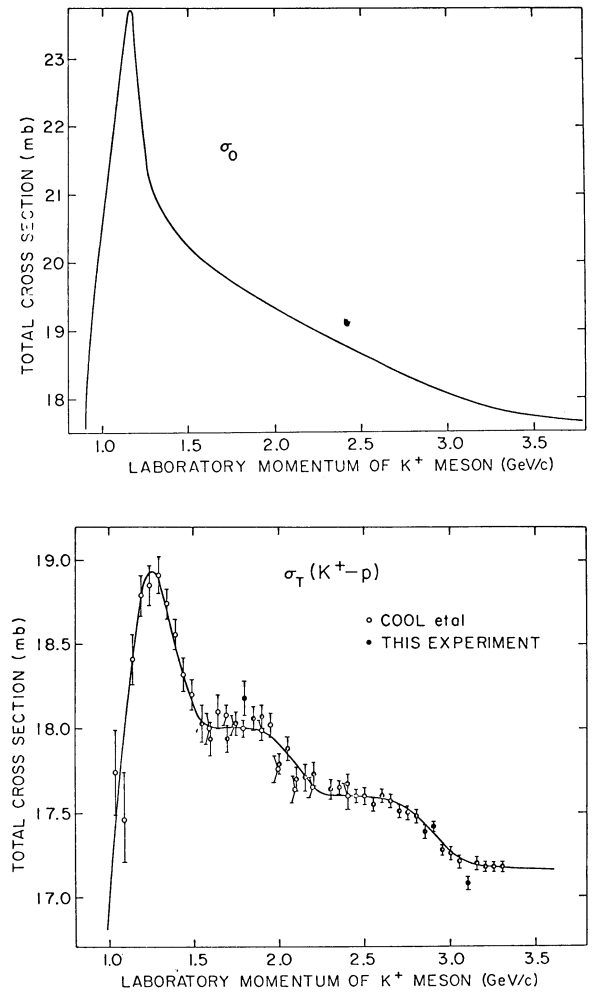

Figure 6 - Recent KN cross-section measurements by Abrams et al. [Ref. 9)] demonstrating additional structure in the S = +1, I = 1 baryon system. The upper curve represents the unfolded I = 0 total cross-section; no structure is apparent above Z_0^* at P_K = 1.15 GeV/c.

To clarify the structure near P_K = 1.2 GeV/c, Goldhaber et al.[10] have been systematically analysing both the elastic and inelastic final states. They find

a) The K^+p elastic cross-section[11] shows no peak near Z_1^*; the differential cross-section, which is essentially isotropic at low momenta, tends smoothly to a characteristic diffraction pattern at higher momenta.

b) The K-N^*(1238) final state, which dominates the inelastic channels[12], shows a peak near P_K = 1.2 GeV/c; however, the decay angular distributions are in reasonable agreement with the Stodolsky-Sakurai ρ-exchange model[13]. A partial-wave expansion in this channel indicates that <u>both</u> the $p_{1/2}$ and $p_{3/2}$ waves dominate through this region; within statistics, there is no drastic change as the Z_1^* enhancement is traversed.

Goldhaber et al. conclude that their data suggest strongly that Z_1^* does <u>not</u> correspond to a resonance in a single partial wave, but most likely reflects the rapid onset of production in inelastic channels. This suggests that the higher-mass enhancements observed by Abrams et al. may reflect significant production of N^*(1688) and N^*(1920) near their thresholds. Since the

Z_0^* represents a stronger and sharper enhancement, it is possibly a more likely candidate for a resonance; any conclusion, however, must await the detailed analysis of inelastic K^+d interactions through this region.

If the structure in the KN system reflects the rapid onset of inelastic channels, the situation would be analogous to that in the nucleon-nucleon system. For example, Bugg et al.[14] find that between 1.0 and 1.5 GeV/c the I = 1 pp cross-section increases almost 25 mb to a plateau of about 48 mb; other experiments have demonstrated that this results predominantly from the rapid increase in $N^*(1238)$ production through pion exchange. Above 2.0 GeV/c the pp cross-section decreases monotonically except for a broad peak of about 0.5 mb centred near 3.0 GeV/c; this enhancement could result from significant threshold production of $N^*(1688)$. No clear structure is observed in the I = 0 nucleon-nucleon system; however, the smoothing due to Fermi motion in the pd measurements could easily obscure any I = 0 structure less than 0.5 mb.

We conclude that the classification proposed in Fig. 4 is not yet seriously threatened. Although structure undoubtedly exists in the S = +1 baryon systems, the limited data presently available suggest that it results from the rapid onset of production in inelastic channels as new thresholds are crossed. It is interesting to note, however, that our prejudices are such that analogous structure in other systems may well appear in Fig. 4 as potential candidates for new resonances.

3. THE MESON RESONANCES

In 1964 I had the pleasure of discussing the status of the meson resonances in some detail at the International School of Physics at Varenna and the details appear in the Proceedings[15]. At that time candidates for completing the nonets of $J^P = 0^-$, 1^-, and 2^+ mesons had just been discovered. In addition, several "anomalies" were known; since that period the properties of a few of these have been clarified. The present discussion will concern the work which has been done during the past two years. In his rapporteur's talk at the XIIIth International Conference on High Energy Physics, Professor Goldhaber provided a rather thorough review of much of this work[16]. Nevertheless, it is useful to look a little more leisurely and from a somewhat different perspective to see what things remain unchanged from the hectic period of the Conference, and what things have received different interpretations or further clarification during the few months over which these notes were completed.

I think that the most striking single item presented during the past year came from the missing-mass (MM) spectrometer group at CERN. As a result of a series of runs at π^- momenta ranging from 3 to 12 GeV/c, Focacci et al.[17] have arrived at a proposed spectrum of mesons with $I \geq 1$ and mass between 500 and 2500 MeV. The technique used is simple and elegant. The momentum and angle of the recoil proton is measured for the reaction,

$$\pi^- + p \rightarrow X^- + p \qquad (4)$$

where X^- represents any object produced in association with the proton. For each event the kinematic information allows a calculation of the mass, M, of X^- with a resolution of about $\pm$ 26 MeV; counters are used to determine the number of X^- events with decay into one, three or five charged particles plus possible neutrals; the square of the four-momentum-transfer, $-t$ $(=\Delta^2)$, is measured with an accuracy of ± 0.006 near $-t = 0.025$ $(GeV/c)^2$, and ± 0.07 for

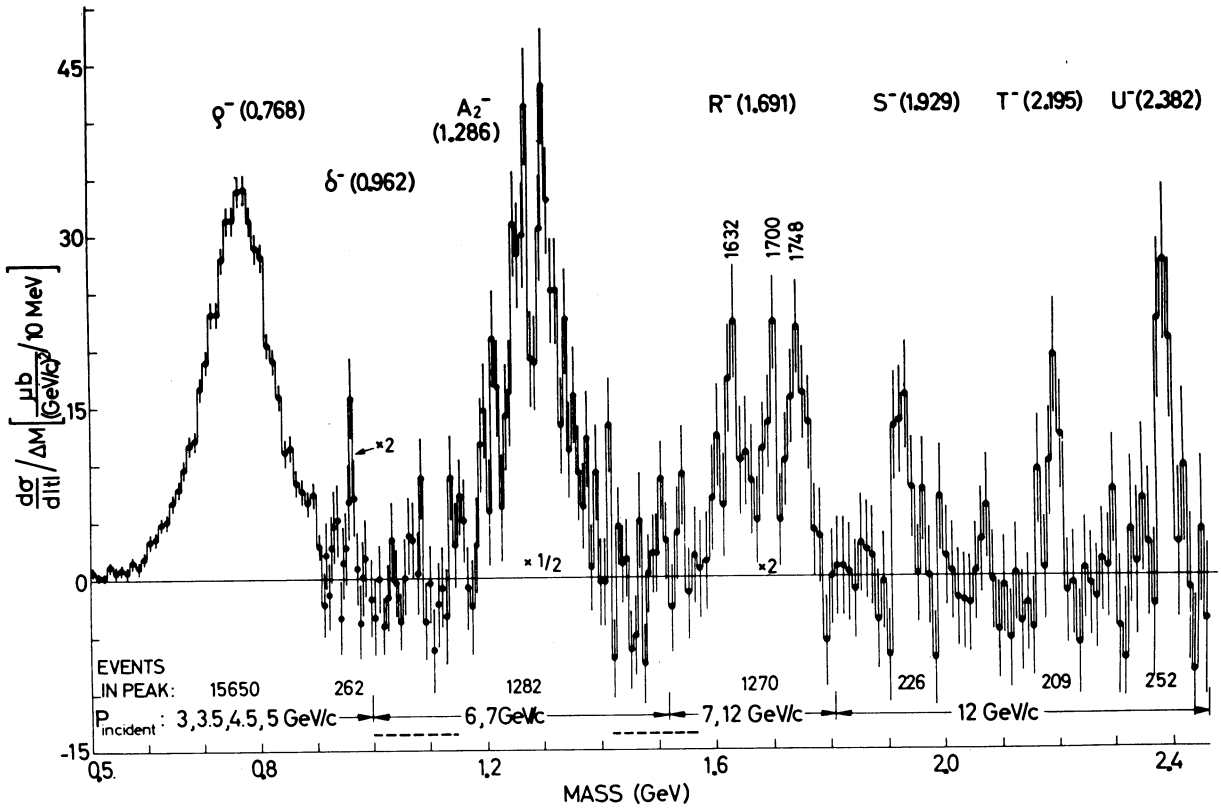

Figure 7 - The S = 0, I ≠ 0, meson spectrum proposed by **Focacci** et al. [Ref. 17)] on the basis of the CERN missing-mass spectrometer data. The spectrum is a composite of data taken at different **incident** π^- momenta.

$-t = 0.1$ to 0.5 $(GeV/c)^2$. The proposed meson spectrum is shown in Fig. 7. It is important to realize that the plot is a composite of data taken at different momenta. For each run, a fit is made to the background and a subtraction performed; a typical run is shown in Fig. 8, which illustrates the original data[18] near $M(X^-) = 1920$ MeV. Consequently, the signals are not very large and a good statistical precision is required to ascertain their validity. A summary of their results is given in Table 2.

In looking for some systematic feature in their data, **Focacci** et al. report another remarkable observation. When the mass-squared, $M^2(X^-)$, of each <u>major</u> peak, i.e. $d\sigma/dt \geq 20\ \mu b/(GeV/c)^2$, is plotted against its sequence-number, the points lie in a straight line; this is shown in Fig. 9. Since the established spins of the ρ and the $A_2(1310)$ are equal to their sequence-numbers, **Focacci** et al. speculate that the correspondence may also apply to the remaining peaks. We shall return to this interesting possibility later.

Since the MM spectrometer represents a new and potentially powerful technique it is important to compare this structure with that observed in the more traditional bubble chamber (BC) investigations where the full kinematic reconstruction of each event is usually possible. In Fig. 10 the $\pi^\pm\pi^0$ effective-mass distributions, $M(\pi^\pm\pi^0)$, for the reactions

$$\pi^\pm + p \rightarrow \pi^\pm + \pi^0 + p \qquad (5)$$

are compared[16] with the spectrum of **Focacci** et al. In principle, all peaks corresponding to

TABLE 2

Data on unstable bosons, X^-, of mass 500 to 2500 MeV, produced in the reaction $\pi^- p \to pX^-$, as observed by a missing-mass spectrometer: p_1 ≡ lab. incident pion momentum; $|t|$ ≡ square of the momentum transfer to recoil proton. [From M.N. Focacci, W. Kienzle, B. Levrat, B.C. Maglić, and M. Martin, Phys.Rev.Letters 17, 890 (1966), with subsequent revision.]

a	b	c	d	e	f	g	h	i	j	k
Particle name	Central mass value (in MeV)	Expt'l. resolution	Physical width Γ (deduced)	Incident π^- momentum, p_1	Statistical significance (st. dev.)	Events in peak above background and statistical error	Signal-to-background ratio	t limits	dσ/dt	Decay mode
ρ^-	768 ± 5	28 ± 5	127 ± 5	3.0 3.5 4.5 5.0		15600 ± 170	1.6:1	0.10 - 0.14 0.14 - 0.17 0.17 - 0.22 0.22 - 0.26	770 ± 150 x) 770 ± 170 580 ± 100 370 ± 110	1c > 97.4%
δ^-	962.5 ± 5	24 ± 4	≤ 5	3.0 3.5 4.5 5.0	5.0	262 ± 52	1:5	0.11 < t < 0.21	8.9 ± 3 y)	$\frac{1c}{\geq 3c} = 1.3 \,^{+0.9}_{-0.7}$
A_2	1286 ± 8	36 ± 4	98 ± 5	6.0 7.0	17	1282 ± 63	1:1.5	0.31 < t < 0.39	400 ± 120	$\frac{1c}{3c} = 1.05 \pm 0.1$
A_2' A_2''	1260 ± 10 1312 ± 10			6.0 7.0	1 peak and 2 peaks equally probable: P = 5% to 10%	$\frac{A_2'}{A_2''} \approx 1:1$	1:6			$\frac{1c}{3c} \approx 1$
R	1691 ± 15	31 ± 3	116 ± 3	7.0 12.0	1 peak: P = 1% 2 peak: P = 1% 3 peak: P = 20 to 60% ($R_{1,2,3}$)	973 ± 84	1:6	0.23 < t < 0.28	125 ± 30	1c = 0.30 ± 0.06 z) 3c = 0.67 ± 0.10 >3c = 0.03 ± 0.03
R_1	1632 ± 15	34 ± 3	< 21		6.7	360 ± 70	1:4.7		35 ± 10	1c = 0.37 ± 0.13 3c = 0.59 ± 0.21 >3c = 0.04 ± 0.04
R_2	1700 ± 15	30 ± 3	< 30	7.0 12.0	6.1	485 ± 73	1:3.3		43	1c = 0.42 ± 0.11 3c = 0.56 ± 0.14 >3c = 0.01 ± 0.01
R_3	1748 ± 15	28 ± 3	< 38		7.3	425 ± 74	1:3.5		47	1c = 0.14 ± 0.08 3c = 0.80 ± 0.18 >3c = 0.05 ± 0.05
S	1929 ± 14	22 ± 2	≤ 35	12.0	5.5	226 ± 41	1:7	0.22 < t < 0.36	35 ± 12	$1c = 0.06 \,^{+0.15}_{-0.06}$ $3c = 0.92 \,^{+0.08}_{-0.20}$ $>3c = 0.02 \,^{+0.13}_{-0.02}$
T	2195 ± 15	39 ± 4	≤ 13	12.0	5.1	209 ± 41	1:7	0.22 < t < 0.36	29 ± 10	$1c = 0.04 \,^{+0.11}_{-0.04}$ $3c = 0.94 \,^{+0.06}_{-0.19}$ $>3c = 0.02 \,^{+0.13}_{-0.02}$
U	2382 ± 24	62 ± 6	≤ 30	12.0	5.9	252 ± 43	1:6	0.28 < t < 0.36	42 ± 14	1c = 0.30 ± 0.10 3c = 0.45 ± 0.15 >3c = 0.25 ± 0.10

x) dσ/dt normalized to 4 GeV/c (average momentum).

y) dσ/dt weighted between p_1 = 3, 3.5, and 4.5 GeV/c.

z) errors are one standard deviation.

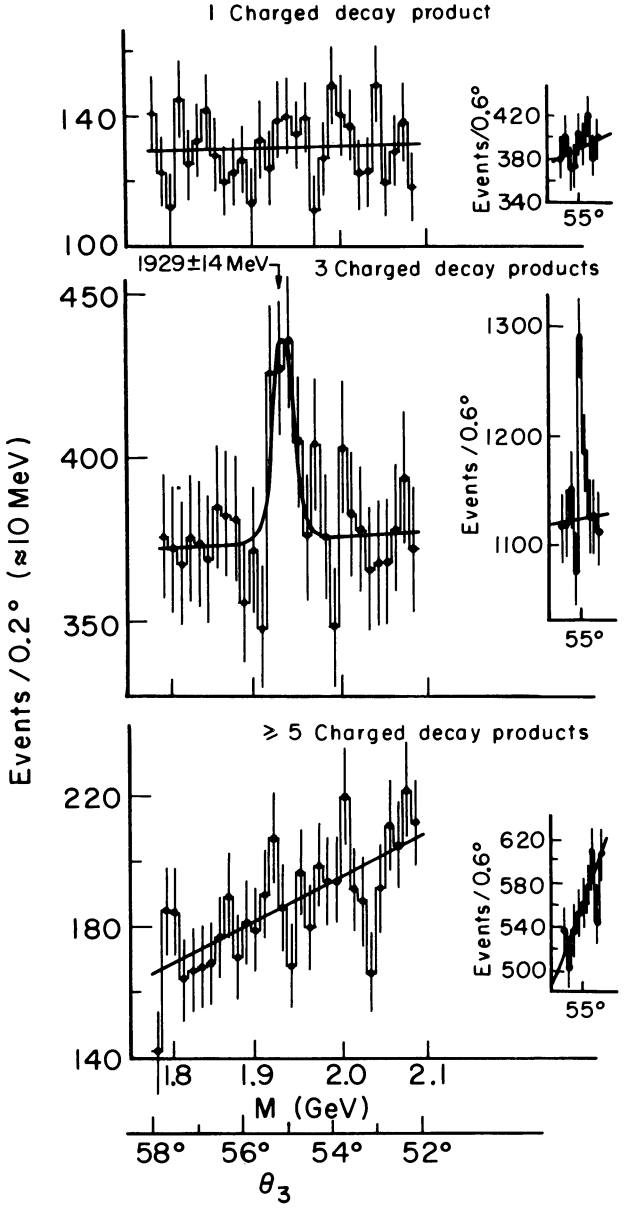

Figure 8 - The original missing-mass spectrometer data of Chikovani et al. [Ref.18)] in the region of the S-peak at 1929 MeV.

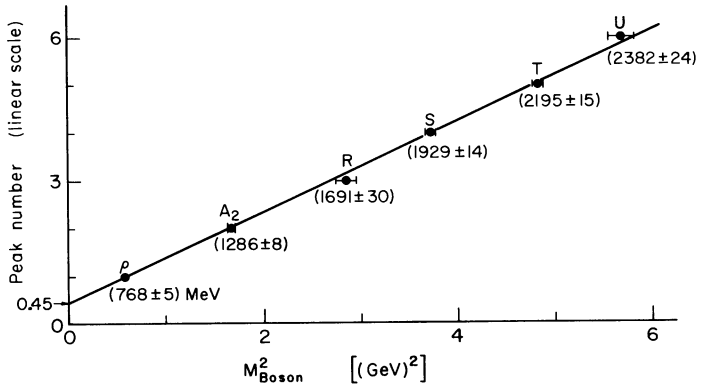

Figure 9 - Plot by Focacci et al. [Ref. 17)] of M^2 for major peaks versus sequence number. The straight line plot suggests that the higher mass peaks represent Regge recurrences of the ρ and A_2 mesons.

mesons with $I \geq 1$, $G = +1$, and $P = (-1)^J$ should appear in each plot. Above the very large peak at the $\rho^{\pm}$ mass, both the π^+p and π^-p experiments show significant enhancements near 1.62 GeV, in good agreement with the R_1 component of the R-peak in the MM-spectrometer data in Table 2. In addition, the $M(\pi^+\pi^0)$ histogram shows a clear peak near 1.91 GeV consistent with the S-peak in Table 2; there is no corresponding signal apparent in the $M(\pi^-\pi^0)$ plot. At this point it is important to emphasize the differences in these experiments: (a) the R, S, and T peaks were observed at 12 GeV/c while the $M(\pi^-\pi^0)$ spectrum was measured at 6 GeV/c; (b) both high mass peaks in the 8 GeV/c $M(\pi^+\pi^0)$ spectrum occur in the strong $N^*(1238)$ band which is not produced in the π^-p interactions.

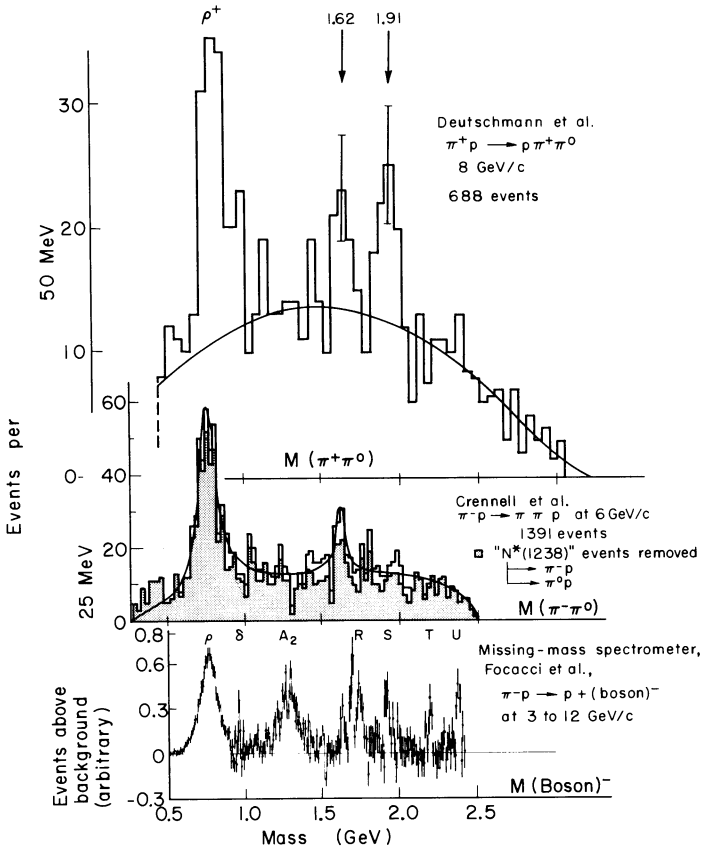

Figure 10 - Compilation of $M(\pi^{\pm}\pi^0)$ distributions and comparison with missing-mass spectrometer data [Ref. 16)]

Further evidence for mesons with $I \geq 1$ is available in the $M(\pi^+\pi^-)$ spectra obtained above 6 GeV/c in the reactions

$$\pi^- + p \rightarrow \pi^+ + \pi^- + n \qquad (6)$$

and

$$\pi^+ + d \rightarrow \pi^+ + \pi^- + p + p \,. \qquad (7)$$

However, these distributions will also contain enhancements corresponding to mesons with $I = 0$, $G = +1$, and $P = (-1)^J$. The available data for reaction (6) are compared[16] in Fig. 11. Above the dominant ρ^0 and f_0 peaks there is a persistent enhancement from about 1.5 to 1.8 GeV, referred to as the g meson. Since this appears to be statistically different in mass and width from the $M(\pi^+\pi^0)$ peaks at 1.62 to 1.63 GeV, Crennell et al.[19] refer to the latter as the g_1 meson; they suggest that the differences in mass and width may indicate the existence of an unresolved $I = 0$ $\pi^+\pi^-$ state near 1750 MeV. No significant structure is observed at higher mass; within statistics, the structure which appears in the $M(\pi^+\pi^-)$ distributions from reaction (7) is consistent with that observed in reaction (6).

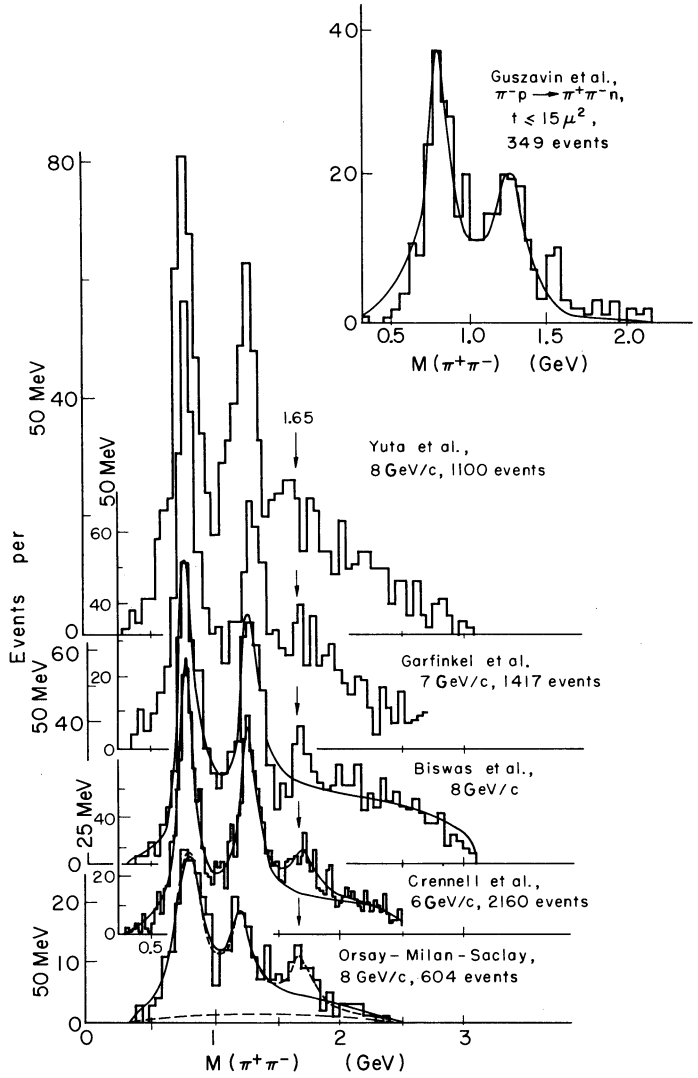

Figure 11 - Compilation of $M(\pi^+\pi^-)$ distributions showing consistent pattern of ρ, f_0, and g enhancements. [Ref. 16)]

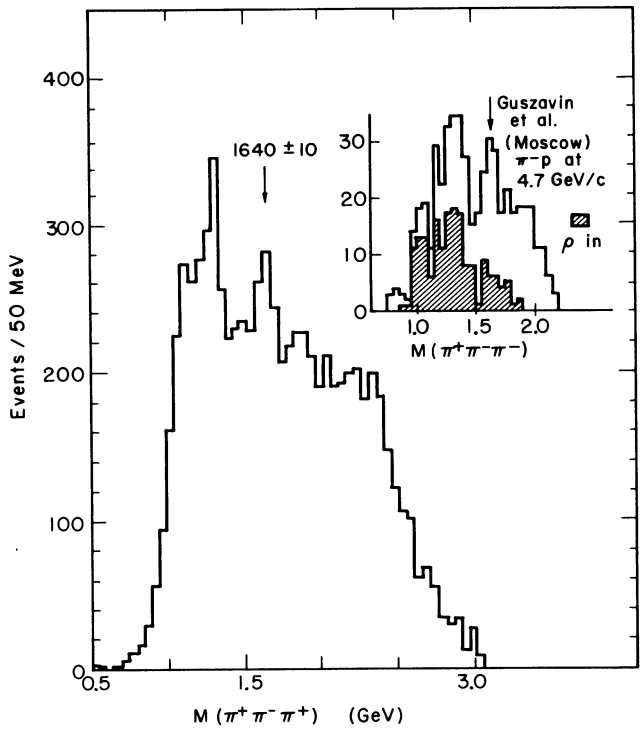

Figure 12 - Compilation by Ferbel [Ref. 20)] with no selection criteria imposed. The A enhancement occurs at 1.0 to 1.4 GeV; a well-defined peak (A_3) appears at 1640 MeV. Analogous effects are observed in the data of Guszavin et al. [Ref. 16)].

Mesons with G = -1 and $J^P \neq 0^+$ may decay into three pions; consequently we may also look for structure corresponding to the peaks reported by Focacci et al. in the reactions

$$\pi^{\pm} + p \rightarrow \pi^{\pm} + \pi^+ + \pi^- + p \ . \qquad (8)$$

The $M(\pi^+\pi^+\pi^-)$ distributions for π^+p interactions near 8 GeV/c have been compiled by Ferbel[20]; the data for <u>all</u> events (no selection criterion imposed) are shown in Fig. 12. The strong A enhancement between 1.0 and 1.4 GeV dominates the distribution; this was first observed by Goldhaber et al. who showed that it was associated entirely with the $\pi^+\rho^0$ combinations. Subsequent experiments have demonstrated that the peak is complicated in structure, consisting of at least a well-defined state at 1310 MeV (the A_2) and possibly a second independent state at 1080 MeV (the A_1). The interesting new feature of the compilation in Fig. 12 is the clear peak at 1640 MeV (the A_3); it is possible that this confirms the 3π P-enhancement near 1600 MeV reported earlier by Fiorini et al.[21] with poorer statistics. Ferbel reports that in contrast with the A enhancement, a more detailed analysis indicates that this peak is <u>not</u> associated with the ρ^0. The nearest MM-spectrometer peak is the R_1 at 1632 MeV; since this peak consists predominantly of decays into one charged and three charged particles plus possible neutrals, it is not unlikely that it represents a superposition of the g_1 meson and the $A_3(1640)$.

To complete our summary of the major peaks observed in three-pion combinations, it is necessary to consider the reaction

$$\pi^+ + d \rightarrow \pi^+ + \pi^- + \pi^0 + p + p \ . \qquad (9)$$

In this case the $M(\pi^+\pi^-\pi^0)$ spectrum shows the well-known I = 0 states $\eta(549)$ and $\omega(784)$. At higher masses, a clear peak due to $A_2^0(1310)$ is observed; as an example, the data of the BBFO Collaboration[22] are shown in Fig. 13; the η and ω peaks have been suppressed by the imposition of the ρ^0-selection criterion. Of particular importance, however, is the absence of any peak which might correspond to the $A_1^0(1080)$. In most experiments which report evidence for $A_1^{\pm}(1080)$, it is produced with intensity comparable to the $A_2^{\pm}(1310)$.

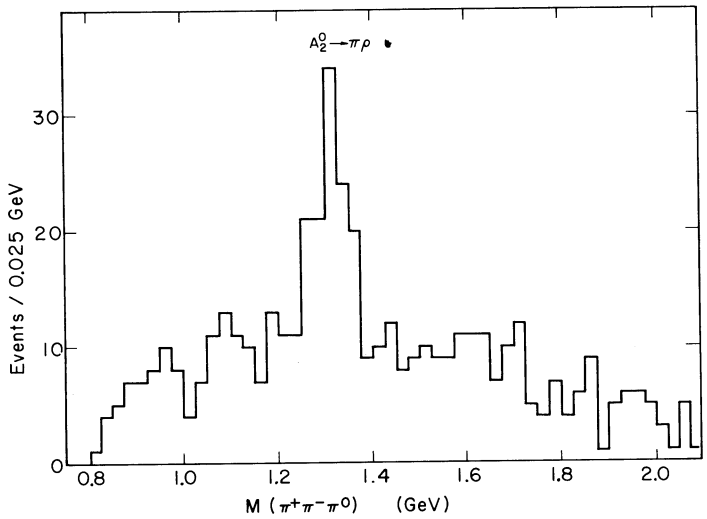

Figure 13 - Data of Bari-Bologna-Florence-Orsay Collaboration [Ref. 22)] with ρ selection criterion imposed. Although the $A_2^0(1310)$ occurs strongly, no $A_1^0(1080)$ is observed.

Finally, the charged four-pion systems have been studied in the reactions

$$\pi^{\pm} + p \to \pi^{\pm} + \pi^+ + \pi^- + \pi^0 + p \ . \tag{10}$$

The only clear evidence for structure occurs in events corresponding to the $\pi^{\pm}\omega$ combinations. The major feature is a low-mass peak, the B(1220), to which we return later; in addition, some evidence for an additional peak in the $\pi^{\pm}\omega$ combinations near 1640 MeV has been reported[23].

Perhaps the most complete comparison between BC data and the MM-spectrometer results has been carried out by the ABC Collaboration[24] in their study of $\pi^+ p$ interactions at 8 GeV/c. To look for mesons with G = -1, three-pion spectra were summed over all possible channels

$$\pi^+ + p \to p + \pi^+ + \pi^+ + \pi^- \quad (N^{*++} \text{ excluded}) \tag{11a}$$

$$\pi^+ + p \to N^{*++} + \pi^+ + \pi^- + \pi^0 \tag{11b}$$

$$\pi^+ + p \to p + \pi^+ + Z^0 \tag{11c}$$

where Z^0 is two (or more) π^0's. The data are shown in Fig. 14; the resolution may be inferred from the widths of the η and ω peaks. The A enhancement stands out clearly above the estimated background shown by the solid curve. A general enhancement occurs near 1.65 GeV (the P-enhancement of Fiorini et al.[21]?) corresponding to the complex R-peak in the MM-spectrometer experiment. For direct comparison with Fig. 7 the data with background subtracted are shown in Fig. 14b; there is no significant evidence for the S, T, or U peaks.

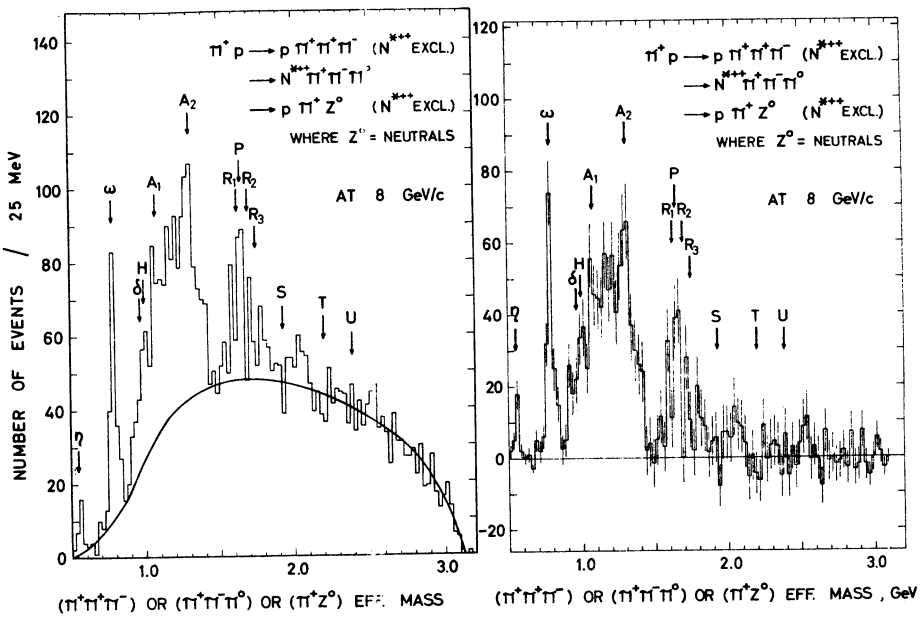

Figure 14 - Search for S = 0, G = -1 mesons by Aachen-Berlin-CERN Collaboration [reported in Ref. 24)]; the data are summed over all possible decay modes. At right the estimated background has been subtracted; regions corresponding to peaks observed in the missing-mass spectrometer are indicated.

The ABC Collaboration has studied the G = +1 systems in an analogous way; all possible two- and four-pion spectra were summed

$$\pi^+ + p \rightarrow p + \pi^+ + \pi^+ + \pi^- + \pi^0 \qquad (12a)$$

$$\pi^+ + p \rightarrow N^{*++} + \pi^+ + \pi^- + Z^0 \qquad (12b)$$

$$\pi^+ + p \rightarrow p + \pi^+ + \pi^0 \ . \qquad (12c)$$

The combined spectrum appears in Fig. 15; after subtraction of the estimated background, the spectrum shown in Fig. 15b is obtained. Small peaks occur near the S, T, and U masses in addition to the expected peak at the R_1 mass. It is apparent that the statistical significance of these peaks depends sensitively on the way in which the background is estimated; nevertheless, they may be interpreted as providing some support for the assumption that at least some component of the S, T, and U peaks has G = +1. It may also be noticed that a peak persists near 2600 MeV, suggesting a further resonance (V meson) with positive G-parity[24].

Since the MM-spectrometer results were obtained with π^-p interactions, we have compared the spectrum with those observed in BC studies of π^+p and π^+d interactions. Let us summarize the results at this point:

a) Both the MM and BC experiments show clearly the charged ρ peak; the masses and widths are consistent.

b) Both experiments exhibit strong $A_2(1310)$ peaks with comparable masses and widths. In the MM-spectrometer measurements the peak is associated with events decaying equally into one and three charged particles plus possible neutrals, consistent with the decay of an I = 1 state in $\pi^0\rho^-$ and $\pi^-\rho^0$.

c) The MM spectrometer shows no evidence for a peak near $A_1^-(1080)$.

d) The MM spectrometer shows no evidence for a peak near $B^-(1220)$, but this could be obscured by the strong $A_2(1310)$ peak.

e) The R_1 peak at 1632 MeV in the MM-spectrometer data could represent a superposition of the g_1 and A_3 enhancements, although the reported width of the R_1, 34 ± 3 MeV, may be too narrow for this interpretation. No clear BC peaks corresponding to R_2 and R_3 have been observed.

f) The S-peak in the MM-spectrometer data at 1929 MeV may correspond to the 1910 MeV enhancement observed in the 8 GeV/c π^+p interactions. Since the width in the $M(\pi^+\pi^0)$ spectrum is comparable with the experimental resolution[24] this interpretation is not incompatible with the reported width, ≤ 34 MeV, of the S-peak. However, an apparent discrepancy remains. The S-peak is associated primarily with events decaying into three charged particles plus possible neutrals; this suggests the decays $\pi^-\omega$ or $\rho^-\rho^0$. We know that the 1910 MeV peak in Fig. 15 results from $\pi^+\pi^0$ pairs from (12c); where is the <u>much</u> stronger $\pi^+\pi^+\pi^-\pi^0$ peak we expect from (12a) if the S-meson has G = +1?

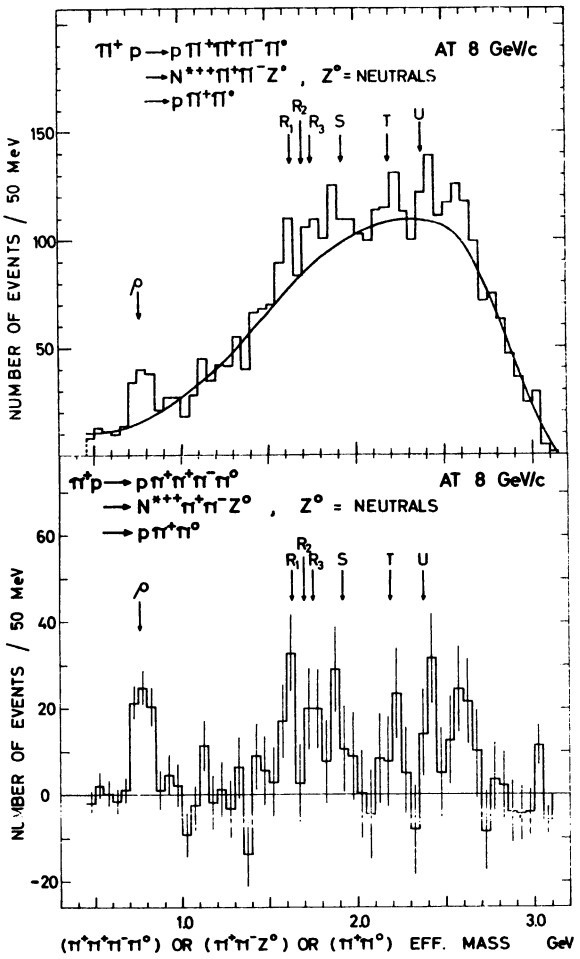

Figure 15 - Search for S = 0, G = +1 mesons by Aachen-Berlin-CERN Collaboration [reported in Ref. 24)]; the data are summed over all possible decay modes. At bottom the estimated background has been subtracted; the corresponding missing-mass spectrometer peaks are indicated.

We conclude that although areas of apparent inconsistency persist, the general agreement between the MM and BC experiments is rather good. Probably the major difference lies in the reported widths for the resonant systems. In the MM experiment, widths of the higher-mass systems (R, S, T, and U) are comparable with the resolution ($\lesssim$ 30 MeV); such small widths are never observed in the BC experiments. Whether this results from the particular technique of background subtraction in the MM-spectrometer data, or reflects the poorer resolution in the BC analyses is not clear at present. In general, the MM experiments cannot determine the G-parity of an observed peak, or resolve accidental superpositions of systems with similar masses. However, these experiments point out the regions of the mass spectrum where new states exist --- where the BC's should start their investigations to determine the properties of the states.

4. SPINS AND PARITIES

Let us turn now to the present knowledge of the spins and parities of the multipion systems discussed thus far.

4.1 The ρ meson and the $\pi\pi$ interaction below 1 GeV

No one can doubt that $J^P = 1^-$ for the ρ meson. However, the difference in the decay angular distributions for the $\pi^+\pi^0$ and $\pi^+\pi^-$ systems has provided a long-standing anomaly. To illustrate this we show in Fig. 16 a recent compilation by Walker et al.[25] for the reactions

$$\pi^- + p \rightarrow \pi^- + \pi^0 + p \qquad (13a)$$

and

$$\pi^- + p \rightarrow \pi^+ + \pi^- + n \ . \qquad (13b)$$

To combine data at various momenta Walker et al. represent the production cross-section by the formula

$$d^2\sigma/d\Delta^2\, dm^* = K\, m^{*2}\, \sigma(\pi\pi)\, f(\Delta^2) \qquad (14)$$

where $f(\Delta^2)$ is an empirically determined function; Δ^2 is the square of the four-momentum-transfer to the nucleon, K is the pion momentum in the c.m. of the dipion, and m^* is the dipion effective mass. The scattering angle is defined by $\cos\vartheta = \hat{p}_o \cdot \hat{p}_-$, where p_o is the beam momentum and p_- the final-state π^- momentum measured in the c.m. of the dipion.

We note that the $\pi^-\pi^0$ angular distribution shows a small backwards asymmetry below the ρ^- peak at 760 MeV, becomes essentially symmetric in the region of the ρ^-, and then develops a small forward asymmetry. This is consistent with the behaviour expected for a resonant I = 1 p-wave amplitude interfering with a small I = 2 s-wave amplitude. In contrast, the $\pi^+\pi^-$ angular distribution exhibits a strong forward asymmetry which remains essentially constant from 500 to 950 MeV. Since the asymmetry does <u>not</u> change sign through the region of the ρ^0 it has long been argued that it most likely arises from an I = 0 s-wave phase shift which also increases smoothly through this region.

Many groups who have studied reactions (13) have attempted to deduce the $\pi\pi$ phase shifts directly from the measured distributions. Unfortunately, a serious limitation occurs in all such analyses. It is well-known that both the production and decay angular distributions differ significantly from predictions based on unmodified single-particle exchange models.

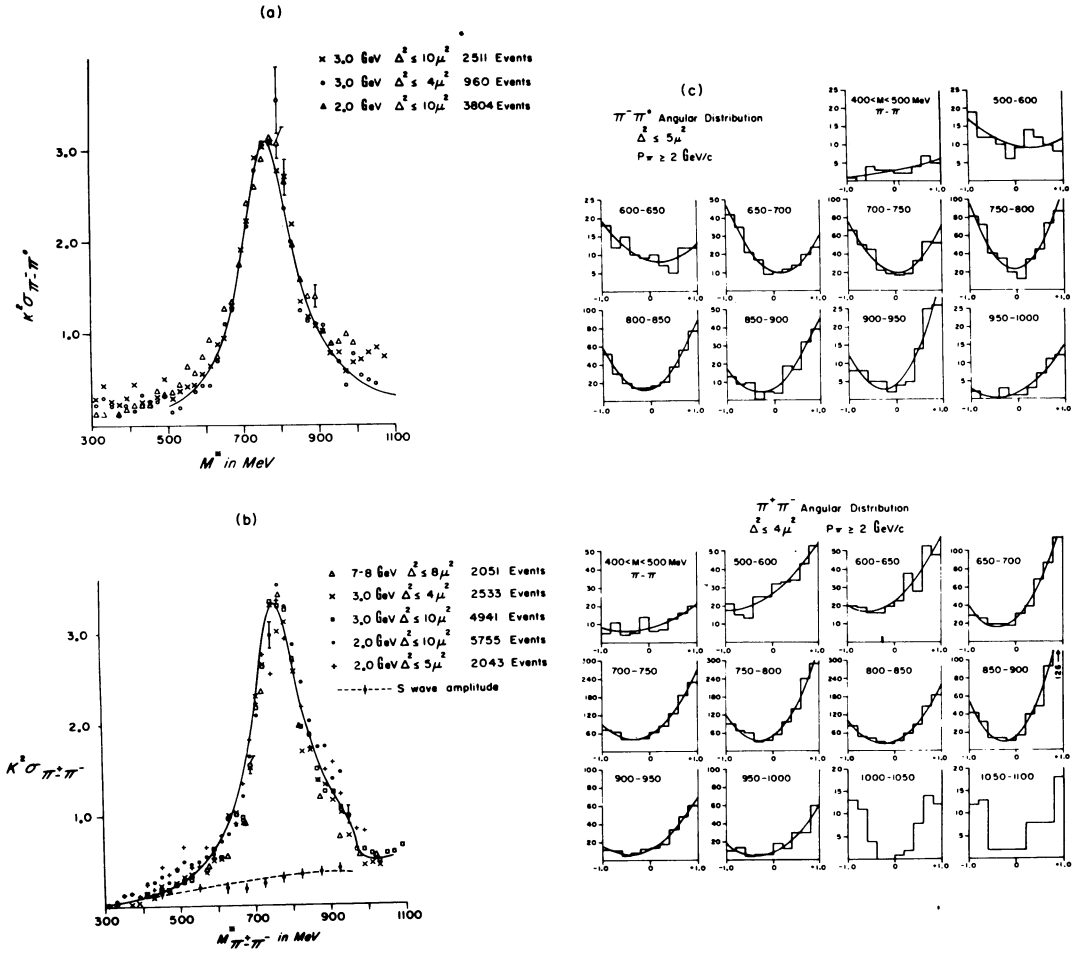

Figure 16 - Compilation by Walker et al. [Ref. 25)] of effective $\pi\pi$ cross-sections and scattering angular distributions. The data give a good fit to a p-wave Breit-Wigner resonance with $M_r^* = 760$ MeV and $\Gamma = 160 + 10$ MeV.

Gottfried and Jackson[26] and others have obtained good agreement with a substantial body of experimental data when the incoming and outgoing waves were modified for absorptive effects. The idea may be applied in a straightforward way when the ρ is considered a long-lived system; then its production and decay properties may be calculated independently. To determine phase shifts, absorption must also be properly introduced in the production of s-wave dipion systems, and the appropriate interference with the p-wave dipion systems calculated. In general, the individual phase-shift determinations differ in the particular way in which the absorptive corrections are applied. We shall briefly discuss only two recent attempts to determine the phase shifts.

In their analysis of reactions (13) at 2.7 GeV/c Gutay et al.[27] assume:

a) The s-wave and p-wave $\pi\pi$ production amplitudes calculated in Born approximation and modified for absorption correctly describe the data for c.m. production angles with $\cos \vartheta^* > 0.8$.

b) The $\pi\pi$ scattering angular distributions at the smallest accessible momentum-transfers correspond closely to those in the Chew-Low limit, $\Delta^2 \to -\mu^2$.

c) Only the I = 0, $J^P = 0^+$, and I = 1, $J^P = 1^-$ partial waves need be considered in the region of the ρ^0. Gutay et al. argue that the small asymmetry above and below the ρ^- implies an I = 2 s-wave phase shift which contributes negligibly to the asymmetry in the ρ^0.

d) The p-wave phase shift is given by a p-wave Breit Wigner resonance.

With these assumptions, Gutay et al. fit their data to the absorption model and obtain the density matrix elements for forward production, i.e. $\cos\vartheta^* = 1$, where the angular distribution for $\pi\pi$ scattering (averaged over azimuthal angle) is approximated by

$$d\sigma/d\Omega = \lambda^2 \left\{ \tfrac{4}{9} \sin^2 \delta_0^0 + 4 \cos(\delta_0^0 - \delta_1^1)\sin\delta_0^0 \sin\delta_1^1 \cos\vartheta + 9 \sin^2\delta_1^1 \cos^2\vartheta \right\}. \tag{15}$$

Since incoherent background should contribute most strongly to the isotropic term, it is not used in the analysis. Since the behaviour of δ_1^1 is assumed known [assumption (d)] the value of δ_0^0 may be inferred from the ratio of the second and third terms in Eq. (15). The two solutions, δ_0^0 and $\delta_0^{0\prime} = \pi/2 - (\delta_0^0 - \delta_1^1)$ are shown in Fig. 17b and compared with earlier estimates. A similar analysis at 4.2 GeV/c by the same group[27] yields similar results; in this case the effects of neglecting δ_0^2 were carefully studied and again found to be negligible. The authors believe that the reasonable fit of the absorption model to their data justifies the extrapolation of the calculated density matrix elements to $\cos\vartheta^* = 1$. Unfortunately, it is precisely near $\cos\vartheta^* = 1$ that the absorption model gives the poorest fit to their data, seriously underestimating $\rho_{00} - \rho_{11}$. For this reason it is difficult to understand the improvement gained through use of the absorption model; it is not at all obvious why the phase shifts obtained by straightforward fitting of the scattering angular distributions at low Δ^2 to Eq. (15) are not at least equally valid.

In their analysis of the combined data in Fig. 16, Walker et al.[25] argue that δ_0^2 cannot be neglected if meaningful phase shifts are to be deduced for $\pi\pi$ energies below 700 MeV. To estimate the s-wave phase shift the square of the scattering amplitude is written

$$(\pi^-\pi^0): |A|^2 = [\sin\delta_2 \cos(\delta_p - \delta_2) + 3x \sin\delta_p]^2 + \sin^2\delta_2 \sin^2(\delta_2 - \delta_p) \tag{16a}$$

$$(\pi^+\pi^-): |A|^2 = \left\{ [\tfrac{1}{3}\sin\delta_2 \cos(\delta_p - \delta_2) + \tfrac{2}{3}\sin\delta_0 \cos(\delta_p - \delta_0)] + 3x \sin\delta_p \right\}^2 + [\tfrac{1}{3}\sin\delta_2 \sin(\delta_p - \delta_2) + \tfrac{2}{3}\sin\delta_0 \sin(\delta_p - \delta_0)]^2 \tag{16b}$$

where $x = \cos\vartheta$ and δ_0, δ_2 are the I = 0 and I = 2 s-wave phase shifts; δ_p is calculated from a p-wave Breit-Wigner resonance with E = 760 MeV and Γ = 160 MeV. Walker et al. argue that the minimum in the angular distribution provides the most reliable determination of δ_0 or δ_2. However, without modification they claim that this technique greatly overestimates the s-wave amplitude. A correction factor (for absorption?) is deduced by comparing the cross-sections in the reactions

$$\pi^+ + p \rightarrow \pi^+ + \pi^+ + n \tag{17a}$$

and

$$\pi^+ + p \rightarrow \pi^+ + \pi^0 + p \ . \tag{17b}$$

They conclude that the corrected value of cos ϑ_{min} is approximately 0.8 times the value obtained by fitting Eqs. (16) to the angular distributions. The result of their analysis is shown in Fig. 17a. Their preferred solution for the I = 0 s-wave phase shift is indicated by the solid line. The dashed line illustrates a second family of phase shifts in qualitative agreement with those of Gutay et al., but Walker et al. report that they are less satisfactory in fitting the mass spectra. There is no doubt that Walker et al. have invented a technique for correcting for absorption or other effects; unfortunately, there appears to be little theoretical (or experimental) justification at present for the conviction that this correction applied uniformly over the mass interval 300 to 950 MeV and to beam momenta 2 to 8 GeV/c leads to valid phase-shift analysis. Perhaps the qualitative agreement with results obtained with other techniques provides the strongest justification for the procedure used.

In Figs. 17a and 17b there are solutions for the I = 0 s-wave phase shift which increase rapidly through 90° between 700 and 750 MeV, implying the existence of a sharp resonance. In their study of reaction (13b) Hagopian et al.[28] searched for such a state by selecting $\pi^+\pi^-$ events with $|\cos\vartheta| < 0.3$, where the ρ^0 contribution should be a minimum; they concluded that their data provided some evidence for the existence of such a state. The most recent data[16] are shown in Fig. 18. In Selove's compilation there is a suggestion of a small peak centred at 720 MeV superimposed on a wider peak due to the ρ^0; in Jacobs' data, the 720 MeV peak does not appear. Unfortunately, even the combined data are statistically inadequate for any definite conclusion.

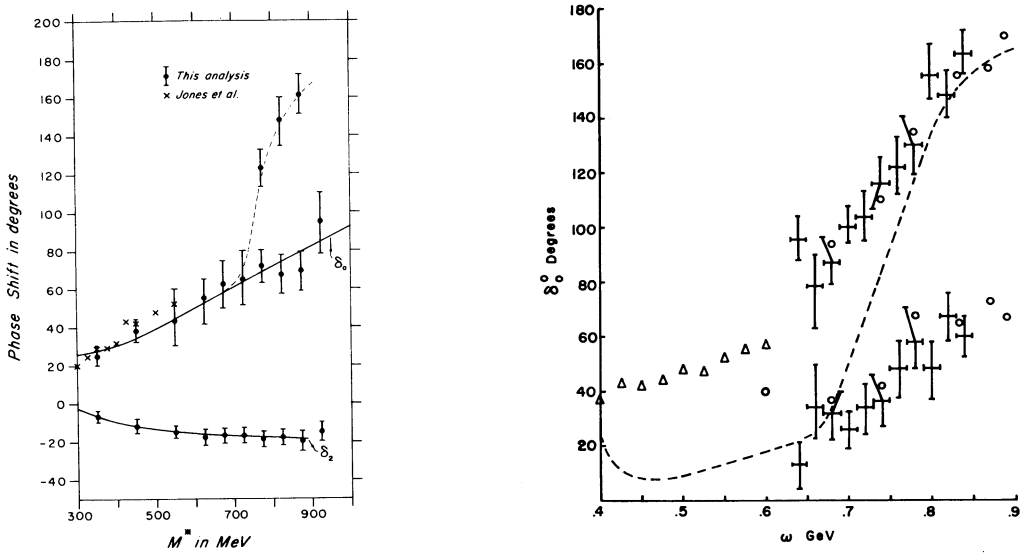

Figure 17 - (Left) I = 0 and I = 2 s-wave phase shifts deduced by Walker et al. [Ref. 25)]; the solid curves represent their preferred solutions. (Right) the I = 0 s-wave phase shifts derived by Gutay et al. [Ref.27)]; the two branches result from neglect of the isotropic term in the scattering angular distribution, where incoherent background may contribute significantly. The dashed curve is due to Wolf; o, from Baton and Reignier; and Δ, from Jones et al.

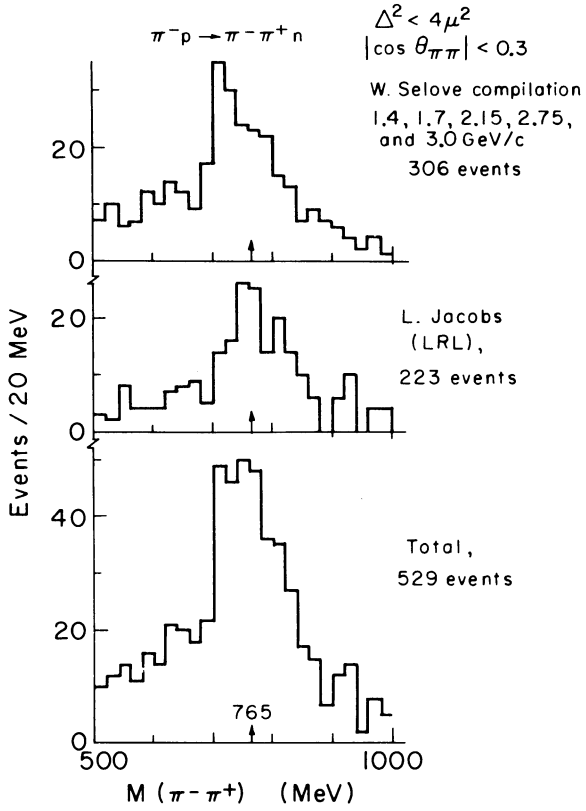

Figure 18 - $M(\pi^+\pi^-)$ distributions for events with scattering angle near 90° where the relative s-wave contribution should be largest. The combined data [Ref. 16)] suggest some distortion in the peak towards lower masses, but do not provide convincing evidence for a narrow I = 0 resonance near 720 MeV.

Possible evidence for a sharp I = 0 resonance has been reported by Feldman et al.[29] in a preliminary analysis of the reaction

$$\pi^- + p \to \pi^0 + \pi^0 + n \qquad (18)$$

at 1.52 GeV/c. Neutron momenta were determined by time-of-flight measurements; π^0 decay γ-rays were detected in lead-plate spark chambers. Although statistics were limited, there was some indication in the 4γ events for enhanced neutron counts corresponding to a $\pi\pi$ mass near 700 MeV with $\Gamma \lesssim 50$ MeV. At present, the same group has undertaken a more comprehensive experiment to check this result. This may be unnecessary however, since Buhler-Broglin et al.[30] have redone the experiment with great care at the same incident momentum and with the same angular acceptance. Their spectrum for the missing mass recoiling against the neutron is shown in Fig. 19. A clear enhancement is observed corresponding to the decay $\omega \to \pi^0\gamma$; no deviation from a smooth background is apparent near 700 MeV. Normalizing to the ω peak of Feldman et al.[29], 350 to 600 events should have been observed near 700 MeV. Buhler-Broglin et al. conclude that their data disagree strongly and show no evidence for a narrow peak near 700 MeV.

Reaction (18) has also been studied by Corbett et al.[31] at 1.7 and 2.5 GeV/c. In this case only the 4γ's were detected; kinematically reconstructed events gave a mass resolution of about 100 MeV. The peripherally-produced events showed no evidence for any narrow resonance near 700 MeV, but rather a broad enhancement centred at 600 MeV with a width of about 400 MeV.

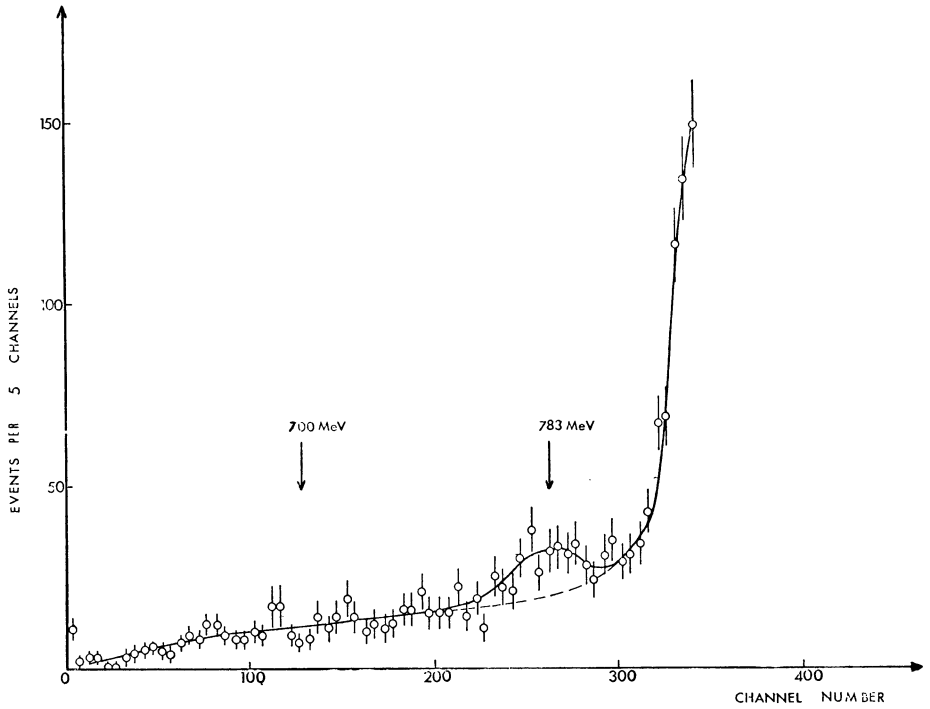

Figure 19 - The missing-mass data of Buhler-Broglin et al. [Ref. 30)]. Although the neutral decay of the ω is observed clearly, there is no evidence for a neutral state near 700 MeV.

If this enhancement is interpreted as an I = 0 s-wave resonance, Corbett et al. estimate that the asymmetry in the ρ^0 decay could be reproduced with an I = 2 s-wave phase shift of about -40° at a mass of 750 MeV. Theoretical support for such a broad, low-mass I = 0 s-wave resonance has been deduced by Lovelace et al.[32] from a dispersion analysis of backward pion-nucleon scattering data. However, when Crawford et al.[33] assume the presence of an I = 0 s-wave $\pi\pi$ resonance in the decay $\eta \to \pi^+\pi^-\pi^0$, they obtain the values E = 392 ± 9 MeV and Γ = 88 ± 15 MeV. It may be noted that such a narrow resonance should be easily detected in the $\pi^+\pi^-$ spectrum from reaction (13b); no particular peaking at this mass is apparent in the extensive data shown in Fig. 16.

We conclude that although several experiments independently suggest the existence of an I = 0 s-wave $\pi\pi$ resonance somewhere between 350 and 800 MeV, there is little agreement about the position and width. Because of statistical limitations and/or theoretical uncertainties in the analyses, no consistent set of I = 0 s-wave phase shifts can be deduced at present.

4.2 The $\pi\pi$ system above 1 GeV/c

It is apparent from Fig. 11 that above 1 GeV the $M(\pi^+\pi^-)$ distributions are dominated by the f_0 meson, with E = 1250 MeV and Γ = 120 MeV. Extensive analyses[16] of both the $\pi^+\pi^-$ and $\pi^0\pi^0$ systems have confirmed the early speculations that $I^GJ^P = 0^+2^+$ for the f_0.

In Fig. 10 the data of Crennell et al.[19] show a $\pi^-\pi^0$ peak about four standard deviations above the background at E = 1630 MeV with Γ = 100 MeV. The peak is reduced negligibly when $N^{*+}(1238)$ events are removed. Since no $\pi^+\pi^+$ peak is observed in reaction (17a) at the same incident momentum, Crennell et al. conclude that I = 1 for the 1630 MeV peak. To determine the spin, the scattering angular distribution for $\pi^-\pi^0$ events in the peak was expanded in a Legendre series. The P_4 moment shows a bump at 1630 MeV and the P_6 moment shows an interference

oscillation at the same mass. From this Crennell et al. argue that although $J^P = 1^-$ cannot be definitely excluded, $J^P = 3^-$ is the most likely assignment. No evidence for decay into any other final state was observed. As discussed earlier, Fig. 11 suggests that the $\pi^+\pi^-$ (g) enhancement extending from about 1560 to 1800 MeV differs significantly from the (g_1) peak in the $\pi^-\pi^0$ system. Since the possibility of an I = 2 enhancement has been excluded, Crennell et al. tentatively ascribe the differences in mass and width to the existence of an unresolved I = 0 $\pi^+\pi^-$ state near 1750 MeV. We note that although considerably broader, the g_1 enhancement corresponds closely in position with the R_1 peak observed in the MM spectrometer; in particular, the $J^P = 3^-$ assignment is eminently consistent with the linear plot of Focacci et al. shown in Fig. 9.

The properties of possible higher-mass $\pi\pi$ enhancements remain to be clarified in future experiments.

4.3 The $A_1(1080)$ and $A_2(1310)$ enhancements

The existence of a broad 3π enhancement from 1.0 to 1.4 GeV, associated with the $\pi^+\rho^0$ combinations, has already been discussed. Efforts to clarify the detailed character of the structure in the A enhancement have provided a basis for interesting controversy during the past few years, but there is now hope that a consistent interpretation of the data can be achieved in the near future.

Shortly after the discovery of this enhancement, several groups[16] were able to demonstrate that it consisted of at least two peaks; a large well-defined peak occurred at 1310 MeV and a smaller peak appeared near 1080 MeV, somewhat erratic in intensity and clarity. In addition, Chung et al.[34] observed a strong $K\bar{K}$ enhancement near 1310 MeV; with the assumption that the $\pi\rho$ and $K\bar{K}$ peaks represented alternative decay modes of the $A_2(1310)$, the assignment $I^GJ^P = 1^-2^+$ was deduced. However, in some analyses of the $\pi^+\rho^0$ systems alone, the assignment $J^P = 1^+$ or 2^- has been favoured. Consequently, it was desirable that assignments for the $\pi\rho$ and $K\bar{K}$ peaks be deduced separately.

In the analysis of the 3π systems a crucial uncertainty occurs in the subtraction of the background which is usually present. In Fig. 20, Zemach[35] shows the zeros which must occur on the Dalitz plot for given IJ^P assignments. The essential point is the vanishing of the density on the boundary for systems with $P = (-1)^J$; for systems with $P = (-1)^{J+1}$ the density need vanish only at isolated points on the boundary. These conclusions are more generally valid for meson decay into any three pseudoscalar particles. It is apparent that since the parity of the 3π system must be deduced from the density on the Dalitz plot near the boundaries, a precise estimate of background is crucial; for systems with $P = (-1)^J$, a small residual background of collinear events (i.e. those at the boundary of the Dalitz plot) can lead erroneously to the opposite parity assignment; analogously, for systems with $P = (-1)^{J+1}$, the subtraction of too much background, which artificially depletes the population at the boundary, also results in the wrong parity assignment.

The recent data of Chung et al.[34] are shown in Fig. 21; selections in the $\pi^-\rho^0$ events have been chosen to enhance the $A_2(1310)$ peak. The $K\bar{K}$ and $\pi^-\rho^0$ peaks correspond closely in mass, width, and momentum-transfer. In the decay angular distributions for the charged $K\bar{K}$ system, a strong $\cos^2\vartheta$ component appears, so that the lowest consistent assignment is $I^GJ^P = 1^-2^+$. In fitting the $\pi^-\rho^0$ decay distributions to theoretical predictions for possible J^P assignments, backgrounds were calculated using 3π phase space with varying admixtures of

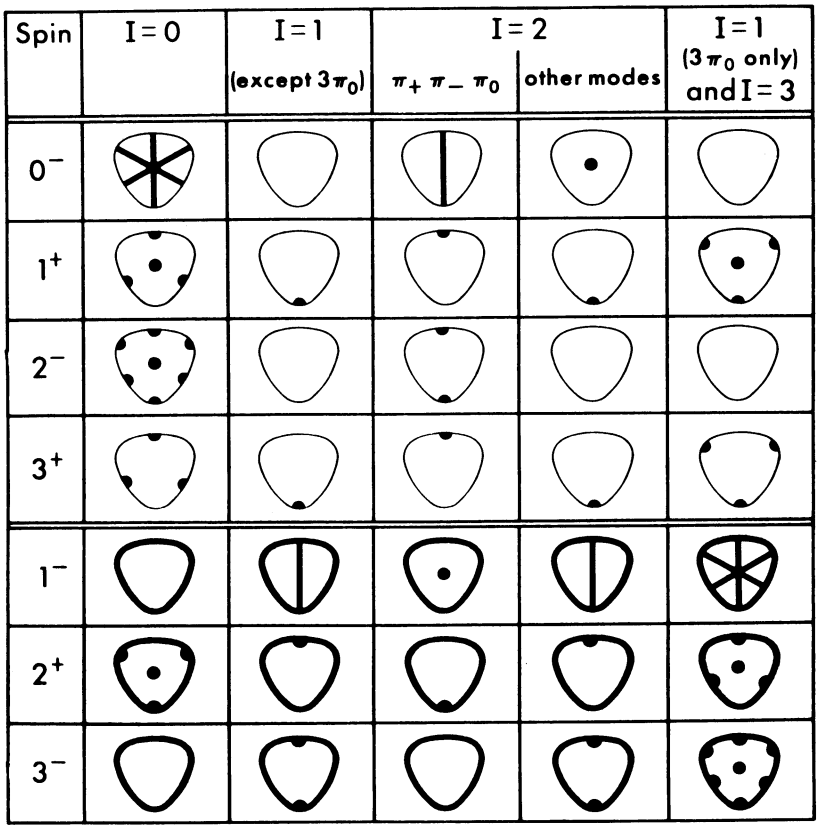

Figure 20 - Schematic representation of Dalitz plots for 3π decays by Zemach [Ref. 35)]. The density must vanish in the dark regions due to parity conservation and Bose statistics. Note in particular that the density around the perimeter (collinear events) must vanish for the sequence $J^P = 1^-, 2^+, 3^-$, etc.

$J^P = 1^+$ $\pi\rho^0$ systems. For the background level suggested by the data, 40 to 60%, only the $J^P = 2^+$ assignment provides an acceptable fit. With somewhat weaker statistics, Benson et al.[36] reached a similar conclusion.

With analogous data obtained in π^+p interactions at 8 GeV/c, the ABC Collaboration[24] favour the $J^P = 2^+$ assignment only when a 3π phase-space background larger than 50% is used. With an approximate $J^P = 1^+$ $\pi\rho^0$ background (with no phase-space contribution) only the $J^P = 2^-$ and 1^+ assignments appear acceptable. However, the ABC Collaboration also observe a peak near 1300 MeV in the reaction

$$\pi^+ + p \rightarrow \pi^+ + \pi^- + \pi^0 + N^{*++}(1238)\,. \qquad (19)$$

In this case the $J^P = 2^+$ hypothesis with suitable background provides an excellent fit to the data. Morrison[24] emphasizes that the 1310 MeV peak observed in the $\pi^+\rho^0$ final state at 8 GeV/c may not be the $J^P = 2^+$ system observed at lower momenta since cross-sections for exchange processes are decreasing while those for diffraction production are increasing. It is apparent that this interesting possibility can be tested only when background processes have been successfully investigated over a wide range of momenta.

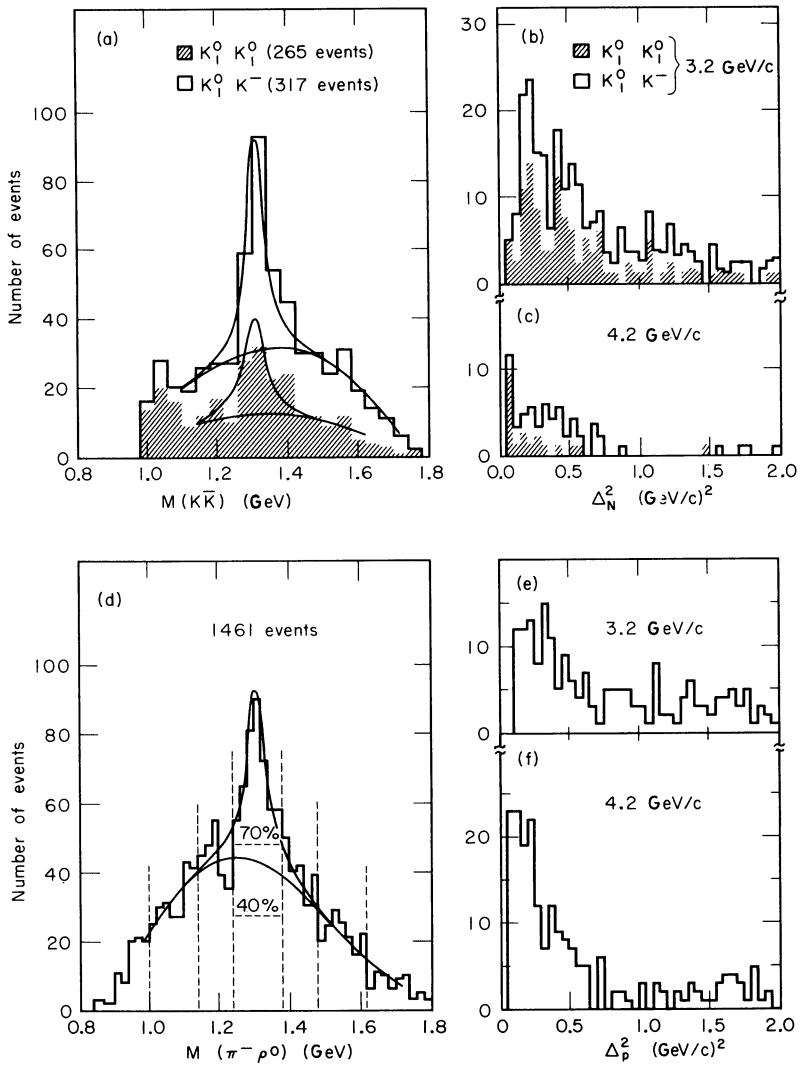

Figure 21 - Data of Chung et al. [Ref. 34)] showing similarity in mass, width, and Δ^2 distribution for $\bar{K}K$ and $\pi\rho$ peaks near 1300 MeV.

We have now described the properties of the upper half of the A enhancement; the lower half of the enhancement is usually interpreted as an independent resonance (sometime clearly resolved and sometimes not[16]) called the $A_1(1080)$. First, we must emphasize some aspects of the mass spectrum in the $A_1(1080)$ region:

a) In general, the enhancement appears somewhat larger in $\pi^+\rho^0$ systems from π^+p interactions than in the $\pi^-\rho^0$ systems from π^-p interactions. The $A_2^{\pm}(1310)$ are produced with comparable strengths.

b) Although the $A_2^-(1310)$ peak is observed clearly in the MM spectrometer, there is no evidence for an $A_1^-(1080)$ peak.

c) The $A_2^0(1310)$ has been observed in a variety of experiments; little evidence for the $A_1^0(1080)$ has been reported.

d) In the coherent production of $\pi^-\pi^-\pi^+$ states by 16 GeV/c π^-'s on complex nuclei, the Orsay-Milan-Saclay-Berkeley Collaboration[37] find that almost all events contain at least one $\pi^+\pi^-$ combination in the ρ^0 interval; in addition, the $\pi^-\rho^0$ mass spectrum peaks near the $A_1^-(1080)$. No production of $A_2^-(1310)$ is observed.

Are these observations consistent with the assumption that the $A_1(1080)$ is a valid resonance? We note first that the more diffuse $A_1^-(1080)$ enhancement observed in the π^-p interactions could be obscured in the MM-spectrometer experiment because of uncertainties in background subtraction, so that (a) and (b) need not be incompatible without more extensive data. On the other hand (c) implies that although $A_2(1310)$ production appears consistent in all respects with ρ exchange, the $A_1(1080)$ is produced only by exchange of I = 0 systems. Perhaps the clue is contained in (d); if the dominant mechanism for $A_1(1080)$ production can lead to coherent production on complex nuclei, ρ exchange will be suppressed. For coherent production (limit of extreme forward direction) the only vector quantity is the beam momentum; taking into account the negative intrinsic parity of the incident pion, the allowed sequence for coherently produced meson systems is then 1^+, 2^-, 3^+, etc. In addition, for $J^P = 1^+$, the normal to the 3π decay plane should exhibit a $\sin^2\vartheta$ distribution with respect to the beam direction. In their 16 GeV/c π^- data, the Orsay-Milan-Saclay-Berkeley Collaboration obtain an excellent fit to the $J^P = 1^+$ hypothesis, although $J^P = 2^-$ cannot be unambiguously excluded; in addition, the expected $\sin^2\vartheta$ correlation is observed.

Deck has emphasized[38] that the resonance interpretation cannot be accepted without detailed investigation; the problem is to distinguish between diagrams (a) and (b) in Fig. 22. Since the scattering at the lower vertex in (b) is highly diffractive at large c.m. πp energies, this diagram results in a low mass $\pi\rho$ enhancement. If this diagram accounts for the $A_1(1080)$ enhancement we obtain two predictions: (i) the ρ^0 decay angular distribution with respect to the beam direction will be similar to that observed in reaction (13b); (ii) the angular distribution at the lower vertex should be similar to that for real πp scattering at the corresponding c.m. energy. The predictions have been neatly verified by Shen et al.[39] and Chung[40] for $\pi^\pm p$ interactions below 4.2 GeV/c. However, some uncertainty arises because of the complexity of the analysis; this is apparent from Fig. 23 which shows Chung's data at 3.2 and 4.2 GeV/c. In (a) we observe three horizontal bands corresponding to copious production of $N^*(1238)$, $N^*(1512)$, and $N^*(1688)$; in addition, two vertical bands corresponding to $A_1(1080)$ and $A_2(1310)$ are apparent. The mass projections in the A_1 and A_2 bands show the strong production of nucleon isobars. However, (d) shows an important difference between the $A_2(1310)$ and the $A_1(1080)$ enhancements; the latter is confined almost completely to $\Delta^2_{p\pi^-} < (0.55\ \text{GeV/c})^2$, consistent with the mechanism suggested by Deck. In fact, the $A_1(1080)$ enhancement may be almost completely separated from the $A_2(1310)$

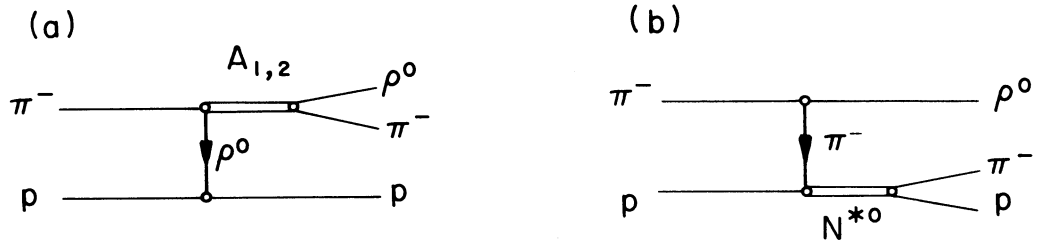

Figure 22 - (a) Resonance production through ρ exchange. (b) ρ^0 production through π exchange. Since the lower vertex involves low momentum-transfers at high c.m. energies for the final π^-p system, Deck [Ref. 38)] has emphasized that this diagram results in a kinematically induced low mass enhancement.

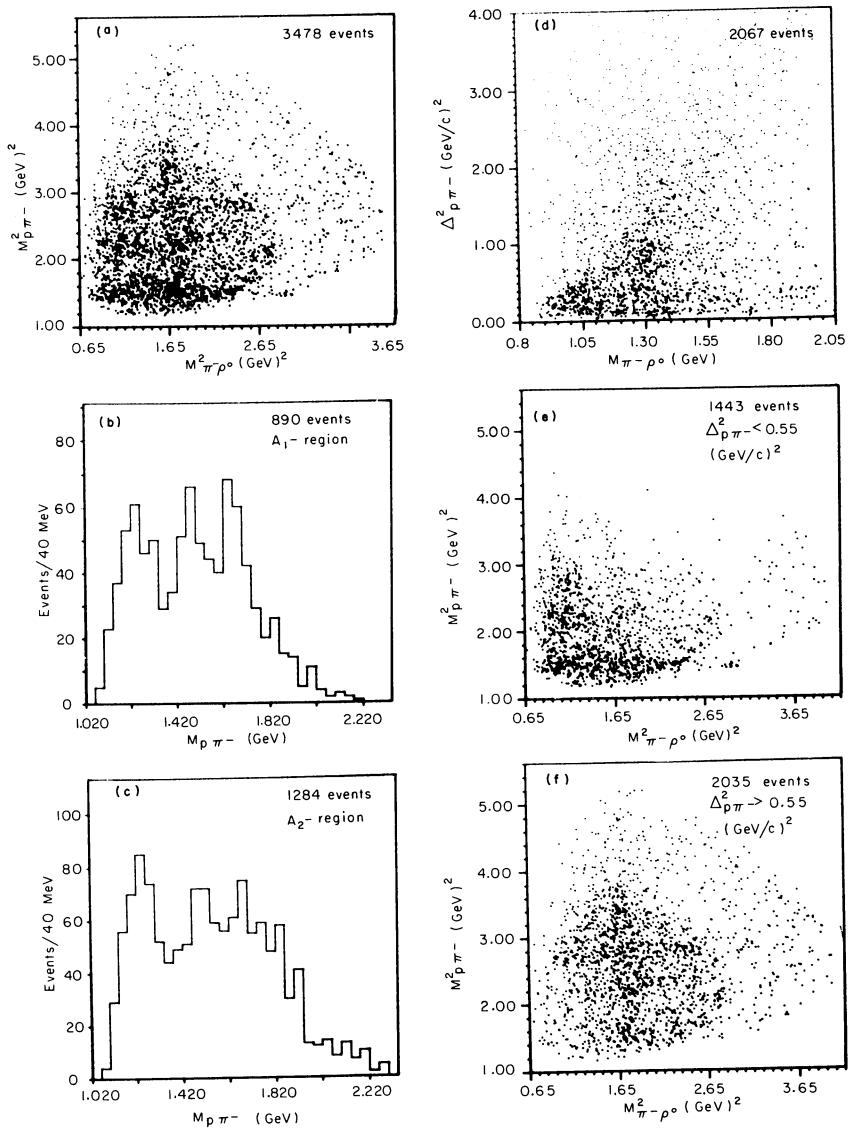

Figure 23 - Data of Chung [Ref. 40)] on A_1 and A_2 enhancements. See text for discussion.

peak by the simple selection applied in (e) and (f). We must conclude that the Deck mechanism contributes significantly in the region of the $A_1(1080)$ enhancement. Since the virtual scattering at the lower vertex in Fig. 22b is highly diffractive at high final state πp c.m. energies, it may be expected that the $A_1(1080)$ enhancement will be confined to events with very low Δ^2_p. This is precisely what is observed; when events are selected with $\Delta^2_p > 0.3$ (GeV/c)^2 no significant enhancement is observed in the region of $A_1(1080)$. This accounts then, for the absence of the $A_1(1080)$ in the MM-spectrometer experiment where only the Δ^2_p interval 0.31 to 0.39 (GeV/c)^2 was studied in this mass region. The Deck mechanism can also partially account for the absence of any $A_1^0(1080)$ effect since a virtual charge-exchange scattering is required at the nucleon vertex in Fig. 22b.

Despite the circumstantial evidence that the $A_1(1080)$ may result from the Deck mechanism, the clear possibility remains that there is a genuine resonance in this region superimposed on a substantial "Deck" background. This situation is especially suggested by the analyses of data

above 5 GeV/c, where explicit calculations of the "Deck effect" cannot reproduce the sharpness of the peak in the A_1 (1080) region[16]. Unfortunately, the production and decay correlations for a kinematically induced peak in the A_1 (1080) region are similar to those expected for a resonance with $J^P = 1^+$ produced in a diffractive process; consequently, the inability of the Deck mechanism to reproduce the sharpness of the observed peak constitutes the major argument for the existence of an independent resonance. Clearly, the observation of A_1 (1080) in other reactions would quickly settle the issue; we return to this possibility in our discussion of multipion systems produced in $\bar{p}p$ annihilations.

4.4 The B(1220) meson

In studies of the reactions

$$\pi^+ + p \rightarrow \pi^+ + \omega + p \qquad (20)$$

above 3 GeV/c, an enhancement near 1220 MeV with full-width 120 MeV is observed in the mass spectrum of the $\pi\omega$ combinations; this is referred to as the B meson. However, after our discussion of the A_1 (1080) enhancement it is apparent that we must distinguish between the two possibilities indicated in Fig. 24: does the B enhancement represent the production of a meson system through the exchange diagram in (a), or does it merely reflect the strong forward peaking expected at the lower vertex in (b). To investigate the latter possibility Chung et al.[40,41] selected events with $\Delta^2_{p\pi^-} < 1.0$ (GeV/c)^2; these are shown in Fig. 25. Although the B enhancement is particularly strong in these events, the $M(\pi^- p)$ distribution shows that N^*'s are also produced copiously. Using these events it is then possible to determine the dependence of the B enhancement on the angular distribution of the $\pi^- p$ system in its c.m. They find that essentially the entire B enhancement is confined to the angular interval $\cos\vartheta > 0.6$; since forward peaking is not unlikely for $\pi^- p$ systems produced through the diagram in Fig. 24b, Chung et al. concluded that the properties of the B enhancement, as observed in their data, could not be unambiguously distinguished from those expected for a kinematic reflection of N^* production through ρ exchange.

However, if the B enhancement is a genuine resonant state, it should be observed in other reactions. Recently, Baltay et al.[42] investigated the reaction

$$\bar{p} + p \rightarrow \omega + \pi^+ + \pi^- \rightarrow 2\pi^+ + 2\pi^- + \pi^0 \qquad (21)$$

for $\bar{p}$'s absorbed at rest. The strong ω peak in these events is shown in Fig. 26; when the $\pi^\pm\omega$ combinations are plotted, the distributions in Fig. 26a and b are obtained. A well-defined peak is observed at 1200 MeV with full-width 100 MeV; the relative significance of the peak is increased in Fig. 26b where only those events in the central region of the ω Dalitz plot are used.

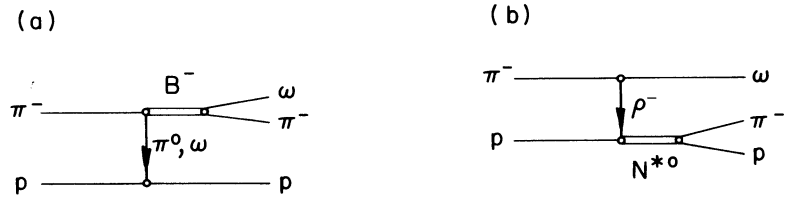

Figure 24 - (a) Diagram for B meson production through π or ω exchange; (b) ω production through ρ exchange which may lead to a low mass $\pi\omega$ enhancement at high incident π^- momentum.

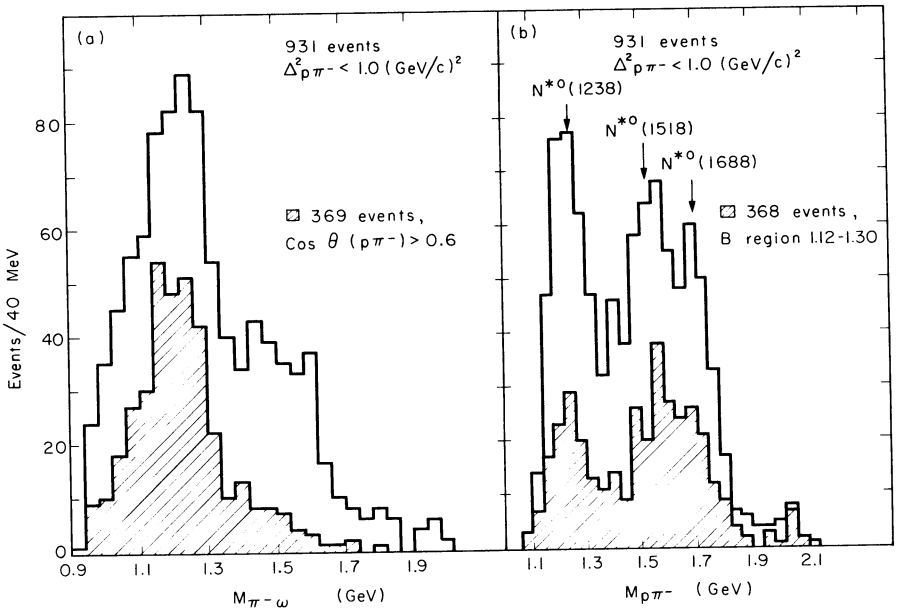

Figure 25 - Data of Chung et al. [Ref. 41)] showing simultaneous production of B meson with nucleon isobars.

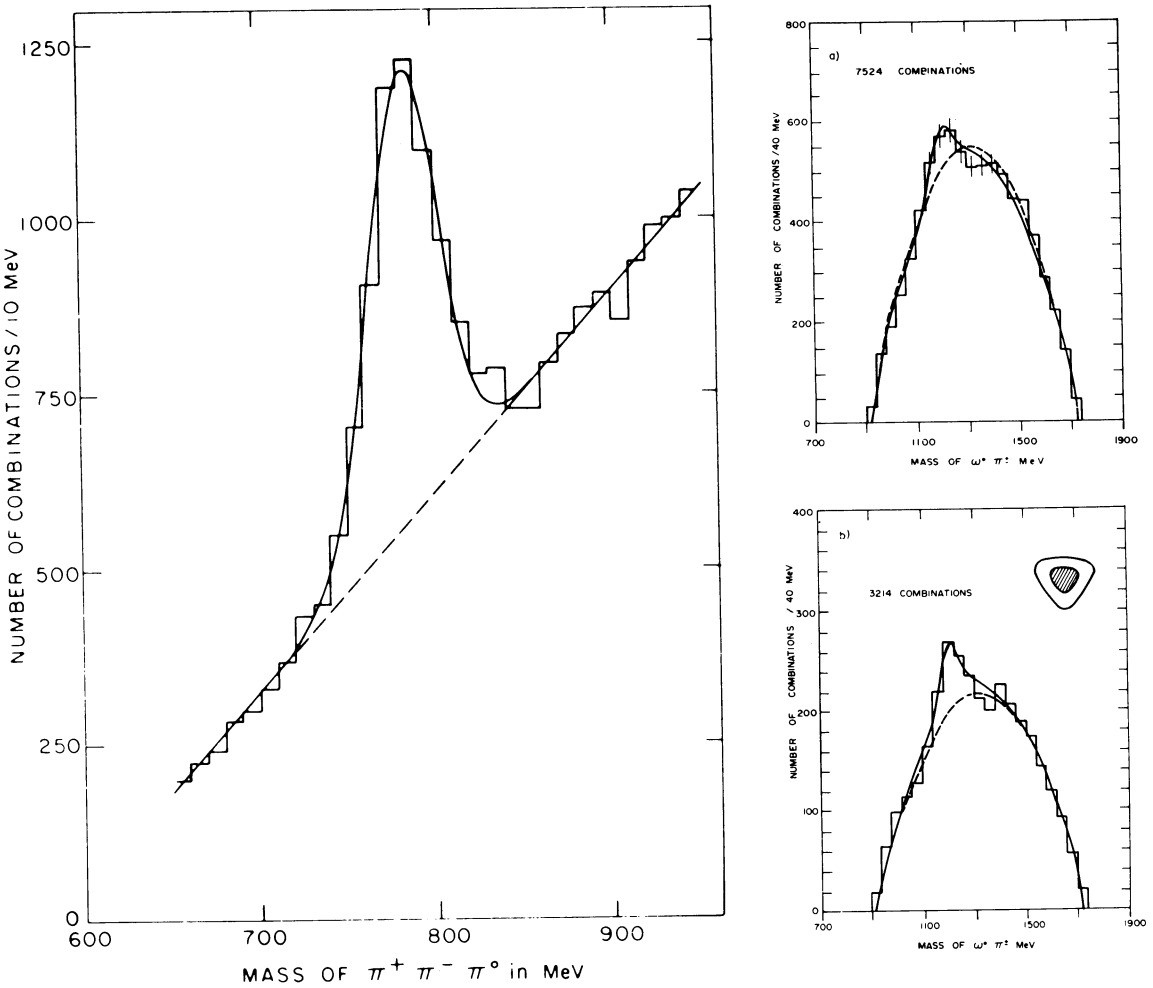

Figure 26 - Data of Baltay et al. [Ref. 42)]; (left) ω peak observed in $\bar{p}p$ annihilations; (right) evidence for B meson in $\pi^\pm\omega$ combinations; in (b) only events in the central region of the ω Dalitz plot are used.

No peak is observed for events <u>not</u> having a $\pi^+\pi^-\pi^0$ combination in the ω interval. It is unlikely that a completely independent kinematic effect would generate a peak with mass and width similar to that observed in reaction (20); consequently, Baltay et al. conclude that the B enhancement represents an independent meson state.

Although the simultaneous production of N^*'s with the B meson precludes any rigorous conclusion, it is of interest to ask what J^P assignment is suggested by the data of Chung et al. Almost the entire B enhancement is preserved with the selection $\Delta_p^2 < 0.35$ $(GeV/c)^2$, as shown in Fig. 27a. The angular distribution between the decay pion momentum ($\underset{\sim}{p}$) and the normal ($\underset{\sim}{n}$) to the ω-decay plane is shown in Fig. 27b. A comparison with the control region suggests a $\sin^2\vartheta$ distribution for B events; the simplest decay matrix element would then be $M_D \propto \underset{\sim}{n} \times \underset{\sim}{p}$, implying the assignment $I^G J^P = 1^+1^-$. In this case the B meson has the same quantum numbers as the ρ meson; the absence of any $\pi\pi$ decay would then be remarkable. It is likely, however, that decay correlations are severely distorted by the simultaneous N^* production, and a valid J^P analysis must await the discovery of a clean source of B mesons.

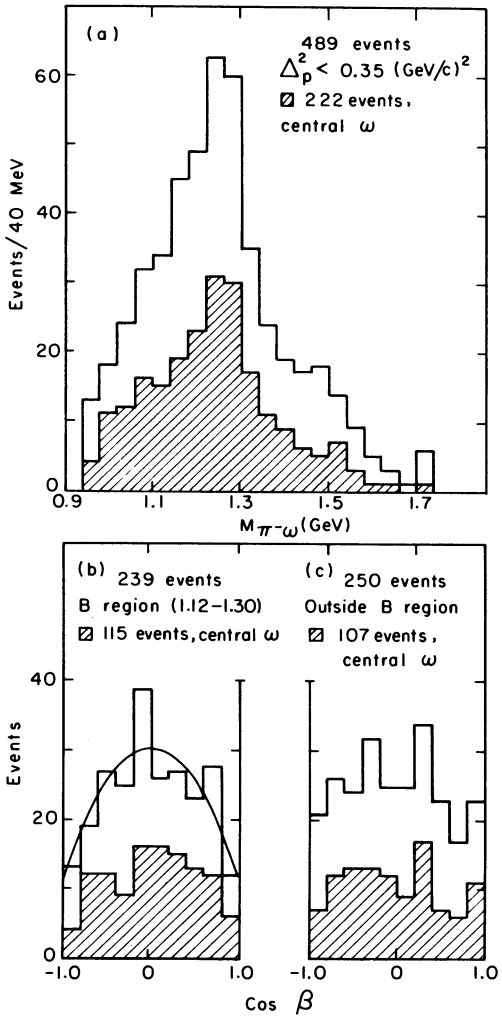

Figure 27 - Data of Chung [Ref. 40)] in which the B meson is analysed as a valid resonance; (a) essentially the entire B meson peak is retained with the selection $\Delta_p^2 < 0.35$ $(GeV/c)^2$; (b) angular correlation between B decay pion and normal to ω decay plane; (c) same correlation for control region.

4.5 Multipion systems in $\bar{p}p$ annihilations

Since the early discovery of the $\omega(784)$ in reaction (21) by Maglić et al.[43] it has been apparent that the $\bar{p}p$ annihilation process provides a rich source of multipion final states for the study of meson systems. In addition, we have just discussed the use of these systems to demonstrate the validity of the B meson when its properties were obscured by simultaneous N^* production in πp interactions. We now ask what other systems decaying into pions have been suggested by studies of the $\bar{p}p$ annihilation process.

The most useful final states are obtained from the copiously produced four- and six-pronged events

$$\bar{p} + p \rightarrow 2\pi^+ + 2\pi^- + (n\,\pi^0) \qquad (22)$$

and

$$\bar{p} + p \rightarrow 3\pi^+ + 3\pi^- + (n\,\pi^0)\ . \qquad (23)$$

For stopped $\bar{p}$'s it has been possible to investigate the production and decay of the η, ω, f_0, and $A_2(1310)$ mesons.

With higher c.m. energies it has been possible to explore the regions of the S, T, and U peaks observed in the MM-spectrometer studies. In their analysis of five-pion annihilations at 5.7 GeV/c, Alles-Borelli et al.[44] report an enhancement in the $\pi^+\pi^-\pi^0$ mass distribution at 2207 ± 13 MeV with Γ = 62 ± 52 MeV which could correspond to the neutral state of the T-peak in Fig. 7. In six-pion final states at 2.5, 3.0, and 3.6 GeV/c Danysz et al.[45,46] observed peaks in the $2\pi^+2\pi^-$ combinations near 1710 MeV with Γ = 40 ± 12 MeV and near 1834 MeV with Γ = 42 ± 11 MeV. In each case the peaks persist when either a single or double ρ^0 selection is imposed; the authors emphasize, however, that this does not establish the decays $\pi^+\pi^-\rho^0$ or $\rho^0\rho^0$ because of the high background of $\pi^+\pi^-$ combinations having a mass in the ρ^0 region.

In the seven-pion annihilations at 3.0 and 3.6 GeV/c Danysz et al.[46] selected events with a $\pi^+\pi^-\pi^0$ combination in the ω region and a $\pi^+\pi^-$ combination in the ρ^0 region. The $\omega\rho^0$ mass spectrum shows peaks at 1689 ± 10 MeV with Γ = 38 ± 18 MeV and at 1848 ± 11 MeV with Γ = 67 ± 27 MeV. Again, because of the large background under the ρ^0 peak it is not possible whether the decay is predominantly $\omega\rho^0$ or $\omega\pi^+\pi^-$. The $\pi^+\rho^0$ mass spectrum for these <u>same</u> events is shown in Fig. 28; deviations from phase space are observed in the regions of the $A_1(1080)$ and $A_2(1310)$ systems. Fitting the distributions with Breit-Wigner resonances and phase space backgrounds yields the masses and widths

$$A_1: \quad 1054 \pm 7 \text{ MeV} \quad \text{with} \quad \Gamma = 33 \pm 19 \text{ MeV}$$

$$A_2: \quad 1269 \pm 9 \text{ MeV} \quad \text{with} \quad \Gamma = 45 \pm 22 \text{ MeV}\ .$$

Although the masses and widths appear somewhat small for identification with the $A_1(1080)$ and $A_2(1310)$, they may converge with further data.

Unfortunately, all the peaks discussed in this section represent effects of 2.5 to at most 4.0 standard deviations, consequently, even though highly suggestive they cannot yet be accepted as established effects. However, it is apparent that should the existence of these peaks be verified in further studies of $\bar{p}p$ annihilations, the existence of an A_1 meson may soon be unambiguously established.

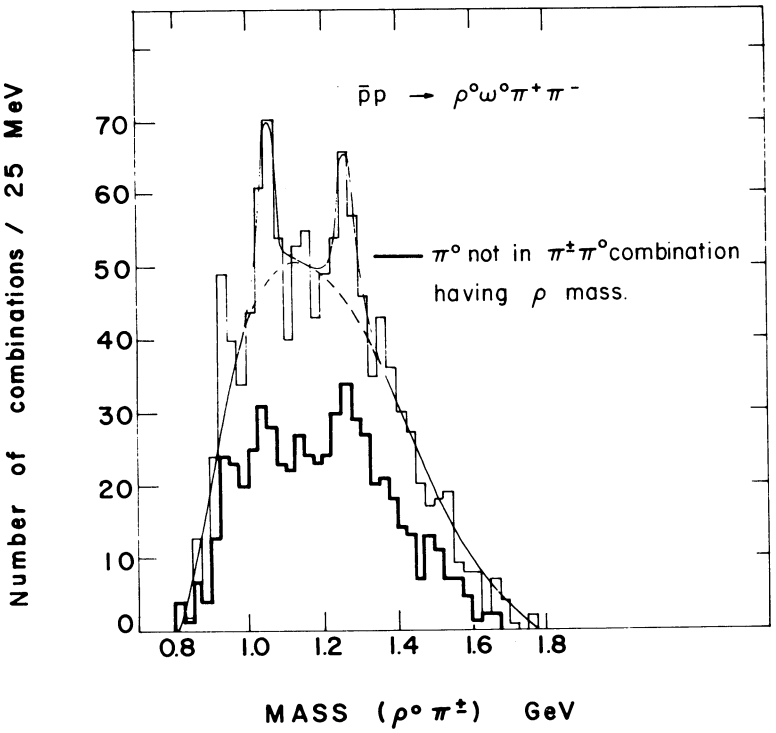

Figure 28 - Data of Danysz et al. [Ref. 46)] showing suggestive evidence for A_1 and A_2 peaks in $\bar{p}p$ annihilations at 3.0 and 3.6 GeV/c.

4.6 Systems involving $K\bar{K}$ pairs

Thus far we have examined only the properties of multipion systems in our review of the non-strange meson resonances. However, this does not exhaust the possibilities; for example, we have already mentioned the $K\bar{K}$ spectrum obtained by Chung et al. and used in their analysis of $A_2(1310)$. To pursue further the relation between the BC experiments and the MM-spectrometer results we shall now discuss in more detail what has been learned from the investigation of systems involving $K\bar{K}$ pairs.

In Fig. 29 we show two $M(K^{\pm}K_1)$ spectra obtained in the reactions[16)]

$$\pi^{\pm} + p \rightarrow K_1 + K^{\pm} + p \ . \qquad (24)$$

We note first that possible assignments for these systems are $I^GJ^P = 1^-0^+$, 1^+1^-, 1^-2^+ etc. In each case the $A_2(1310)$ peak is clearly visible; the apparent difference in widths may represent a difference in statistics and resolution. The observed $\Delta^2_{K^{\pm}K_1}$ distributions (not shown) demonstrate that most of the $K^{\pm}K_1$ pairs are produced peripherally. In this case the 1^-0^+ systems would most reasonably result from η exchange and the 1^+1^- system from π or ω exchange. We may conclude that there exists no low-mass I = 1 system strongly coupled to both the $\pi\pi$ and $K\bar{K}$ channels; in addition, should any 1^-0^+ state exist, it will not be produced copiously in πp interactions.

For contrast, we show in Fig. 30 a comparison of K_1K_1 mass spectra[16)] obtained in the reaction

$$\pi^- + p \rightarrow K_1 + K_1 + n. \qquad (25)$$

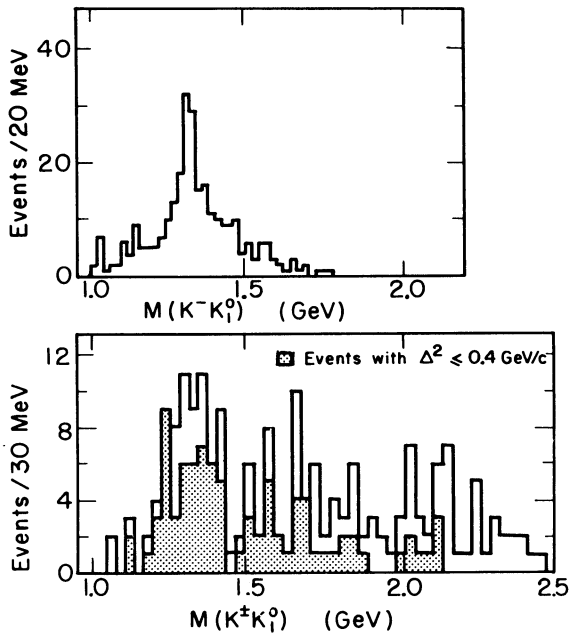

Figure 29 - $M(K^{\pm}K_1)$ distributions observed in $\pi^{\pm}p$ interactions [Ref. 16)]

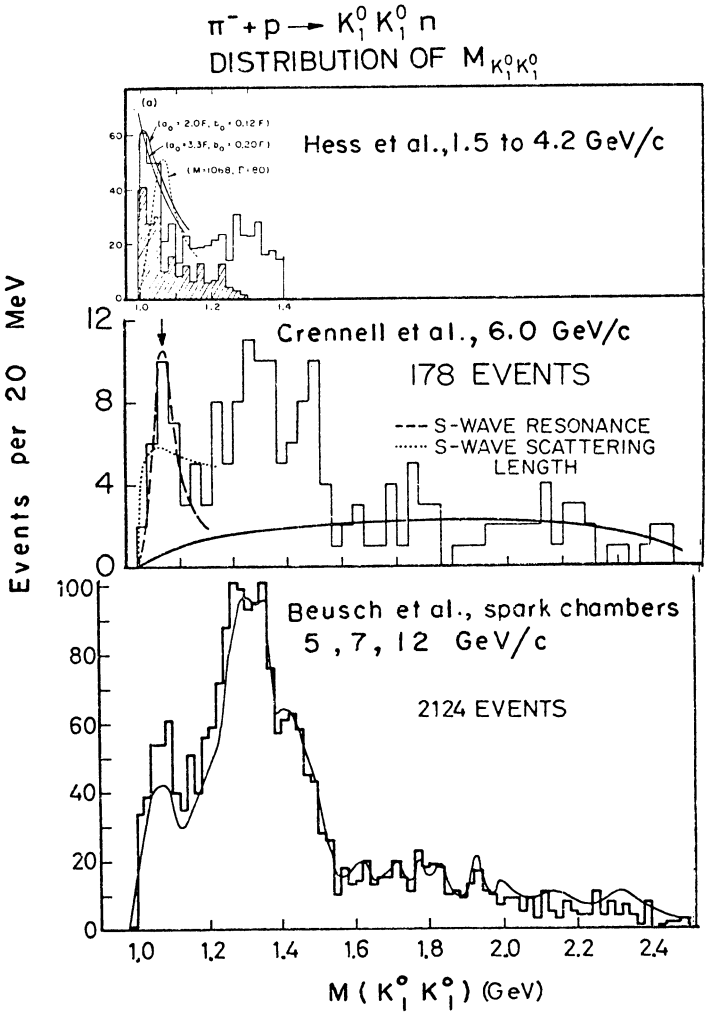

Figure 30 - $M(K_1K_1)$ distributions observed in $\pi^{-}p$ interactions [Ref. 16)].

Again, strong enhancements in the region of the $A_2(1310)$ are observed. However, in this case all spectra show a strong peak at low K_1K_1 mass; in addition, the low mass events are highly peripheral. Extending the arguments above, possible assignments are $I^GJ^P = 0^+0^+$, 0^+2^+, 1^-2^+, etc. Since the angular distributions in the K_1K_1 rest frame are isotropic for events with $M(K_1K_1) < 1.15$ GeV, the 0^+0^+ assignment is preferred. However, the detailed spectra differ in one important respect. In the data corresponding to pion momenta below 5 GeV/c the K_1K_1 mass spectrum peaks at threshold; this has been interpreted as evidence for a strong I = 0 s-wave interaction with scattering length $A_0 = \pm$ (2 to 6) + i (0.7 to 3.0) fermi. For pion momenta above 6 GeV/c the K_1K_1 mass spectrum appears to peak near 1070 MeV with Γ = 80 MeV; this suggests the existence of an I = 0 s-wave resonance. Since either effect should be produced through pion-exchange it is difficult to understand the difference in the spectra. Perhaps the difference will vanish with improvements in statistics and mass resolution in these final states.

A study of $K\bar{K}$ systems produced in $\bar{p}p$ annihilations eliminates the constraints imposed by peripheral production in πp interactions. The most extensive investigations are for stopping $\bar{p}$'s. We note first that the reaction

$$\bar{p} + p \rightarrow K_1 + K_1 \tag{26}$$

is allowed only for initial states with C = +1 and $P = (-1)^J$. For the $^1S_0$ $p\bar{p}$ system, C = +1 but $J^P = 0^-$; for the $^3S_1$ system C = -1. Consequently, if capture occurs from S-orbitals, reaction (26) cannot occur. The observed upper limit[47] for the K_1K_1/K_1K_2 ratio is less than $1/333$, setting an upper limit of 10% (with 90% confidence level) for capture from other than S-orbitals. The simplicity of the initial states places strong restrictions on the properties of the final states; these may be used effectively in the analysis of the data.

As an example we may consider the properties of the final states

$$\bar{p} + p \rightarrow K^{\pm} + K_1 + \pi^{\mp} \tag{27}$$

and

$$\bar{p} + p \rightarrow K_1 + K_1 + \pi^0 \tag{28}$$

which have been studied in detail by Conforto et al.[48]. The Dalitz plot for reaction (27) is shown in Fig. 31. The structure in the plot is a challenge to the experimenter since it appears that a complete quantitative fit should be possible. The well-defined $K^*(890)$ bands dominate the plot. However, two diagonal $K^{\pm}K_1$ enhancements can be easily identified. The first occurs along the line corresponding to $M(K^{\pm}K_1) \simeq 1280$ MeV; the second represents a concentration of events at low $K^{\pm}K_1$ mass along the boundary of the plot. The $M(K^{\pm}K_1)$ projection for events in the triangular region between the $K^*(890)$ bands is shown in Fig. 32a. To fit the plot Conforto et al. first assumed a coherent superposition of two body effects:

a) I = 1/2 and I = 3/2 s-wave $K\pi$ interactions in the zero-effective range approximation.

b) $K^*(890)$ production.

c) a resonant I = 1 $\bar{K}K$ interaction at 1280 MeV with Γ = 90 MeV and possible $J^P = 0^+$, 1^-, or 2^+. The choice $J^P = 2^+$ gave the best fit, suggesting that although somewhat low in mass, the enhancement most likely corresponds to $A_2(1310)$ production.

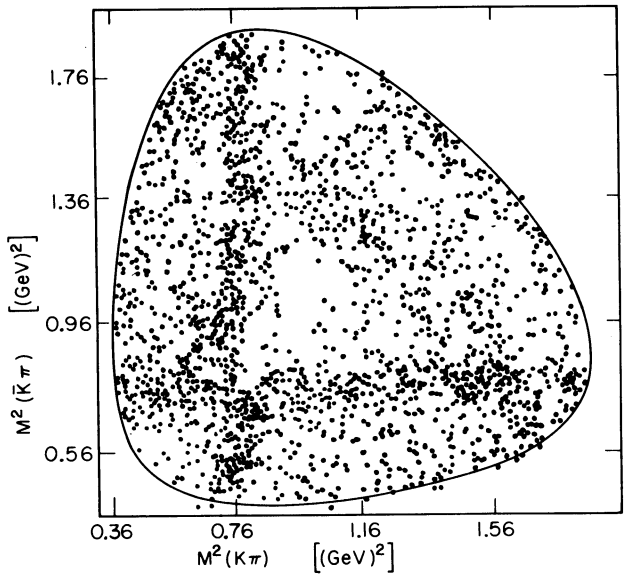

Figure 31 - Dalitz plot for $\bar{p}p \to K^{\pm}K_1\pi^{\mp}$ at rest. The analysis by Conforto et al. [Ref. 48)] is discussed in the text.

These three effects were sufficient to give an excellent fit everywhere except in the region of low $K^{\pm}K_1$ masses. The angular distribution is isotropic in this region, so that it is natural to include a threshold interaction in the $I^GJ^P = 1^-0^+$ state. Two possibilities were considered:

i) a strong s-wave interaction in the zero-effective-range approximation. In this case the mass distribution was adequately fitted with a scattering length of + 2.5 ± 1.0 fermi. The rapid variation in density near the boundary results from a strong destructive interference with the I = ½ s-wave $K\pi$ amplitude.

ii) a resonant s-wave interaction. Good fits are obtained with a Breit-Wigner resonance centred at 960 to 1020 MeV with Γ = 50 to 90 MeV. In this case the alternative decay $\pi\eta$ is allowed; observation of an enhancement in this system would confirm the resonance hypothesis.

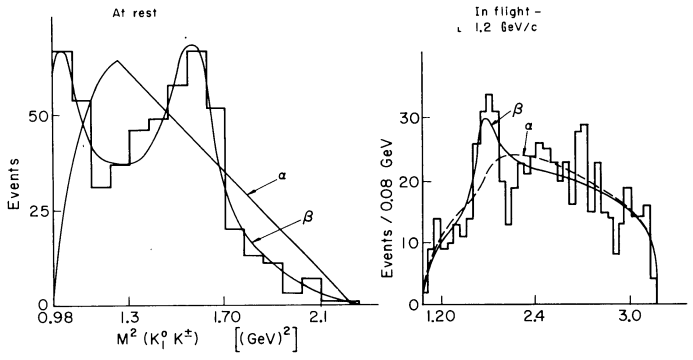

Figure 32 - (Left) the $M^2(K_1K^{\pm})$ distribution for events inside the $K^*(890)$ bands in Fig. 31; peaks are observed corresponding to a threshold enhancement and the $A_2(1310)$. (Right) the $M^2(K_1K^{\pm})$ distribution for the same final state at 1.2 GeV/c; the threshold enhancement is not produced [Ref.16)].

Reaction (28) has also been studied by Conforto et al.[48]. The $M(K_1K_1)$ projection for events between the $K^*(890)$ bands is shown in Fig. 33. In this case the relative size of the threshold enhancement is smaller; however, this may result from destructive interference with the strong $I^GJ^P = 0^+0^+$ threshold interaction discussed earlier.

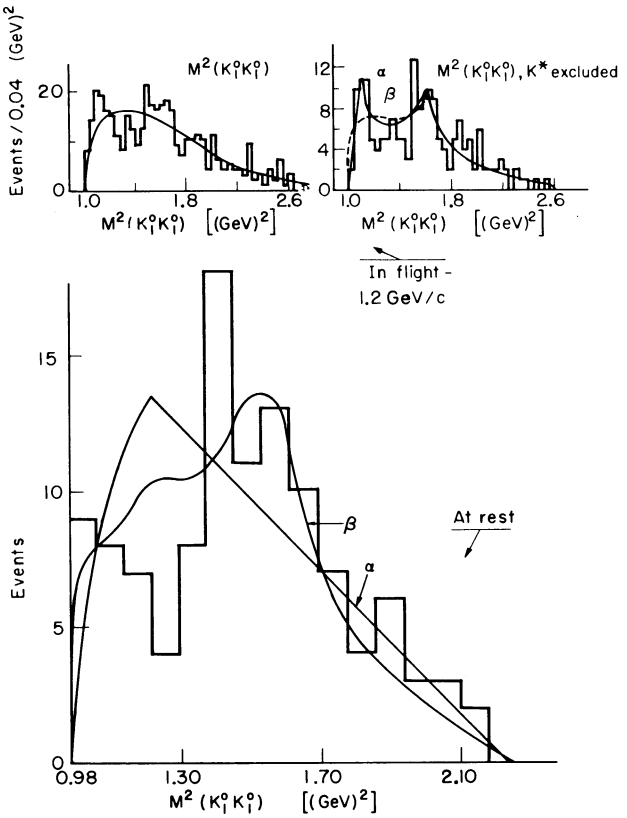

Figure 33 - (Lower) $M^2(K_1K_1)$ distribution for $\bar{p}p \to K_1K_1\pi^0$ at rest; only events inside the $K^*(890)$ bands are included. (Upper) $M^2(K_1K_1)$ distributions for the $K_1K_1\pi^+\pi^-$ final state at 1.2 GeV/c [Ref. 16)].

The same reactions have also been investigated at 1.2 GeV/c by Barlow et al.[49]. The projected $M(K^+K_1)$ distribution is shown in Fig. 32b; although production of $A_2(1310)$ persists, the low-mass enhancement is gone. The more limited data for the $K_1K_1\pi^0$ final state (not shown) are consistent with this observation. For further comparison, the $M(K_1K_1)$ spectrum for the reaction

$$\bar{p} + p \to K_1 + K_1 + \pi^+ + \pi^- \qquad (29)$$

is shown in Fig. 33. An enhancement, probably corresponding to $A_2(1310)$ appears near $(1260\ \text{MeV})^2$. In addition, a peak of comparable intensity appears near $(1045\ \text{MeV})^2$; the sharpness of the peak cannot be reproduced with an s-wave scattering length, but is consistent with a Breit-Wigner resonance centred at 1045 MeV with $\Gamma = 50$ MeV.

To summarize, we may say that a low-mass K_1K_1 enhancement is observed in most experiments; it is consistent with $I^GJ^P = 0^+0^+$. In several cases the mass spectrum peaks near 1050 to 1070 MeV

suggesting a resonance with Γ = 50 to 70 MeV; due to statistical limitations, the possibility of a large s-wave scattering length, as suggested by the low-momentum πp data, cannot be completely excluded. In addition, the stopping $\bar{p}p$ analyses indicate the existence of a strong threshold interaction in the $I^G J^P = 1^- 0^+$ state. The model used by Conforto et al.[48] leads to a positive scattering length of about 2.5 fermi. However, it is not clear that reasonable modification of the model would not permit a good fit with a negative scattering length. Should the scattering length have a negative real part larger than the range of interaction, a bound-state resonance may be expected below the $K\bar{K}$ threshold; the observation of an s-wave $\pi\eta$ peak <u>below</u> 1 GeV would strongly suggest this interpretation.

At this point it is interesting to return to the spectrum observed in the MM-spectrometer experiment. In Fig. 7 a sharp peak, referred to as the δ^-, occurs at 962 MeV. The validity of the peak has been confirmed by Oostens et al.[50] in a study of the reaction

$$p + p \rightarrow X^+ + d \qquad (30)$$

where X^+ is an unknown object produced in association with the deuteron. The recoil deuteron spectrum is shown in Fig. 34a; after subtracting background the data are plotted in terms of $M(X^+)$ in Fig. 34b. A peak appears at 966 ± 8 MeV with width equal to the experimental resolution. This is indeed a surprise, since it is remarkably similar in mass and width to the $\eta'(958)$ which has been given the assignment $I^G J^P = 0^+ 0^-$. Can it be that the $\eta'(958)$ actually represents the neutral member of a state with I = 1?

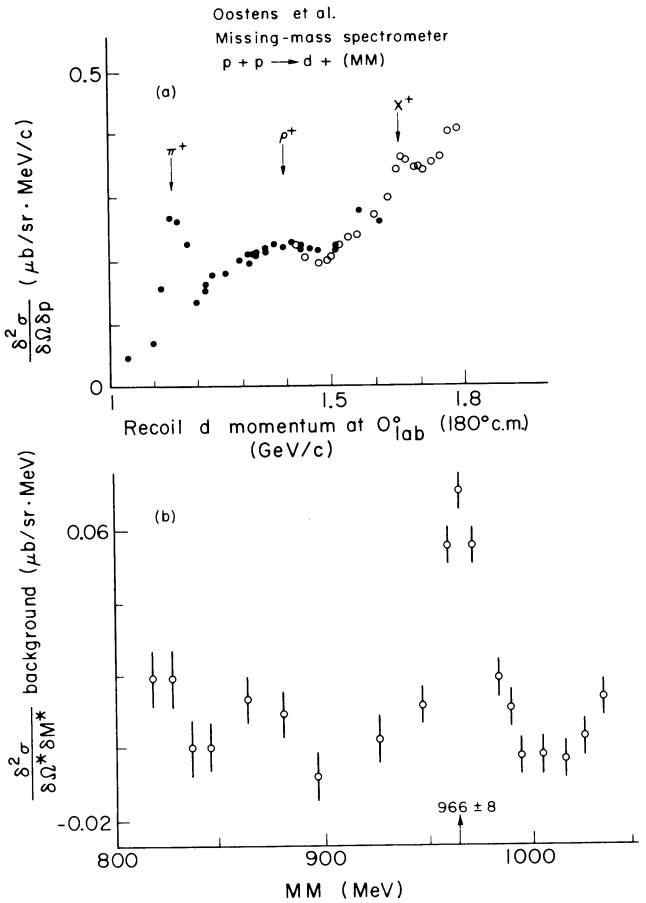

Figure 34 - Data of Oostens et al. confirming the existence of the δ [Ref. 50)]. In (b) the estimated background has been subtracted.

The $\eta'(958)$ has been studied most extensively in the reactions

$$K^- + p \rightarrow \Lambda + \pi^+ + \pi^- + MM \qquad (31a)$$

and

$$K^- + p \rightarrow \Lambda + \pi^+ + \pi^+ + \pi^- + \pi^- + MM \qquad (31b)$$

where MM is the missing mass. When the $\pi^+\pi^-$MM distribution is plotted for events in reaction (31a) with MM = $\eta(549)$ a sharp peak appears at 958 MeV with a width equal to the experimental resolution. It is useful now to establish clearly the existence of the decay $\eta' \rightarrow \pi^+\pi^-\gamma$. Using events not fitting the $\Lambda\pi^+\pi^-$ or $\Sigma^0\pi^+\pi^-$ final states, Rittenberg et al.[51] have plotted the $M^2(\pi^+\pi^-MM)$ distributions for two intervals of MM; these are shown in Fig. 35. A peak at 958 MeV is observed only for events in the "γ band"; a prominent ω peak is observed in the "π^0 band". The $M^2(\pi^+\pi^-)$ distribution for events in the $\pi^+\pi^-\gamma$ peak at 958 MeV is shown in Fig. 36a; a good fit is obtained when phase space is multiplied by a Breit-Wigner resonance corresponding to the ρ meson. The decay angular distribution in the ρ rest frame, shown in Fig. 36b, fits $\sin^2\vartheta$. The simplest possibilities correspond to the electric dipole transition $0^+ \rightarrow 1^- + \gamma$, or the magnetic dipole transition $0^- \rightarrow 1^- + \gamma$; in either case C = +1 for the final state. Rittenberg et al. consider what other decays might be expected for the two possible assignments I = 0 or I = 1.

	$J^P = 0^-$	$J^P = 0^+$
I = 0	$\pi\pi\eta$	$\pi\pi$
I = 1	$\pi\pi\pi$	$\pi\eta$

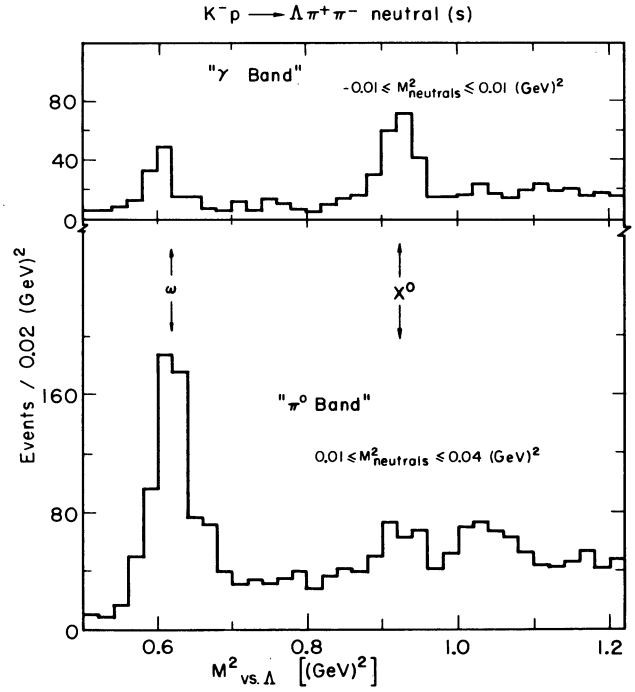

Figure 35 - Data of Rittenberg et al. [Ref. 51)] demonstrating the existence of the decay $\eta'(958) \rightarrow \pi^+\pi^-\gamma$.

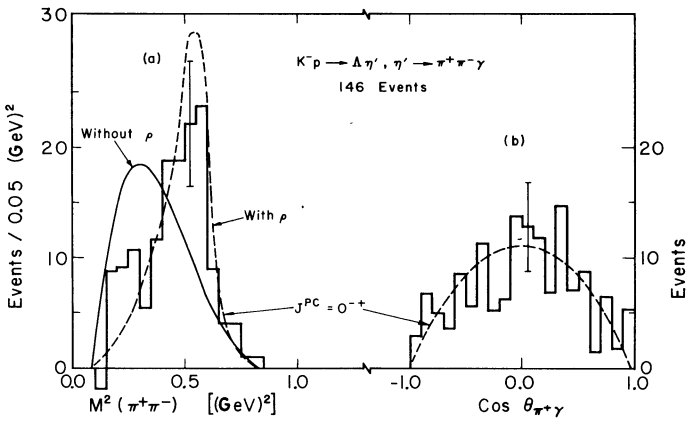

Figure 36 - Mass distribution and angular correlation for events in the $\pi^+\pi^-\gamma$ peak at 958 MeV in Fig. 35 [Ref. 51)].

Only the $\pi\pi\eta$ combinations show a peak at 958 MeV, consistent with the earlier assignment $I^GJ^P = 0^+0^-$. To study the decay correlations in the $\pi^+\pi^-\eta$ final state Rittenberg et al. use only the events from reaction (31a) with MM = $\eta(549)$; in this case there is no serious ambiguity between pions resulting from η' and η decay. The angular distribution is isotropic, again consistent with the assignment $I^GJ^P = 0^+0^-$.

In any case, there is at present no reason to suspect the assignment usually given the $\eta'(958)$; we must find some other explanation for the $\delta^\pm(962)$. A possible clue lies in the strong $K^\pm K_1$ threshold enhancement observed in the stopping $p\bar{p}$ annihilations. Conforto et al. have found that a real scattering length of about 2.5 fermi is sufficient to fit their data; however, the analysis is complicated, and it is unlikely that a complex scattering length with negative real part can be unambiguously excluded. If this is the case, then a bound-state resonance will occur below the $K\bar{K}$ threshold with the properties

$$E_r = 2\,M_K - 4\,(M_K\,a_1^2)^{-1}$$

and

$$\Gamma_r = 4\,b_1\,(M_K\,a_1^2)^{-1}$$

where $A_1 = a_1 + i\,b_1$ is the complex scattering length in the I = 1 $K\bar{K}$ system. Since the assignment would then be $I^GJ^P = 1^-0^+$ the most likely decay is $\delta^\pm \to \pi^\pm\eta$. The $\pi^\pm\eta$ combinations can be studied conveniently in the reactions

$$\pi^\pm + p \to \pi^\pm + \eta + p \qquad (32)$$

where we know that the $\delta^\pm(962)$ is produced from the original MM-spectrometer measurements. Unfortunately, the cross-section listed in Table 2 for $\delta^\pm(962)$ production is small, so that large numbers of events must be measured before the peak could be observed; such studies are now in progress and we should know the answer in the next year.

4.7 The $K\bar{K}$ enhancement near 1300 MeV

The $K\bar{K}$ peaks near 1300 MeV observed by Chung et al.[34] in π^-p interactions below 5 GeV/c appear consistent with the assumption that they represent alternative decay modes of $A_2(1310)$. A similar conclusion was reached by Conforto et al. in their analysis of the reaction $\bar{p}p \to K\bar{K}\pi$, although the mass of the observed $K\bar{K}$ peak appeared to be nearer to 1280 MeV.

For $\pi^{\pm}p$ interactions above 5 GeV/c, Figs. 29 and 30 suggest that the structure in the 1300 MeV peak may be more complex. Crennell et al.[52] invoke a C = +1 resonance near 1480 MeV which they identify with the f'(1515). Beusch et al.[53] report that their data are best fitted with C = +1 resonances at

$$E_r = 1253 \text{ MeV}; \quad \Gamma = 115 \text{ MeV} \quad \text{(identified as the } f_o\text{)}$$

$$E_r = 1325 \text{ MeV}; \quad \Gamma = 90 \text{ MeV}$$

$$E_r = 1439 \text{ MeV}; \quad \Gamma = 45 \text{ MeV} .$$

The parameters of the f_o were fixed in the fitting process; no evidence for any peak corresponding to $f_o'(1515)$ was observed.

At present we may feel reasonably confident in accepting the $K\bar{K}$ decay of the $A_2(1310)$; confirmation and/or clarification of additional structure must await further data.

4.8 The $K\bar{K}$ enhancement at 1515 MeV

In their study of the reactions

$$K^- + p \rightarrow \Lambda(\Sigma^0) + K_1 + K_1 \tag{33}$$

and

$$K^- + p \rightarrow \Lambda(\Sigma^0) + K^+ + K_1 + \pi^+ \tag{34}$$

Barnes et al.[16,54] found evidence for a meson with mass near 1515 MeV and width about 90 MeV; their most recent data are shown in Fig. 37. Their initial analysis suggested the assignment $I^G J^P = 0^+2^+$; with improved statistics this assignment has become more secure. However, the importance of the $K\bar{K}\pi$ decay mode is obscured by a possible contribution to the peak in this final state from the nearby E^0 meson. It may be noticed that decay into $\pi\pi$ is allowed; however, no evidence for this decay mode or any other not involving the $K\bar{K}$ system has been reported.

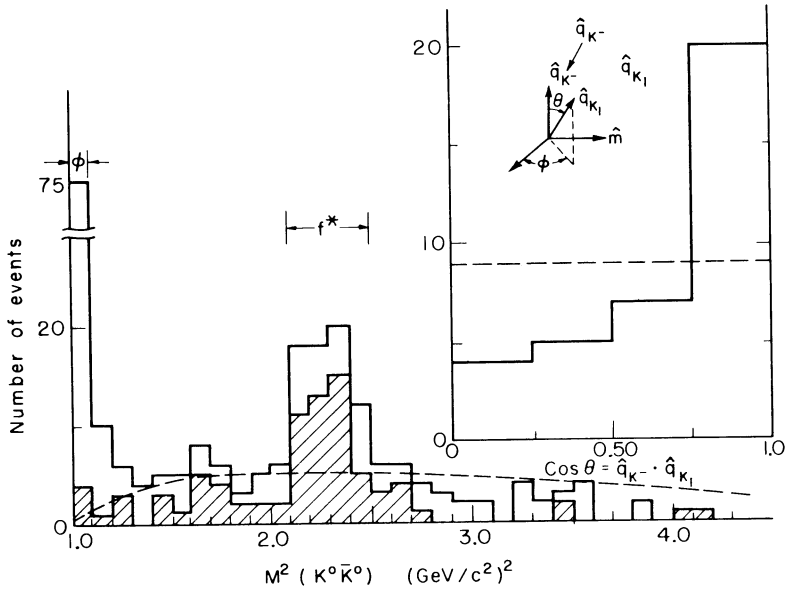

Figure 37 - Recent data of Barnes et al. [Ref. 54)] on $f^*(1500)$. Copious production of $\varphi(1019)$ is observed in the low-mass $K^0\bar{K}^0$ systems.

4.9 Properties of the $K\bar{K}\pi$ systems

Several groups have studied $\bar{p}p$ annihilations in which $K\bar{K}$ pairs are produced in association with two or more pions. These are convenient systems for searching for mesons of the sequence 0^-, 1^+, 2^-, etc., where decay into $K\bar{K}$ is forbidden. Let us consider first the reactions

$$\bar{p} + p \rightarrow K_1 + K_1 + \pi^+ + \pi^- \qquad (35)$$

$$\bar{p} + p \rightarrow K_1 + (K^0) + \pi^+ + \pi^- \qquad (36)$$

and

$$\bar{p} + p \rightarrow K_1 + K^\pm + \pi^\mp + \pi^0 \ . \qquad (37)$$

Using stopped $\bar{p}$'s, Armenteros et al.[55] found that the two-body combinations showed peaks corresponding to ρ and $K^*(890)$ production. The $K\pi\pi$ combinations contained a well-defined enhancement centred at 1230 MeV with Γ = 60 MeV to which we return later; within statistics, no structure was apparent in the $M(K\pi\pi)$ distribution for these events. The same reactions have been analysed at 1.2 GeV/c by Barlow et al.[49] Peaks corresponding to the $A_2(1310)$ and the threshold enhancement are apparent in the $M(K_1K_1)$ spectrum shown in Fig. 33; the K_1K_2 combinations (not shown) contain a peak at the $\varphi(1090)$ and both ρ and $K^*(890)$ production are observed. However, in this case <u>no</u> $K\pi\pi$ enhancement occurs at 1230 MeV; again, little evidence for structure appears in the $K\bar{K}\pi$ combinations.

The situation is dramatically different in the reactions

$$\bar{p} + p \rightarrow K_1 + K^\pm + \pi^\mp + \pi^- + \pi^+ \qquad (38)$$

$$\bar{p} + p \rightarrow K_1 + K^\pm + \pi^\mp + \pi^0 + \pi^0 \qquad (39)$$

$$\bar{p} + p \rightarrow K_1 + K_1 + \pi^+ + \pi^- + \pi^0 \qquad (40)$$

and

$$\bar{p} + p \rightarrow K_1 + (K^0 + \pi^0) + \pi^+ + \pi^- \ . \qquad (41)$$

The major feature is shown in the $M(K\bar{K}\pi)$ distributions in Fig. 38, which represents the data of Baillon et al.[56]. A strong peak occurs in the neutral $K\bar{K}\pi$ combinations near 1425 MeV. Since the two-body combinations demonstrate copious production of the $K^\pm K_1$ threshold enhancement and of $K^*(890)$, Baillon et al. attempted to reproduce the peak with just these two effects. This was not possible, so the peak is attributed to a $K\bar{K}\pi$ resonance with E_r = 1425 ± 7 MeV and width Γ = 80 ± 10 MeV called the E meson. Since the charged $K\bar{K}\pi$ combinations show no peak, Baillon et al. conclude that I = 0 for the E meson.

With the assumption of an I = 0 $K\bar{K}\pi$ resonance the spectra for reactions (38) and (39) can be accounted for almost entirely by production through the intermediate state $\bar{p}p \rightarrow E^0\pi\pi \rightarrow K\bar{K}\pi\pi\pi$. Reaction (40) is dominated by ω production, but the matrix element for the $K_1K_1\omega$ final state (which has C = +1 and results from the initial $^1S_0$ state) can be written explicitly and the reflected background in the $M(K\bar{K}\pi)$ distribution evaluated. A small, but significant, $K_1K_1\pi^0$ enhancement persists near 1425 MeV. To obtain the $K_1K_2\pi^0$ spectrum it is adequate to subtract one-half the $K_1K_1\pi^0$ spectrum in reaction (40) from the $K_1(K^0\pi^0)$ spectrum in reaction (41);

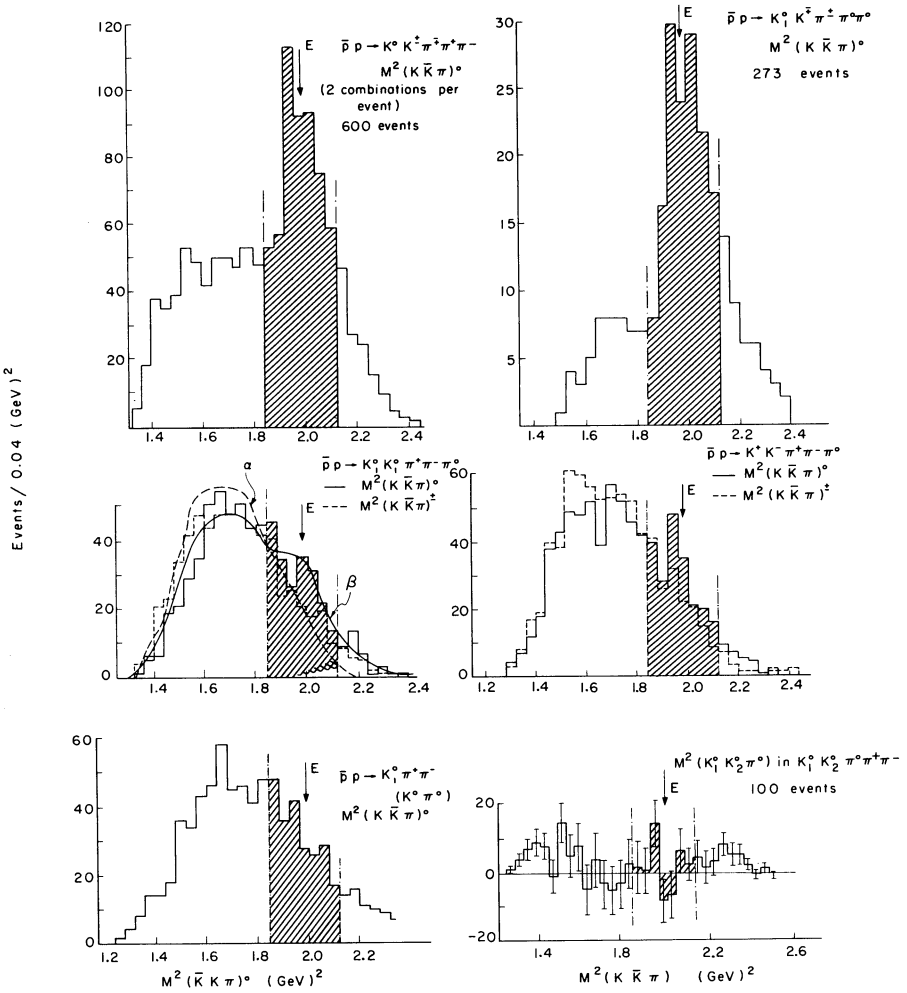

Figure 38 - Data of Baillon et al. [Ref. 56) demonstrating the existence of the E^0 meson. A small enhancement persists in the $M(K_1K_1\pi^0)$ distribution; no effect is observed in the subtracted $M^2(K_1K_2\pi^0)$ distribution.

in this case, no enhancement is observed near 1425 MeV. The fitted number of E^0 events in each channel is found to be:

Final state	Total number of events	Number of E^0 events	Predicted number C = +1	Predicted number C = -1
$K_1K^{\pm}\pi^{\mp}$ (38)	600	$600 \begin{smallmatrix}+0\\-60\end{smallmatrix}$	$600 \begin{smallmatrix}+0\\-60\end{smallmatrix}$ ≡ normalization	
$K_1K^{\pm}\pi^{\mp}$ (39)	273	208 ± 20	---	---
$K_1K_1\pi^0$ (40)	657	83 ± 21	90	0
$K_1K_2\pi^0$ (41)	757	20 ± 25	0	300

The predicted numbers are based on the assumption that I = 0 and a detection efficiency of ⅔ for the K_1. Clearly, the results are compatible only with $C(E^0) = +1$. Then, since C = +1 for the $E^0\pi^0\pi^0$ final state as well, it is possible to conclude that most events result from

the $^1S_0$ state of the $\bar{p}p$ system; less than 30% of E^0 production in reaction (38) comes from the initial $^3S_1$ state.

The spin and parity of the E^0 meson may in principle be deduced from its production and decay correlations. The two-body mass distributions for events in the E^0 peak indicate that ~ 50% result from $E^0 \to K^*(890)\bar{K}$ or c.c.; the remainder appear to represent decays through the proposed I = 1 s-wave $K\bar{K}$ threshold enhancement. If the latter decays are correctly identified, this implies $I^G = 0^+$ and the sequence $J^P = 0^-, 1^+, 2^-$, etc., for the E^0. It may be noted that this sequence would provide a simple explanation for the absence of $E^0\pi^0$ events in reaction (37). Since $C(E^0\pi^0) = +1$, only the $^1S_0$ $\bar{p}p$ state with $J^P = 0^-$ can contribute; a pion in a state with angular momentum J has $P = -(-1)^J$, consequently, the reaction is forbidden if $P(E^0) = -(-1)^J$.

The spin-parity analysis is considerably simplified when attention is focused on events with $M^2(K\bar{K}) < (1.08\ \text{GeV})^2$, i.e. in the region of the s-wave threshold enhancement. These events may be characterized by three vectors:

$\underset{\sim}{k}$: the relative momentum of the dipions in their rest frame

$\underset{\sim}{P}$: the relative momentum of the decay pion and the $K\bar{K}$ system in the E^0 rest frame

$\underset{\sim}{K}$: the relative momentum of the dipion system and the E^0 meson in the $\bar{p}p$ rest frame.

The vectors $\underset{\sim}{k}$ and $\underset{\sim}{P}$ may be transformed to the $\bar{p}p$ rest frame using the techniques discussed by Zemach[35], where Baillon et al. define the angles

$$\cos\varphi = \hat{\underset{\sim}{P}} \cdot \hat{\underset{\sim}{K}} \ ; \quad \cos\psi = \hat{\underset{\sim}{P}} \cdot \hat{\underset{\sim}{k}} \ ; \quad \text{and} \quad \cos\chi = \hat{\underset{\sim}{k}} \cdot \hat{\underset{\sim}{K}} \ . \tag{42}$$

In the $\bar{p}p$ rest frame it is now straightforward to evaluate the correlations for the lowest spin-parity assignments:

Initial state	$J^P(E^0)$	Matrix element	Correlation
$^1S_0$	0^-	1	1
	1^+	$\underset{\sim}{P} \cdot \underset{\sim}{K}$	$\cos^2\varphi$
	2^-	$(\underset{\sim}{P} \cdot \underset{\sim}{K})^2 - (\frac{1}{3})K^2P^2$	$(\cos^2\varphi - \frac{1}{3})^2$
$^3S_1$	0^-	$\underset{\sim}{k} \times \underset{\sim}{K}$	$\sin^2\chi$
	1^+	$\underset{\sim}{k} \times \underset{\sim}{P}$	$\cos^2\psi$
	2^-	$\underset{\sim}{P}\,\underset{\sim}{P} \cdot (\underset{\sim}{k} \times \underset{\sim}{K}) - (\frac{1}{3})P^2(\underset{\sim}{k} \times \underset{\sim}{K})$	$\sin^2\chi$ $5\text{-}3\cos^2\varphi$ $5\text{-}3\cos^2\psi$

In each case the lowest allowed partial wave is assumed for the dipion system.

The essential experimental result may be summarized by the statement that Baillon et al. find that all distributions are essentially isotropic. Since the $E^0\pi^0\pi^0$ final state comes only from the $^1S_0$ initial state, the predictions are unique to the extent that centrifugal barriers inhibit the I = 0, L = 2 dipion systems. Consequently, it is difficult to reconcile either the $J^P = 1^+$ or 2^- assignments with the data. The small contribution of initial $^3S_1$ state to the $E^0\pi^+\pi^-$ events allows some additional flexibility in fitting the data in this final state; nevertheless, the 1^+ and 2^- assignments must still be rejected. In the unlikely possibility that the dipion system is dominated by the L = 2 partial wave, only the $J^P = 1^+$ assignment is compatible with the data.

Although angular correlations are reasonably fitted with the assumption $I^GJ^P = 0^+0^-$ for the E^0, the $M(\pi\pi)$ distributions are poorly reproduced; both the $\pi^+\pi^-$ and $\pi^0\pi^0$ combinations tend toward higher mass values than expected from phase space. To obtain good fits, Baillon et al. find it adequate to introduce an I = 0 s-wave resonance with mass 445 to 460 MeV and width 65 to 80 MeV. Once again, the interesting possibility of an I = 0 low-mass s-wave $\pi\pi$ resonance provides a convenient explanation for distortions in the $\pi\pi$ mass spectrum.

Despite its complexity the analysis is quite thorough; it appears difficult to escape the conclusion that the E^0 represents another state in the sequence $\eta(549)$, $\eta'(958)$, and $E^0(1425)$, all with $I^GJ^P = 0^+0^-$. This is the first significant evidence that states exist which cannot be accommodated within the now-familiar nonet structure of the SU(3) symmetry scheme.

To determine whether the E^0 was produced in other reactions, Hess et al.[57] analysed the reactions

$$\pi^- + p \rightarrow K^\pm + K_1 + \pi^\mp + n \qquad (43)$$

$$\pi^- + p \rightarrow K_1 + K_1 + \pi^- + p \qquad (44)$$

and

$$\pi^- + p \rightarrow K^- + K_1 + \pi^0 + p \qquad (45)$$

obtained over the interval 2.7 to 4.2 GeV/c. The $M(K\bar{K}\pi)$ distributions for charged and neutral combinations are shown in Fig. 39; no clear evidence for any structure is apparent in the charged combinations. The neutral combinations show the E^0 peak at 1425 MeV.

However, the more striking effect is the sharp neutral peak which occurs at 1280 MeV with width $\Gamma < 30$ MeV called the D meson. The existence of this state was deduced independently by d'Andlau et al.[58] in their study of the reaction $\bar{p}p \rightarrow K\bar{K}\pi\pi\pi$ at 1.2 GeV/c.

As observed in the decay of the E^0 meson, the K^+K_1 pairs tend to concentrate in the low mass region, suggesting the presence of the I = 1 s-wave threshold enhancement; consequently, one again suspects $I^G = 0^+$ and the sequence $J^P = 0^-$, 1^+, 2^- etc. for the D meson. The $J^P = 1^+$ hypothesis fits the data most naturally; when a strong I = 1 s-wave $K\bar{K}$ interaction is included, the hypothesis $I^GJ^P = 0^+0^-$ also provides an adequate fit. The determination of the correct J^P assignment would be greatly facilitated if possible alternative decay modes, such as $\pi\pi\eta$, were available for analysis; thus far, none has been observed.

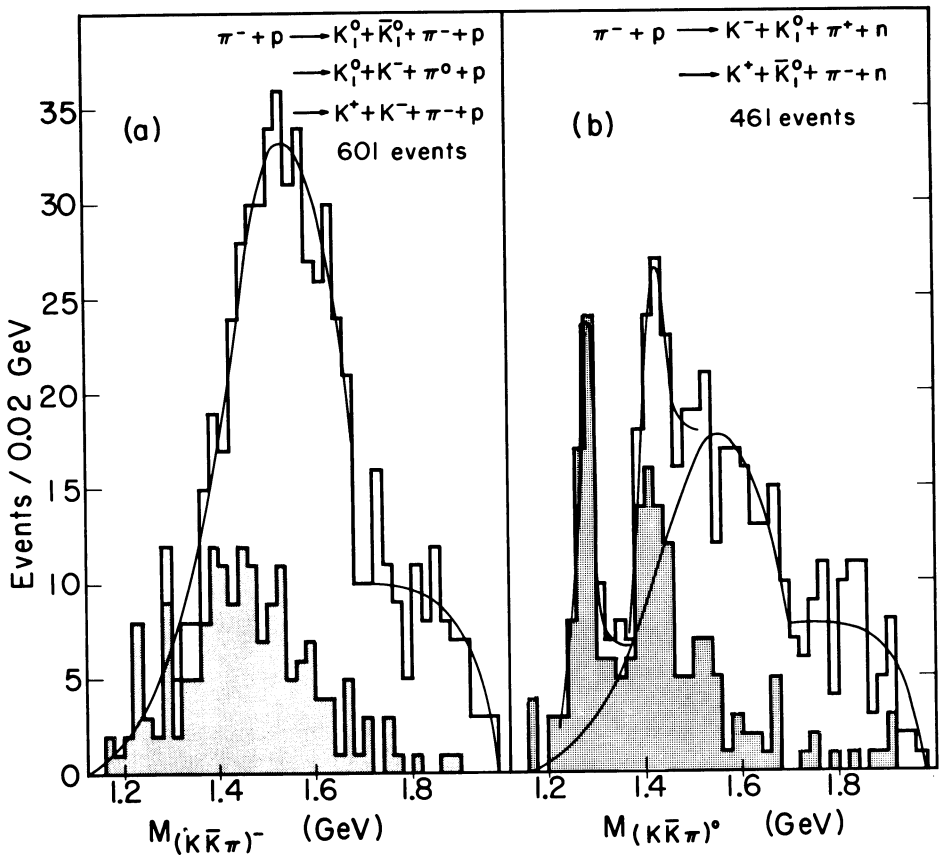

Figure 39 - Charged and neutral $M(K\bar{K}\pi)$ distributions observed by Hess et al. [Ref. 57)] in π^-p interactions. The neutral combinations show the D meson at 1280 MeV.

4.10 The strangeness $\pm 1/2$ systems

The status of the S = ± 1 systems with allowed decay into Kπ can be conveniently summarized with the data of deBaere et al.[59] who studied the reaction

$$K^+ + p \rightarrow K^0 + \pi^+ + p \qquad (46)$$

with good statistics at 3.0 and 3.5 GeV/c. The Dalitz plot for this final state is shown in Fig. 40; the projections appear in Fig. 41. The $K^0\pi^+$ mass distribution is dominated by the production of $K^*(890)$ and $K^*(1415)$; with some optimism a third enhancement can be observed near 1080 MeV. It is particularly interesting to note that the $K^*(1415)$ enhancement occurs almost entirely in the $N^*(1238)$ interference band; the enhancement near 1080 MeV is also confined to this band. We have now discussed several instances in which enhancements are particularly strong in regions where the kinematics permit the simultaneous production of two resonances -- both by essentially peripheral processes. Professor Goldhaber has called this effect "catalytic interference" and I think that we shall see more of it as production processes are studied further.

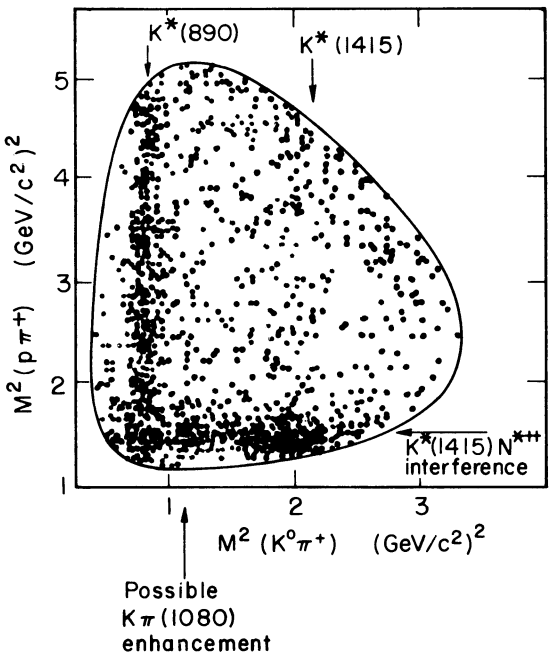

Figure 40 - Data of deBaere et al. [Ref. 59)] for the $K_1\pi^+p$ final states at 3.0 and 3.5 GeV/c. The reaction is dominated by production of $K^*(890)$ and $N^*(1238)$.

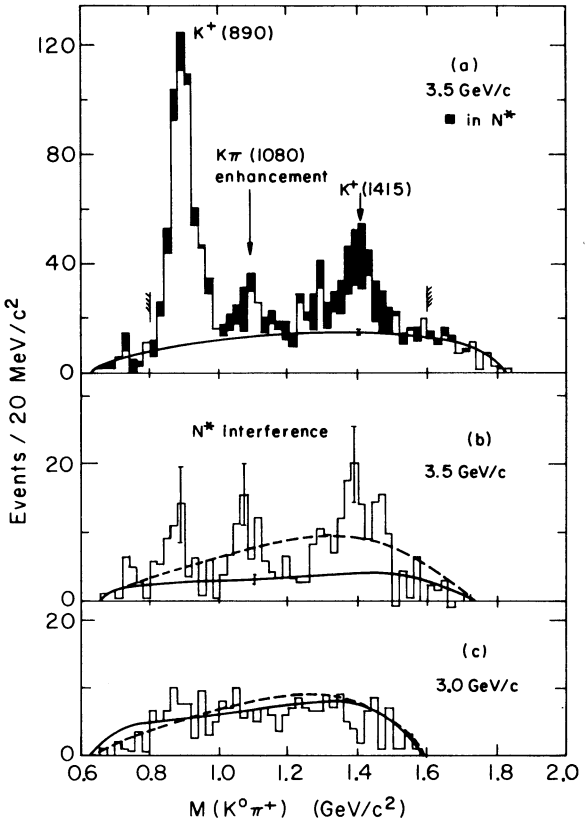

Figure 41 - $M(K_1\pi^+)$ mass distributions for Fig. 40 show that a strong $K^*(1415)$ enhancement occurs in the $N^*(1238)$ interference band; the data suggest the presence of an additional peak near 1080 MeV, also confined to the $N^*(1280)$ band.

The assignment $J^P = 1^-$ has long been established for the $K^*(890)$. In addition, all analyses[16] have led to $J^P = 2^+$ as the preferred assignment for $K^*(1415)$. The most recent analysis is that reported by Goldberg et al.[60] who studied the reactions

$$K^- + p \rightarrow \bar{K}^0 + \pi^- + p \qquad (47)$$

and

$$K^- + p \rightarrow \bar{K}^0 + \pi^+ + \pi^- + n \qquad (48)$$

at 4.6 and 5.0 GeV/c. The neutral $K^0\pi^+\pi^-$ combinations for events with $\Delta_n^2 < 0.2$ (GeV/c)^2 showed a strong peak at 1425 ± 5 MeV with Γ = 70 ± 10 MeV; angular correlations between the normal to the decay plane and the incident K^- were consistent with production through pion exchange. The charged $K^0\pi^-$ systems showed a strong peak near 1425 MeV only for events with $0.2 < \Delta_n^2 < 0.5$ (GeV/c)^2. In the same experiment the production and decay angular distributions for charged $K^*(890)$ events are consistent with a production process dominated by ω exchange. Goldberg et al. argue that it is reasonable to assume that the same production mechanism for charged $K^*(1425)$ events accounts for the difference in observed Δ^2 distributions. With this assumption possible decay correlations in the $K^*(1425)$ rest frame may be calculated:

J^P	Matrix element	Decay correlation
1^-	$\underset{\sim}{\varepsilon}^* \cdot (\underset{\sim}{p}_0 \times \underset{\sim}{p})$	$(1-x^2)$
2^+	$\underset{\sim}{\varepsilon}^* \cdot (\underset{\sim}{p}_0 \times \underset{\sim}{p})(\underset{\sim}{p}_0 \cdot \underset{\sim}{p})$	$(1-x^2)\,x^2$
3^-	$\underset{\sim}{\varepsilon}^* \cdot (\underset{\sim}{p}_0 \times \underset{\sim}{p})\,(\underset{\sim}{p}_0 \cdot \underset{\sim}{p})^2 - (1/5)(p_0^2 p^2)$	$(1-x^2)(x^2 - 1/5)^2$

where $\underset{\sim}{\varepsilon}$ is the polarization of the exchanged ω; $\underset{\sim}{p}_0$ is the beam momentum and $\underset{\sim}{p}$ the relative $K\pi$ momentum; $x = \hat{\underset{\sim}{p}}_0 \cdot \hat{\underset{\sim}{p}}$.

An acceptable fit to the data is obtained only for the hypothesis $J^P = 2^+$. Although the result is model-dependent, the essential validity of the model has been tested in a wide variety of reactions in which the properties of the resonant state were known. With regard to the $K^*(1080)$ we need say little more at present since its existence has yet to be unambiguously established.

Many groups have extended the search for new $S = \pm 1$ resonances to $K\pi\pi$ systems. We have already mentioned that Armenteros et al.[55] observed a well-defined enhancement (the C meson) at 1230 MeV with Γ = 60 MeV in their study of $K\bar{K}\pi\pi$ final states produced in $\bar{p}p$ annihilations at rest. French et al.[61] have analysed the $\bar{K}K\pi\pi\pi\pi$ final states from $\bar{p}p$ annihilations at 3 to 4 GeV/c; they find some evidence for a peak in the $I_z = \pm 3/2$ $K^*(890)\pi$ combinations which they interpret as a resonance with E_r = 1265 ± 10 MeV and width Γ = 50 ± 20 MeV. Unfortunately, the properties of these systems remain obscure since little additional evidence for either state has yet been reported in studies of $K\pi\pi$ systems produced in other reactions.

As a more accessible source of $K\pi\pi$ combinations, several groups have turned their attention to the reactions

$$K^{\pm} + p \rightarrow (K\pi\pi)^{\pm} + p \qquad (49)$$

and

$$K^{-} + p \rightarrow (K\pi\pi)^{0} + n \; . \qquad (50)$$

The characteristic structure in these reactions is demonstrated by the 10 GeV/c $K^{-}p$ data of the ABCLV Collaboration[62] shown in Fig. 42. The charged $K\pi\pi$ systems peak strongly near 1320 MeV; at higher beam momenta a second peak occurs near 1790 MeV. In contrast, no enhancements are observed in the neutral $K\pi\pi$ combinations. It is apparent that the charged peaks must be mediated by the exchange of I = 0 systems.

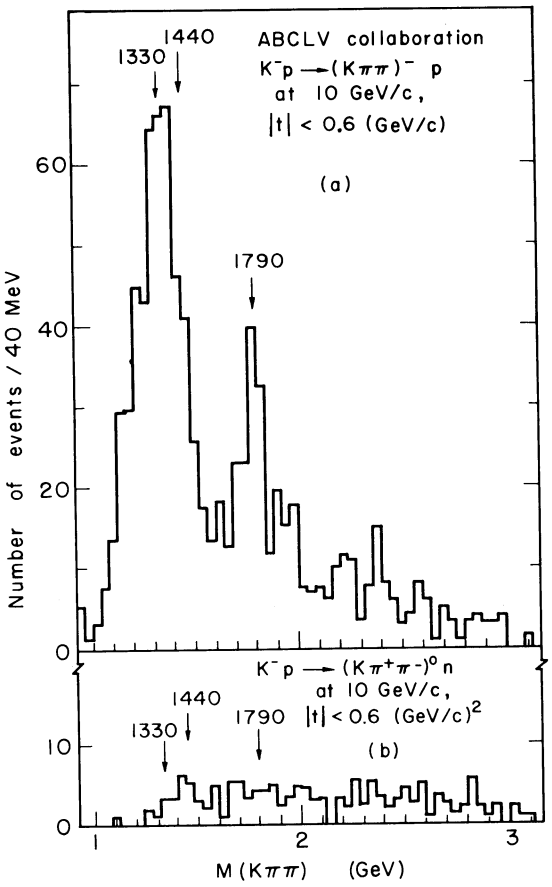

Figure 42 - Data of ABCLV Collaboration [Ref. 62)]. Although two well-defined peaks occur in the charged combinations, no structure is observed in the neutrals.

From our discussion of the A_1 and B enhancements it is easy to see that, in principle, $K^{*}(890)$ production with diffraction scattering of a virtual pion on the nucleon could account for the low mass peak. In this case, we must expect a strong $\cos^2 \vartheta$ component in the $K^{*}(890)$ decay correlation with the incident beam. Using $K^{+}p$ interactions at 4.6 GeV/c, Shen et al.[63] divided their events into two groups: those with $|\cos \vartheta| <$ or > 0.8. The low mass enhancement persisted most strongly in the group with $|\cos \vartheta| < 0.8$; from this they conclude that the Deck mechanism cannot account for the observed peak. In addition, with the improved statistics shown in Fig. 43, Shen et al. report that the low mass peak can be resolved into a resonance at 1320 MeV with $\Gamma = 80 \pm 20$ MeV and the $K^{*}(1430)$.

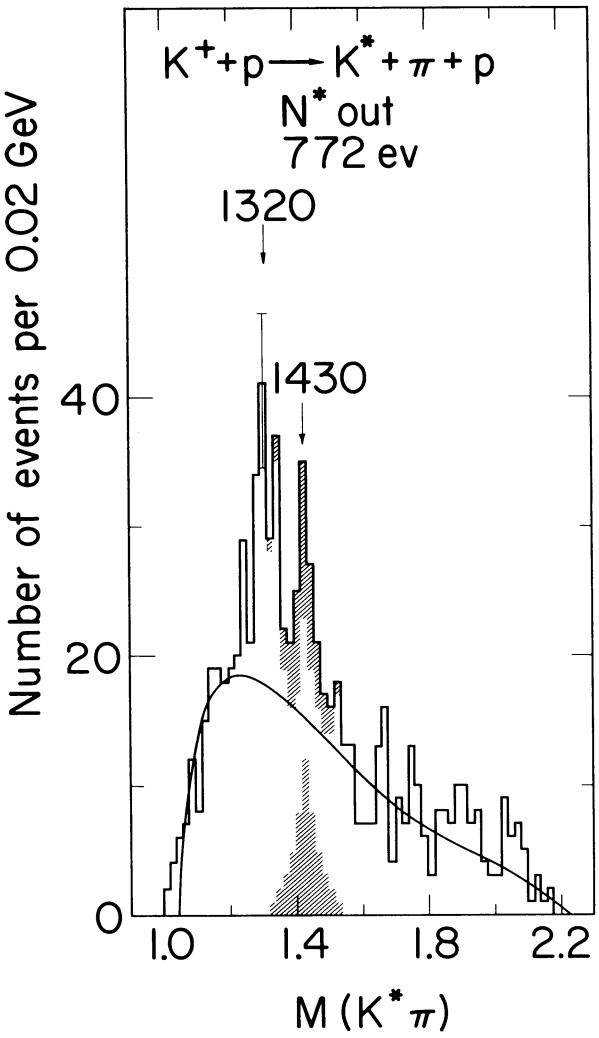

Figure 43 - Data of Shen et al. [Ref. 63)] suggesting that the broad low-mass enhancement in the $(K\pi\pi)^{\pm}$ combinations is a superposition of a resonance near 1320 MeV and the well-established $K^*(1415)$.

A new analysis of the low mass enhancement has been provided by Berlinghieri et al.[64] from their study of K^+p interactions at 12.7 GeV/c. Because of the (almost ten times) narrower Δ^2 distribution to the proton than to the π^+p system, they argue that the enhancement cannot be attributed to the Deck effect. The weak dependence of the cross-section on beam momentum and the absence of an effect in the neutral $K\pi\pi$ combinations suggest production through a diffraction mechanism. If this is so, the likely assignments are $I = \frac{1}{2}$ and $J^P = 0^-, 1^+$, etc.; this is consistent with the absence of observed decay into $K\pi$ or $K\eta$.

The peak at 1320 MeV is associated with both $K^*(890)\pi$ and $K\rho$ combinations; the vector mesons are aligned along the beam axis ($\cos^2\vartheta$) decay. For consistency with the diffraction hypothesis, Berlinghieri et al. invoke production through exchange of an $I^GJ^P = 0^+0^+$ system (the vacuum?). At this point it is necessary to note the difference in emphasis in this analysis and that given by Shen et al. By selecting events with $|\cos^2\vartheta| < 0.8$ Shen et al. conclude that the enhancement is associated predominantly with vector mesons which are <u>not</u> aligned; by looking at the decay angular distribution for vector mesons <u>in</u> the enhancement

(which presumably includes background) Berlinghieri et al. conclude that the vector mesons are alighed. Clearly, this is an important point which must be resolved before a consistent interpretation of all the data is possible. Although it is possible that the effect merely reflects a difference in production mechanisms at 4.6 and 12.7 GeV/c, it may also represent a serious ambiguity in the analyses.

Berlinghieri et al. have studied the decay correlations in the $K\rho$ final states and obtain good agreement with the $J^P = 1^+$ hypothesis. They find that the $K^*(890)\pi$ spectrum peaks near 1280 MeV while the $K\rho$ spectrum peaks near 1320 MeV. Nevertheless, they conclude that their data are consistent with a single resonance at 1280 ± 20 MeV with Γ = 130 ± 15 MeV. The shift in mass of the $K\rho$ spectrum can be adequately accounted for as a distortion of the Breit-Wigner resonance form by the limited phase space available for this decay mode whose nominal threshold is 1255 MeV. In fact, the phase-space-corrected (2.0 ± 0.2) decay rates give $K\rho/K^*\pi = 0.91 \pm 0.25$, consistent with equal strengths for the two decay modes. While the analysis is suggestive, these conclusions regarding the properties of the $K\pi\pi$ enhancement near 1320 MeV can hardly be regarded as conclusive until various groups agree that the mass spectrum represents a composite as suggested by Shen et al., or (at least at higher momenta) that it corresponds to a single broad resonant state.

The L meson near 1780 MeV with Γ = 100 MeV is an interesting new object for future study. Although it is likely[16] that I = ½, its J^P assignment remains undetermined.

5. SUMMARY

It is of interest to try to summarize those areas which appear particularly exciting for future study. However, our understanding is progressing at a sufficiently rapid rate that the summary would have to be revised almost daily to be cogent. But let us proceed anyway!

5.1 Baryons

Certainly the discovery and classification of states fitting comfortably within the frameworks of SU(3) and Regge recurrences must continue. But the urgent problem is the clarification of the structure known to exist in the S = +1 systems. Even since the writing of the early part of these notes progress has occurred. First, Carter[65] has reported the results of a dispersion-theoretic calculation of the real parts of the I = 0 and I = 1 forward scattering amplitudes using the most recent total cross-section measurements; the imaginary parts are obtained with the use of the optical theorem. The I = 1 amplitude has an approximately constant phase over the interval 0.7 to 7.0 GeV/c. In contrast, the I = 0 amplitude exhibits a rapid change in phase near Z_o^*; Carter suggests that it resembles a circle superimposed on a smoothly varying background. By subtracting "reasonable" smoothly varying backgrounds from the real and imaginary parts separately, Carter obtains an Argand diagram for the (hopefully) rapidly varying single partial wave; it corresponds to a resonance with E_r = 1860 ± 15 MeV with Γ = 200 ± 50 MeV. If J = ½, then x = 0.31 ± 0.05. We may look forward to the resolution of this interesting question with the completion of BC studies presently in progress.

As a second example of recent progress Berman[66] reports that near threshold the cross-section, the slope with respect to energy, the production angular distribution, and the N^* decay angular distribution for the reaction $K^+p \rightarrow K^0N^*(1238)^{++}$ can be reasonably accounted for by the same current algebra and mass extrapolation leading to the s-wave pion-nucleon scattering lengths. In the present case an extrapolation in K-meson mass is required, but an analogous

calculation of the s-wave K^+p scattering length agrees with the experimental value within 30%. Remarkably, the predicted decay correlations agree well with those calculated by Stodolsky and Sakurai[13] using the $\rho - \gamma$ analogy; Berman considers this fortuitous since it is unlikely that perturbation theory would be valid near threshold. Unfortunately, however, the rapid fall of the inelastic cross-section (which accounts for most of the apparent peak in the I = 1 K^+p total cross-section) cannot be explained by the current algebras and low energy theorems. Berman conjectures that the decrease may be due to the onset of the p-wave unitarity limit which his theoretical expression reaches at the peak of the experimental cross-section. Clearly, this possible non-resonant explanation of the Z_1^* does not contradict Carter's conclusion, since he suggests a resonance only in the I = 0 state.

5.2 Mesons

The existence of the nonet patterns for the well-established $J^P = 0^-$, 1^-, and 2^+ mesons [see Ref. 16) for discussion of these classifications] has led to a variety of attempts to account for their structure in terms of the quark-antiquark models. The linear relation between spin and mass-squared (experimentally verified for the ρ, A_2, and g_1) observed by Focacci et al. suggests the existence of Regge trajectories for the mesons; this pattern could be accounted for if the quark-antiquark system is assumed to move in a three-dimensional harmonic oscillator potential. In his extensive discussion of such models, Dalitz[67] has shown that many features of the known meson systems can be reproduced.

While the quark-antiquark models neatly account for the $J^P = 0^-$, 1^-, and 2^+ systems, they simultaneously imply the existence of many other nonets. The $^1S_0$ and $^3S_1$ configurations correspond to the $J^P = 0^-$ and 1^- systems; $^1P_1$ corresponds to systems with $J^P = 1^+$ and C = -1 for the neutral non-strange members; $^3P_0$, $^3P_1$, and $^3P_2$ correspond to systems with $J^P = 0^+$, 1^+, and 2^+ with C = +1 for the neutral non-strange members. However, it is apparent from our discussion that the properties of possible candidates for both the $J^P = 0^+$ and 1^+ nonets remain particularly obscure. Although there are indeed many candidates, not a single member of these nonets has been unambiguously established. Clearly, this is the area of interest in the immediate future.

The importance of the $J^P = 1^+$ mesons has been emphasized recently in another context. Weinberg[68] argues that the successes of current algebra imply that some sort of chiral symmetry operates in nature; the existence of the ρ meson then leads one to expect the existence of an associated axial vector meson. He tries to answer the question: what relations are imposed by current algebra upon the spectra of 1^- and 1^+ mesons? Using a weak form of vector- and axial-vector meson dominance, Weinberg is led to the relation

$$M^2(A) = 2\, M^2(\rho)$$

precisely the relation satisfied by the $A_1(1080)$ and the $\rho(760)$! This result would be most remarkable should the $A_1(1080)$ be nothing more than a kinematic enhancement; it is apparent that the experimental clarification of the properties of the $A_1(1080)$ and other candidates for $J^P = 1^+$ systems has become crucial.

For reference, the table of known baryons and mesons and their decay properties is appended; they are the work of Rosenfeld et al.[69].

REFERENCES

1) A. Barbaro-Galtieri, Strong and Weak Interactions; Present Problems, Proc. of the 1966 International School of Physics "Ettore Majorana" (Academic Press, N.Y., 1966). A more complete version appears in UCRL-17054 (1966).

2) R.M. Heinz and M.H. Ross, Phys.Rev.Letters 14, 1091 (1965).

3) S.W. Kormanyos, A.D. Krisch, J.R. O'Fallon, K. Ruddick, and L.G. Ratner, Phys.Rev. Letters 16, 709 (1966).

4) V. Barger and D. Cline, Phys.Rev.Letters 16, 913 (1966); and Phys.Rev. 155, 1792 (1967).

5) F. Ned Dickmen, Phys.Rev.Letters 18, 798 (1967).

6) R.L. Cool, G. Giacomelli, T.F. Kycia, B.A. Leontić, K.K. Li, A. Lundby and J. Teiger, Phys.Rev.Letters 16, 1228 (1966), and to be published.

7) J.D. Davies, J.D. Dowell, P.M. Hattersley, R.J. Homer, A.W. O'Dell, A.A. Carter, K.F. Riley, R.J. Tapper, D.V. Bugg, R.S. Gilmore, K.M. Knight, D.C. Salter, G.H. Stafford, and E.J.N. Wilson, Phys.Rev.Letters 18, 62 (1967).

8) R.L. Cool, G. Giacomelli, T.F. Kycia, B.A. Leontić, K.K. Li, A. Lundby, and J. Teiger, Phys.Rev.Letters 17, 102 (1966).

9) R.J. Abrams, R.L. Cool, G. Giacomelli, T.F. Kycia, B.A. Leontić, K.K. Li, and D.N. Michael, New structures in the K^+p and K^+d total cross-sections between 1.55 and 3.30 GeV/c, submitted to Phys.Rev.Letters.

10) G. Goldhaber, The search for hyperons and bosons belonging to higher symmetries, UCRL-17388 (1967).

11) C. Wohl, R. Bland, J.L. Brown, G. Goldhaber, S. Goldhaber, and G.H. Trilling, to be published.

12) R.W. Bland, M.G. Bowler, J.L. Brown, G. Goldhaber, S. Goldhaber, V.H. Seeger, and G.H. Trilling, Phys.Rev.Letters 18, 1077 (1967).

13) L. Stodolsky and J.J. Sakurai, Phys.Rev.Letters 11, 90 (1963).

14) D.V. Bugg, D.C. Salter, G.H. Stafford, R.F. George, K.F. Riley, and R.J. Tapper, Phys.Rev. 146, 980 (1966).

15) D.H. Miller, Proc. of the International School of Physics "Enrico Fermi", Course XXXIII, Strong Interactions (Academic Press, N.Y., 1966), p.1.

16) G. Goldhaber, Proc. of the Thirteenth International Conference on High-Energy Physics, Berkeley, 1966 (University of California Press, Berkeley and Los Angeles, 1967), p.103. I am indebted to Professor Goldhaber for permission to use several figures prepared by him and Dr. B. Shen. References for material used in these figures can be found in the Proceedings.

17) M.N. Focacci, W. Kienzle, B. Levrat, B.C. Maglić, and M. Martin, Phys.Rev.Letters 17, 890 (1966).

18) G. Chikovani, L. Dubal, M.N. Focacci, W. Kienzle, B. Levrat, B.C. Maglić, M. Martin, C. Nef, P. Schübelin, and J. Séguinot, Physics Letters 22, 233 (1966).

19) D.J. Crennell, V.P. Hough, G.R. Kalbfleisch, K.W. Lai, J.M. Scarr, T.G. Schumann, I.O. Skillicorn, R.C. Strand, M.S. Webster, P. Baumel, A.H. Bachman, and R.M. Lea, Phys.Rev.Letters 18, 323 (1967).

20) T. Ferbel, reported in Ref. 16), p.131.

21) A. Forino, R. Gessaroli, L. Lendinara, G. Quareni, A. Quareni-Vignudelli, N. Armenise, B. Ghigini, V. Picciarelli, A. Romano, A. Cartacci, M.G. Dagliana, M. Della Corte, G. Dicapariaco, J. Laberrigue-Frolow, N. Huu Khanh, J. Quinquart, M. Sené, W. Fickinger, O. Goussu, Physics Letters 19, 68 (1965).

22) Bari-Bologna-Florence-Orsay Collaboration, reported in Ref. 16), p.129.

23) Summary by S. Goldhaber, UCRL-16295, May 1965.

24) Summary by D.R.O. Morrison, Preprint CERN/D.Ph.II/PHYSICS 67-4 (1967).

25) W.D. Walker, J. Carroll, A. Garfinkel, and B.Y. Oh, Phys.Rev.Letters 18, 630 (1967).

26) K. Gottfried and J.D. Jackson, Nuovo Cimento 34, 735 (1964).

27) L.J. Gutay, P.B. Johnson, F.J. Loeffler, R.L. McIlwain, D.H. Miller, and R.B. Willmann, Phys.Rev.Letters 18, 142 (1967), see also Purdue University Preprint C00-1428-26, (1967).

28) V. Hagopian, W. Selove, J. Alitti, J.P. Baton, M. Neveu-René, R. Gessaroli, and A. Romano, Phys.Rev.Letters 14, 1077 (1965).

29) M. Feldman, W. Frati, J. Halpern, A. Kanofsky, M. Nussbaum, S. Richert, P. Yamin, A. Choudry, S. Devons and J. Grunhaus, Phys.Rev.Letters 14, 869 (1965).

30) A. Buhler-Broglin, P. Dalpiaz, T. Massam, F.L. Navarria, M.A. Schneegans, F. Zetti, and A. Zichichi, Experimental evidence against the existence of the S^0-meson, submitted to Nuovo Cimento.

31) I.F. Corbett, C.J.S. Damerall, N. Middlemas, D. Newton, A.B. Clegg, W.S.C. Williams, and A.S. Carroll, Nuovo Cimento 39, 979 (1965).

32) C. Lovelace, R.M. Heinz, A. Donnachie, Physics Letters 22, 325 (1966).

33) F.S. Crawford, Jr., R.A. Grossman, L.J. Lloyd, L.R. Price, and E.C. Fowler, Phys.Rev. Letters 11, 564 (1963); 13, 421 (1964).

34) S.U. Chung, O.I. Dahl, L.M. Hardy, R.I. Hess, G.R. Kalbfleisch, J. Kirz, D.H. Miller, and G.A. Smith, Phys.Rev.Letters 12, 621 (1964); 18, 100 (1967).

35) C. Zemach, Phys.Rev. 133, B 1201 (1964).

36) G. Benson, L. Lovell, E. Marquit, B. Roe, D. Sinclair, and J. Vander Velde, Phys.Rev. Letters 16, 1177 (1966).

37) Orsay-Milan-Saclay-Berkeley Collaboration, Study of $\pi^+\pi^-\pi^-$ final states coherently produced on nuclei by 16 GeV/c π^-, submitted to Nuovo Cimento.

38) R.T. Deck, Phys.Rev.Letters 13, 169 (1964).

39) B.C. Shen, G. Goldhaber, S. Goldhaber, and J.A. Kadyk, Phys.Rev.Letters 15, 731 (1965).

40) S.U. Chung, Thesis, UCRL-16981, 1966, to be published.

41) S.U. Chung, M. Neveu-René, O.I. Dahl, J. Kirz, D.H. Miller and Z.G.T. Guiragossian, Phys.Rev.Letters 16, 481 (1966).

42) C. Baltay, J.C. Severiens, N. Yeh, and D. Zanello, Phys.Rev.Letters 18, 93 (1967).

43) B.C. Maglić, L.W. Alvarez, A.H. Rosenfeld, and M.L. Stevenson, Phys.Rev.Letters 7, 178 (1961).

44) V. Alles-Borelli, B. French, A. Frisk, L. Michejda, and E. Paul, Preprint CERN/TC/PHYSICS 66-25 (1966), submitted to Nuovo Cimento.

45) J.A. Danysz, B.R. French, J.B. Kinson, V. Simak, J. Clayton, P. Mason, H. Muirhead, and P. Renton, Physics Letters 24B, 309 (1967).

46) J.A. Danysz, B.R. French, and V. Simak, Preprint CERN/D.Ph.II/PHYSICS 67-1 (1967).

47) P. Baillon, Thesis, Faculté des Sciences, Paris (1966).

48) B. Conforto, B. Maréchal, L. Montanet, M. Tomas, C. d'Andlau, A. Astier, J. Cohen-Ganouna, M. Della Negra, M. Baubillier, J. Duboc, F. James, M. Goldberg, and D. Spencer, Preprint CERN/D.Ph.II/PHYSICS 67-11 (1967), submitted to Nuovo Cimento.

49) J. Barlow, E. Lillestøl, L. Montanet, L. Tallone-Lombardi, C. d'Andlau, A. Astier, L. Dobrzynski, S. Wojcicki, A.M. Adamson, J. Duboc, F. James, M. Goldberg, R.A. Donald, R. James, J.E.A. Lys, and T. Nisar, Preprint CERN/TC/PHYSICS 66-22 (1967), submitted to Nuovo Cimento.

50) J. Oostens, P. Chavanon, M. Crozon, and J. Tocqueville, reported at the French Physical Society Meeting, Dijon, June, 1966.

51) A. Rittenberg and L. Barbaro-Galtieri, reported in Ref. 16), p.105.

52) D.J. Crennell, G.R. Kalbfleisch, K. Wu Lai, J.M. Scarr, T.G. Schumann, I.O. Skillicorn, and M.S. Webster, Phys.Rev.Letters 16, 1025 (1966).

53) W. Beusch, W.E. Fisher, B. Gobbi, M. Pepin, E. Polgar, P. Astbury, G. Brautti, G. Finocchiaro, J.C. Lassalle, A. Michelini, K.M. Terwilliger, D. Websdale, and C.H. West, reported in Ref. 16), p.123.

54) V.E. Barnes, B.B. Culwick, P. Guidoni, G.R. Kalbfleisch, G.W. London, R.B. Palmer, D. Radojicic, D.C. Rahm, R.R. Rau, C.R. Richardson, N.P. Samios, J.R. Smith, B. Goz, N. Horwitz, T. Kikuchi, J. Leitner, and R. Wolfe, Phys.Rev.Letters 15, 322 (1965).

55) R. Armenteros, D.N. Edwards, F. Jacobsen, L. Montanet, J. Vandermeulen, C. d'Andlau, A. Astier, P. Baillon, J. Cohen-Ganouna, C. Deferse, J. Siaud, P. Rivet, Proc. of the XIIth International Conference on High Energy Physics, Dubna, 1964 (Atomizdat, Moscow, 1966), p.577.

56) P. Baillon, D. Edwards, B. Marechal, L. Montanet, M. Tomas, C. d'Andlau, A. Astier, J. Cohen-Ganouna, M. Della-Negra, S. Wojcicki, M. Baubillier, J. Duboc, F. James, and F.R. Levy, Preprint CERN/TC/PHYSICS 66-24 (1966), submitted to Nuovo Cimento.

57) R.I. Hess, S.U. Chung, O.I. Dahl, L.M. Hardy, J. Kirz, and D.H. Miller, Proc. of the XIIth International Conference on High Energy Physics, Dubna, 1964 (Atomizdat, Moscow, 1966), p.426; and Phys.Rev.Letters 14, 1074 (1965).

58) C. d'Andlau, A. Astier, M. Della Negra, L. Dobrzynski, S. Wojcicki, J. Barlow, T. Jacobsen, L. Montanet, L. Tallone, M. Tomas, A.M. Adamson, M. Baubillier, J. Duboc, M. Goldberg, F. Levy, D.N. Edwards, J.E.A. Lys, Physics Letters 17, 347 (1965).

59) W. deBaere, J. Debaisieux, P. Dufour, F. Grard, J. Heughebaert, L. Pape, P. Peeters, F. Verbeure, R. Windmolders, Y. Goldschmidt-Clermont, V.P. Henri, B. Jongejans, W. Koch, A. Moisseev, F. Muller, J.M. Perrau, and V. Yarba, reported in Ref. 16), p.139.

60) M. Goldberg, B. Goz, J. Leitner, V.E. Barnes, P.J. Dornan, G.R. Kalbfleisch, and I.O. Skillicorn, Phys.Rev.Letters 18, 680 (1967).

61) B.R. French, J.B. Kinson, R. Rigopoulos, V. Simak, F. McDonald, G. Petmezas, and L. Riddiford, Preprint CERN/TC/PHYSICS 66-31 (1966), submitted to Nuovo Cimento.

62) Aachen-Berlin-CERN-London(I.C.)-Vienna Collaboration, reported in Ref. 16), p.118.

63) B.C. Shen, I. Butterworth, C. Fu, G. Goldhaber, S. Goldhaber, and G. Trilling, Phys.Rev. Letters 17, 726 (1966).

64) J. Berlinghieri, M.S. Farber, T. Ferbel, B. Forman, A.C. Melissinos, T. Yamanouchi and H. Yuta, Phys.Rev.Letters 18, 1087 (1967).

65) A.A. Carter, Phys.Rev.Letters 18, 801 (1967).

66) S.M. Berman, Phys.Rev.Letters 18, 1081 (1967).

67) R.H. Dalitz, Rapporteur's talk, Proc. of the Thirteenth International Conference on High Energy Physics, Berkeley, 1966 (University of California Press, Berkeley and Los Angeles, 1967), p.215.

68) S. Weinberg, Phys.Rev.Letters 18, 507 (1967).

69) A.H. Rosenfeld, A. Barbaro-Galtieri, W.J. Podolsky, L.R. Price, Matts Roos, P. Söding, W.J. Willis, and C.G. Wohl, Rev.Mod.Phys. 39, 1 (1967).

APPENDIX

Data on Particles and Resonant States: Table S, Stable Particles. Rev. Mod. Phys., January 1967

A. H. Rosenfeld, A. Barbaro-Galtieri, W. J. Podolsky, L. R. Price, Matts Roos, Paul Soding, W. J. Willis, C. G. Wohl

	$I^G(J^P)C_n$	Mass (MeV)	Mass difference (MeV)	Mean life (sec) $c\tau$ (cm)	$(\text{Mass})^2$ $(\text{GeV})^2$	Decays: Partial mode	Fraction	Q (MeV)	p or p_{max} (MeV/c)
γ	$0,1(1^-)^-$	0		stable	0	stable			
ν_e	$J = \frac{1}{2}$	0(<0.2 keV)		stable	0	stable			
ν_μ		0(<2.1 MeV)							
$e^\mp$	$J = \frac{1}{2}$	0.511006 ±.000002		stable ($> 2\times10^{21}$ y)	0.000	stable	$\mu_e = \frac{1.001159622 \pm .000000027}{2} \frac{e\hbar}{mc}$		
$\mu^\mp$	$J = \frac{1}{2}$	105.659 ±.002		2.199×10^{-6} ±.001, S=1.3* $c\tau = 6.592\times10^{4}$	0.011	$e\nu\bar{\nu}$	100 %	105	53
						$e\gamma\gamma$	(< 1.6)10^{-5}	105	53
						3e	(< 1.3)10^{-9}	104	53
$\mu_\mu = 1.001164 \pm .000003 \frac{e\hbar}{2m_\mu c}$			-33.920 ±.014			$e\gamma$	(< 6)10^{-8}	105	53
$\pi^\pm$	$1^-(0^-)^+$	139.579 ±.014		2.608×10^{-8} ±.015, S=3.5* $c\tau = 782$	0.019	$\mu\nu$	100 %	34	30
						$e\nu$	(1.24±0.03)10^{-4}	139	70
						$\mu\nu\gamma$	(1.24±0.25)10^{-4}	34	30
			4.6041 ±.0037	$(\tau^+ - \tau^-)/\bar{\tau} = (.4\pm.2)\%$ (test of CPT)		$\pi^0 e\nu$	(1.01±0.09)10^{-8}	4	5
						$e\nu\gamma$	(3.0 ±0.5)10^{-8}	139	70
π^0	$1^-(0^-)^+$	134.975 ±.014		[b] 0.89×10^{-16} ±.18, S=1.6* $c\tau = 2.67\times10^{-6}$	0.018	$\gamma\gamma$	[c] (98.8)%	135	67
						γe^+e^-	[c] (1.169)%	134	67
						$\gamma\gamma\gamma$	[c] (< 5)10^{-6}	135	67
						$e^+e^-e^+e^-$	[c] (3.47)10^{-5}	133	67
$K^\pm$	$\frac{1}{2}(0^-)$	493.82 ±.11		1.235×10^{-8} ±.006, S=2.4* $c\tau = 3.70$	0.244	$\mu\nu$	[b] (63.4 ±0.5)%	388	236
						$\pi\pi^0$	(21.0 ±0.3)% S=1.5*	219	205
						$\pi\pi^-\pi^+$	(5.6 ±0.1)%	75	126
				$(\tau^+ - \tau^-)/\bar{\tau} = (.09\pm.08)\%$ (test of CPT)		$\pi\pi^0\pi^0$	(1.71±0.08)%, S=1.5*	84	133
						$\mu\pi^0\nu$	(3.41±0.22)%, S=1.9*	253	215
						$e\pi^0\nu$	(4.79±0.18)%, S=2.1*	358	229
						$\pi\pi^\pm e^\mp\nu$	(3.8 ±0.8)10^{-6}	214	204
			-4.05 ±.12			$\pi\pi^\pm e^\mp\nu$	(< 2)10^{-5}	214	204
						$\pi\pi^\pm\mu^\mp\nu$	(≤ 1.4)10^{-6}	109	151
						$\pi\pi^\pm\mu^\mp\nu$	(< 3)10^{-5}	109	151
						$e\nu$	(1.9 ±1.2)10^{-4}	493	247
						$\pi\pi^0\gamma$	(2.2 ±0.7)10^{-5}	219	205
						$\pi\pi^+\pi^-\gamma$	(10 ±4)10^{-6}	75	126
						πe^+e^-	(< 1.1)10^{-6}	353	227
						$\pi\mu^+\mu^-$	(< 3)10^{-6}	143	172
K^0	$\frac{1}{2}(0^-)$	497.87 ±0.16		50% K_{Short}, 50% K_{Long}					
K_{Short}	$\frac{1}{2}(0^-)$			0.87×10^{-10} ±.009, S=1.3* $c\tau = 2.61$	0.248	$\pi^+\pi^-$	(69.3 ±1.2)% S=1.25*	219	206
			-0.48×$\frac{1}{\tau_S}$ ±.02			$\pi^0\pi^0$	(30.7 ±1.2)%	228	209
K_{Long}	$\frac{1}{2}(0^-)$			5.68×10^{-8} ±.26 $c\tau = 1703$	0.248	$\pi^0\pi^0\pi^0$	(23.5 ±2.1)%	93	139
						$\pi^+\pi^-\pi^0$	(11.5 ± .4)%	84	133
						$\pi\mu\nu$	(27.5 ±1.8)%	253	216
						$\pi e\nu$	(37.4 ±1.8)%	358	229
						$\pi^+\pi^-$	(.153 ±.007)%	219	206
						$\pi^+\pi^-\gamma$	(< 0.3)%	219	206
						$\pi^0\pi^0$	(< 2.7)10^{-3}	228	209
						$e\mu$	(< 4)10^{-5}	392	238
						$\gamma\gamma$	(1.3 ±0.6)10^{-4}	498	249
						$\mu^+\mu^-$	(< 4)10^{-6}	287	225
						e^+e^-	(< 4)10^{-5}	497	249
η	$0^+(0^-)^+$	548.6 ±0.4		$1<\Gamma<10$ keV $(2<c\tau<20)\times10^{-9}$	Neutral decays 72.9%	$\gamma\gamma$	(31.4 ±2.2)%	549	274
						$\pi^0\gamma\gamma$	(20.5 ±3.5)% S=1.3*	414	258
						$3\pi^0$	(21.0 ±3.2)% S=1.5*	144	179
					Charged decays 27.1%	$\pi^+\pi^-\pi^0$	(22.4 ±1.8)%	135	174
						$\pi^+\pi^-\gamma$	(4.6 ±0.8)% S=1.1*	269	236
						$\pi^0 e^+e^-$	(< 0.2)%	413	258
						$\pi^+\pi^-e^+e^-$	(0.1 ±0.1)%	268	236
p	$\frac{1}{2}(\frac{1}{2}^+)$	938.256 ±0.005	-1.2933 ±.0001	stable ($> 6\times10^{27}$ y)	0.880				
n	$\frac{1}{2}(\frac{1}{2}^+)$	939.550 ±0.005		$(1.01\pm.03)\times10^{3}$ $c\tau = 3.03\times10^{13}$	0.882	$pe^-\nu$	100 %	1	1
Λ	$0(\frac{1}{2}^+)$	1115.58 ±0.10		2.51×10^{-10} ±.04, S=1.4* $c\tau = 7.52$	1.245	$p\pi^-$	(66.4 ±1.1)% S=1.1*	38	100
						$n\pi^0$	(33.6 ±1.1)%	41	104
						$pe\nu$	(0.88±0.15)10^{-3}	177	163
						$p\mu\nu$	(1.35±0.60)10^{-4}	72	131
Σ^+	$1(\frac{1}{2}^+)$	1189.47 ±0.08		0.810×10^{-10} ±.013 $c\tau = 2.43$	1.412	$p\pi^0$	(52.8 ±1.5)%	116	189
						$n\pi^+$	(47.2 ±1.5)%	110	185
						$p\gamma$	(1.9 ±0.4)10^{-3}	251	225
						$n\pi^+\gamma$	(≈ 0.2)10^{-4}	110	185
						$\Lambda e^+\nu$	(1.5 ±0.9)10^{-5}	73	72
			-7.97 ±.11			$n\mu^+\nu$	(< 1.1)10^{-4}	144	202
						$ne^+\nu$	(< 5)10^{-5}	249	224
Σ^0	$1(\frac{1}{2}^+)$	1192.56 ±0.11		$<1.0\times10^{-14}$ $c\tau<3\times10^{-4}$	1.422	$\Lambda\gamma$	[c] 100 %	77	75
			-4.88 ±.06			Λe^+e^-	[c] (5.45)10^{-3}		
Σ^-	$1(\frac{1}{2}^+)$	1197.44 ±0.09		1.65×10^{-10} ±.03, S=1.4* $c\tau = 4.95$	1.434	$n\pi^-$	100 %	118	193
						$ne^-\nu$	(1.25±0.17)10^{-3}	257	230
						$n\mu^-\nu$	(0.62±0.12)10^{-3}	152	210
						$\Lambda e^-\nu$	(0.61±0.16)10^{-4}	81	79
						$n\pi^-\gamma$	(≈ 1)10^{-5}	118	193
Ξ^0	$\frac{1}{2}(\frac{1}{2}^+)$?	1314.7 ±1.0		3.0×10^{-10} ±.5, S=1.3* $c\tau = 8.99$	1.728	$\Lambda\pi^0$	100 %	64	135
						$p\pi^-$	(< .5)%	237	299
						$pe^-\nu$	(< .6)%	376	323
						$\Sigma^+e^-\nu$	(< .7)%	125	119
						$\Sigma^-e^+\nu$	(< .6)%	117	112
			-6.5 ±.2			$\Sigma^+\mu^-\nu$	(< .7)%	20	64
						$\Sigma^-\mu^+\nu$	(< .6)%	12	49
						$p\mu^-\nu$	(< .6)%	271	309
Ξ^-	$\frac{1}{2}(\frac{1}{2}^+)$?	1321.2 ±0.2		1.74×10^{-10} ±.05 $c\tau = 5.22$	1.746	$\Lambda\pi^-$	100 %	66	139
						$\Lambda e^-\nu$	(2.5 ±1.8)10^{-3}	205	190
						$n\pi^-$	(< 5)10^{-3}	242	303
						$\Lambda\mu^-\nu$	(< 1.2)%	100	163
						$\Sigma^0 e^-\nu$	(< 0.3)%	128	122
						$\Sigma^0\mu^-\nu$	(< 0.5)%	23	70
						$ne^-\nu$	(< 1)%	381	327
Ω^-	$0(3/2^+)$? ?	1674 ±3		1.5×10^{-10} ±.5, $c\tau = 4.5$	2.802	$\Xi\pi$	(~50)%	221	296
						$\Lambda\bar{K}$	(~50)%	66	216

General Atomic and Nuclear Constants[a]

N	= 6.02252	$\times 10^{23}$ mole^{-1} (based on A_{C12} = 12
c	= 2.997925	$\times 10^{10}$ cm sec^{-1}
e	= 4.80298	$\times 10^{-10}$ esu = 1.60210×10^{-19} coulom
1 MeV	= 1.60210	$\times 10^{-6}$ erg
$\hbar$	= 6.5819	$\times 10^{-22}$ MeV sec
	= 1.05449	$\times 10^{-27}$ erg sec
$\hbar c$	= 1.9732	$\times 10^{-11}$ MeV cm = 197.32 MeV fern
k	= 8.6171	$\times 10^{-11}$ MeV deg^{-1} (Boltzmann const
α	= $e^2/\hbar c$	= 1/137.0388
m_e	= 0.511006	MeV/c^2 = 1/1836.10 m_p
m_p	= 938.256	MeV/c^2 = 1836.10 m_e = 6.721 m_π
	= 1.00727663 m_1	(where m_1 = 1 amu = $\frac{1}{12}$ m_{C12} = 931.478 MeV/c^2)
r_e	= $e^2/m_e c^2$	= 2.81777 fermi (1 fermi = 10^{-13} cm
$\lambda\!\!\!^{-}_e$	= $\hbar/m_e c$	= $r_e \alpha^{-1}$ = 3.86144× 10^{-11} cm
a_∞ Bohr	= $\hbar^2/m_e e^2$	= $r_e \alpha^{-2}$ = 0.529167 A (1 A = 10^{-8} cm
$\sigma_{Thompson}$	= $\frac{8}{3}\pi r_e^2$	= 0.66516×10^{-24} cm^2 = 0.66516 barn
R_∞	= $m_e e^4/2\hbar^2$	= $m_e c^2 \alpha^2/2$ = 13.60535 eV (Rydberg

Hydrogen-like atom (non-rel., μ = reduced mass)

$E_n = \frac{\mu z^2 e^4}{2(n\hbar)^2}$; $a_{n=1} = \frac{\hbar^2}{\mu z e^2}$; $\left(\frac{v}{c}\right)_{rms} = \frac{ze^2}{n\hbar c}$

μ Bohr	= $e\hbar/2m_e c$	= 0.578817×10^{-14} MeV gauss^{-1}
μ_{nucl}	= $e\hbar/2m_p c$	= 3.1524 $\times 10^{-18}$ MeV gauss^{-1}
$\frac{1}{2}\omega_{cyclotron}$	= $e/2m_e c$	= 8.79404 $\times 10^{6}$ rad sec^{-1} gauss^{-1}
	= $e/2m_p c$	= 4.7895 $\times 10^{3}$ rad sec^{-1} gauss^{-1}.
$\sigma_{natural}$	= $\pi(\hbar/m_{\pi^\pm}c)^2$	= 62.768 mb

Other Physical Constants

1 year	= 3.1536× 10^7 sec (≈ $\pi\times10^7$ sec)
density of air	= 1.205 mg cm^{-3} (at 20°C)
acceleration by gravity	= 980.67 cm sec^{-2}
gravitational constant	= 6.670×10^{-8} cm^{3}g^{-1} sec^{-2}
1 calorie	= 4.184 joules
1 atmosphere	= 1033.2 g cm^{-2}
1 eV per particle	= 11604.9°K (from E = kT)

Numerical Constants

1 rad	= 57.29578 deg	e	= 2.71828
C	= 0.577216	1/e	= 0.367879
ln 2	= 0.69315	$\log_{10}e$	= 0.43429
ln 10	= 2.30259	$\log_{10}2$	= 0.30103

[a] Based mainly on E. R. Cohen and J. W. M. DuMond, Rev. Mod. Phys. 37, 537 (1965).

Magnetic moment ($e\hbar/2m_p c$)	Decay Parameters[†] Measured: α	Φ(degree)	Derived: γ	Δ(degree)
2.792763 ±.000030				
-1.913148 ±.000066				
-0.73 ±.16	.663±.022	(-7±7)°	.74	(8±8)°
	.73 ±.18	Sign of ϕ and Δ changed after		
	.06 ±.19	RPM printing to correct for		
		wrong sign in listed data card.		
2.3 ±.6	-.960±.067			
	+.008±.037	(180±30)°	-1.0	(0±85)°
	-.010±.043			
	-.33 ±.10			
	-.391±.032	(6±8)°	.92	(14±15)°

[†] The definition of these quantities is as follows

$$\alpha = \frac{2\,\mathrm{Re}(S^*P)}{|S|^2+|P|^2}\ ;\ \beta = \frac{2\,\mathrm{Im}(S^*P)}{|S|^2+|P|^2}\ ;\ \gamma = \frac{|S|^2-|P|^2}{|S|^2+|P|^2}$$

$$\tan\Phi = \frac{\beta}{\gamma}\ ,\ \tan\Delta = \frac{-\beta}{\alpha}\ .$$

* S = Scale factor = $\sqrt{\chi^2/(N-1)}$ where N ≈ number of experiments. S should be ≈ 1. If S > 1, we have enlarged the error of the mean, δx, i.e., $\delta x \to S\,\delta x$. This new convention, is still inadequate, since if S > 1, the real uncertainty is probably even greater than $S\delta x$. See text.

a. See notes on Stable Particles in text. b. See notes in data card listings. c. Theoretical value. See also data card listings.

† In decays with more than two bodies, P_{max} is the maximum momentum that any particle can have.

Particle or resonance	I(J^P) ⊢⊣ = estab.	Beam π, K (BeV) (BeV/c)	Mass (MeV)	Γ (MeV)	M²±ΓM (BeV²)	Partial decay modes: Mode	Fraction (%)	Q (MeV)	p or p‡max (MeV/c)	4πλ² (mb)
p	1/2(1/2⁺)		938.3		0.880		See Table S			
n	⊢⊣		939.6		0.883					
N'(1400)	1/2(1/2⁺) P_{11}	T=0.43πp p=0.55	~1400[a]	~200	1.96 ±0.28	Nπ	70	322	367	36.3
N(1525)	1/2(3/2⁻) D_{13}	T=0.62 p=0.75	1525[a]	105	2.33 ±0.16	Nπ Nππ [Δ(1236)π][e]	65 35 [~ 20]	447 308 149	460 414 229	23.2
N(1570)	1/2(1/2⁻) S_{11}	T=0.69 p=0.82	1570[a]	130	2.46 ±0.20	Nπ Nη	~ 30 ~ 70	492 82	491 242	20.3
N(1670)	1/2(5/2⁻) D_{15}	T=0.87 p=1.00	1670[a]	140	2.79 ±0.23	Nπ Nππ [Δ(1236)π][e] ΛK Nη	40 dominant[a] [?] small small	592 453 294 57 182	560 526 357 200 368	15.6
N(1688)	1/2(5/2⁺) F_{15}	T=0.90 p=1.03	1688[a]	110	2.85 ±0.19	Nπ Nππ [Δ(1236)π][e] ΛK Nη	65 dominant[a] [?] small small	610 471 312 75 200	572 538 372 231 388	14.9
N'(1700)[c]	1/2(1/2⁻) S_{11}	T=0.92 p=1.05	1700[a]	240	2.89 ±0.41	Nπ	100	622	580	14.5
N(2190)	1/2(7/2⁻)	T=1.94 p=2.07	2190	200	4.80 ±0.44	Nπ ΛK	30 ?	1112 577	888 710	6.21
N(2650)	1/2(11/2⁻)[b]	T=3.12 p=3.26	2650 ±10	~300	7.02 ±0.80	Nπ ΛK	7 ?	1572 1037	1154 1022	3.67
N(3030)[c]	1/2(15/2⁻)[b]	T=4.26 p=4.40	3030	400	9.18 ±1.21	Nπ	0.7	1972	1377	2.62
Δ(1236)	3/2(3/2⁺) P_{33}	T=0.195 (++) p=0.304	1236.0 ±0.6	120 ±2	1.53 ±0.15	Nπ Nπ⁺π⁻	100 0	158 18	231 89	91.9
	$m_0 - m_{++} = 0.45 \pm 0.85$		$m_- - m_{++} = 7.9 \pm 6.8$							
Δ(1670)	3/2(1/2⁻) S_{31}	T=0.87 p=1.00	1670[a]	~180	2.79 ±0.30	Nπ Nππ	40 ?	592 453	560 526	15.6
Δ(1920)	3/2(7/2⁺)	T=1.35 p=1.48	1920	200	3.69 ±0.38	Nπ ΣK	50 seen	842 229	722 423	9.37
Δ(2420)	3/2(11/2⁺)[b]	T=2.51 p=2.65	2423 ±10	~275	5.87 ±0.67	Nπ ΣK	10 ?	1345 732	1024 830	4.66
Δ(2850)	3/2(15/2⁺)[b]	T=3.71 p=3.85	2850 ±12	~300	8.12 ±0.86	Nπ	3	1772	1266	3.05
Δ(3230)[c]	3/2(19/2⁺)[b]	T=4.94 p=5.08	3230	440	10.4 ±1.4	Nπ	0.6	2152	1475	2.24
$Z_0(1865)$[c]	0(?)	p=1.15 K^+p	1863	150	3.47 ±0.28	NK	55 (if J = 1/2)	432	579	14.6
Λ	0(1/2⁺)		1115.6		1.24		See Table S			
Λ(1405)[d]	0(1/2⁻)	p<0 K^-p	1405	35	1.97 ±0.05	Σπ	100	68	142	
Λ(1520)	0(3/2⁻)	p=0.392	1518.8 ±1.5	16 ±2	2.31 ±0.02	$N\bar{K}$ Σπ S=1.7* Λππ	39±5 51±6 10±2	81 182 124	235 258 251	83.6
Λ(1670)[a]	0(1/2⁻)	p=0.74	1670	18	2.79 ±0.03	Λη $N\bar{K}$	$K^-p \to \Lambda\eta$ seen	6 233	66 410	28.5
Λ(1700)	0(3/2⁻)	p=0.80	1700 ±10	40 ±10	2.89 ±0.07	$N\bar{K}$ Σπ	20 seen	263 363	438 411	25.0
Λ(1820)	0(5/2⁺)	p=1.06	1819.5 ±3.5	83 ± 8	3.31 ±0.15	$N\bar{K}$ Σπ Σ(1385)π Λη	70 11 18 ~ 1	382 482 295 155	541 502 362 349	16.5
Λ(2100)	0(7/2⁻)	p=1.68	2100	160	4.41 ±0.34	$N\bar{K}$ Σπ	29 seen	663 763	748 699	8.68
Λ(2340)	0(?)	p=2.27	2340 ±20	105	5.48 ±0.25	$N\bar{K}$ seen in σ(total)	10 ↳ if J = 9/2	903	907	5.92
Σ	1(1/2⁺)		(+)1189.5 (0)1192.6 (-)1197.4		1.41 1.42 1.43		See Table S			
Σ(1385)	1(3/2⁺)	p<0 K^-p	(+)1382.2±0.9 S=1.6* (+)37±3 S=2.1*		1.92 ±0.05	Λπ Σπ	91±3 9±3 S=1.4*	130 48	208 117	
			S=4.8* (-)1388.0±3.0 (-)38±8, S=3.7*							
Σ(1660)[a]	1(3/2⁻)	p=0.72	1660	50	2.76 ±0.08	Λ(1405)π Σπ Λπ $N\bar{K}$	large ? ? small	115 323 405 223	197 379 439 400	29.9
	Large contradictions among measured branching ratios.									
Σ(1770)	1(5/2⁻)	p=0.95	1768 ±4 S=1.5*	89 ±12 S=2.0*	3.13 ±0.16	$N\bar{K}$ Λπ Λ(1520)π Σ(1385)π Ση Σπ	49 17 19 12 2 < 1	331 517 110 243 27 431	498 520 192 318 143 463	19.4
Σ(1910)[c]	1(5/2⁺)	p=1.25	1910 ±10	60	3.65 ±0.11	$N\bar{K}$ Λπ Σπ	8 10 3	473 655 573	612 619 568	12.9
Σ(2035)	1(7/2⁺)	p=1.53	2035 ±15	160	4.14 ±0.33	$N\bar{K}$ Λπ Σπ	16 25 seen	598 784 698	703 703 655	9.83
Σ(2260)[c]	1(?)	p=2.06	2260 ±20	180	5.11 ±0.41	$N\bar{K}$ seen in σ(total)	14 ↳ if J = 9/2	823	855	6.66
Ξ	1/2(1/2⁺)		(0)1314.7 (-)1321.2		1.73 1.75		See Table S			
Ξ(1530)	1/2(3/2⁺) p-wave		(0)1528.9±1.1 (-)1533.8±1.9	7.3 ±1.7	2.34 ±0.01	Ξπ	100	69	145	
Ξ(1815)	1/2(?)		1815 ±3	16 ±8 S=2.2*	3.29 ±0.03	ΛK Ξπ Ξππ [Ξ(1530)π][e] ΣK	~ 65 ~ 10 ~ 25 [~ 20] < 3	202 354 215 145	391 409 351 229	
	Branching ratios poorly known									
Ξ(1930)	1/2(?)		1933 ±16	140 ±35	3.74 ±0.27	Ξπ ΛK	seen seen	472 320	501 504	
Ω⁻	0(3/2⁺)		1674		2.80		See Table S			

a. See note in data listings.
b. J^P assignment based on straight-line Regge-trajectory-recurrence hypothesis and supported by fits to πp elastic scattering at 180°. See note following data listings.
c. Evidence for the existence of the effect and/or for its interpretation as a resonance is open to some question.
d. A virtual bound state of the $\bar{K}N$ system with negative scattering length [$a_0 = (-1.6 + 0.6i)$F]; i.e., a pole in the S matrix below the elastic threshold. See notes in main text and data listings.
e. Square brackets indicate a sub-reaction of the previous unbracketed decay mode.

† at left of Table indicates a candidate that has been omitted because the evidence for the existence of the effect and/or for its interpretation as a resonance is open to considerable question. See listings for information on the following: $N_{\gamma}(3245)$, $N(3695)$, $N^*_{5/2}(1560)$, $Z^*_0(1910)$, $\Sigma(1780)$, $\Sigma(3000)$, $\Xi(1705)$, and $\Xi_{\gamma}(2270)$.

* Quoted error includes an S (scale) factor. See footnote to Table S.

‡ For decay modes into ≥3 particles Pmax is the maximum momentum that any of the particles in the final state can have. The momenta have been calculated using the averaged central mass values, without taking into account the widths of the resonances.

Symbol(J^P)	$I^G(J^P)C_n$ ⊢⊣= estab.	Mass M (MeV)	Width Γ (MeV)	$\pm\Gamma M^{(a)}$ M^2 $(GeV)^2$	Partial Decay Modes: Mode	Fraction (%)	Q (MeV)	p or p_{max} (b) (MeV/c)
η(549)	η(0⁻)	0⁺(0⁻)+	548.6 ±0.4	<0.01	0.301 <.000005	all neutral	73	} See Table S
σ, ε §						$\pi^+\pi^-\pi^0+\pi^+\pi^-\gamma$	27	
						$\pi^+\pi^-\pi^0$	≈ 90	369 328
						$\pi^+\pi^-$	seen (c)	504 366
ω(783)	φ'(1⁻)	0⁻(1⁻)-	783.4 ±0.7* S=1.8*	11.9 ±1.5	0.614 ±.009	$\pi^0\gamma$	9.7±0.8	648 380
						$\eta\pi$ neutral	< 1.5	234 199
						$\pi^+\pi^-\gamma$	< 5	504 366
						e^+e^-	0.012±.003	782 392
						$\mu^+\mu^-$	< 0.10	572 377
η'(958) or X^0	η'(0⁻)	0⁺(0⁻)+	958.3 ±0.8	<4	0.918 <.004	$\eta\pi\pi$	75 ± 3 S=1.8*	131 232
H §						$\pi^+\pi^-\gamma$(incl. $\rho^0\gamma$)	25 ± 3	679 458
						for upper limits see footnote (f)		
φ(1019)	φ(1⁻)	0⁻(1⁻)-	1018.6 ±0.5	4.0 ±1.0 S=1.2*	1.039 ±.004	K^+K^-	48 ± 3	31 125
						K_LK_S	40 ± 3	23 107
						$\pi^+\pi^-\pi^0$ (incl. $\rho\pi$)	12 ± 4	604 461
						for upper limits see footnote (g)		
$\eta_V(1050)$ $\to K_SK_S$	η(0⁺) Some data still favor large scattering length	0⁺(0⁺)+	1050	50	1.10 ±.05	ππ	< 70	780 507
						KK	> 30	54 167
f(1250)	η'(2⁺)	0⁺(2⁺)+	1254 ±12	117 ±15	1.57 ±.15	ππ	large	975 611
						$2\pi^+2\pi^-$	< 4	696 547
						$K\bar{K}$	2.3±0.6	258 381
D(1285)	η'(A)	0⁺(1⁺)+	1285 ±4	32 ±8	1.65 ±.04	$K\bar{K}\pi$ (mainly $\pi_V(1003)\pi$) only mode seen		154 304
						$K^*\bar{K}+\bar{K}^*K$		-100
						$\pi\pi\rho$	not seen	256 356
E(1420)	η(A)	0⁺(0⁻)+	1424 ±7	76 ±9	2.03 ±.11	$K\bar{K}+\bar{K}^*K$	50 ±10	38 157
						$\pi_V(1003)\pi$	50 ±10	284 338
						$\pi\pi\rho$	not seen	395 462
K_sK_s §	η(2⁺)	0⁺(2⁺)+	1514 ±16	86 ±23	2.29 ±.13	ππ	< 14	1235 744
ρρ						$K\bar{K}$	> 60	518 570
f'(1500)						$K^*\bar{K}+\bar{K}^*K$	< 40	128 294
						ηη	not seen	417 522
$\pi^\pm$(140)	π(0⁻)	1⁻(0⁻)+	139.58		0.019	See Table S		
π^0(135)			134.98		0.018			
$\rho^\pm$(760)	ρ(1⁻)	1⁺(1⁻)-	778 (h)	160 (h)	0.605 ±.124	ππ	≈100	480 353
						$\pi^+\pi^-\pi^+\pi^-\pi^0$	< 0.2	206 243
						$\pi^+\pi^-\pi^+\pi^-$	< 0.6	199 238
						$\pi^0\gamma$	< 0.4	619 367
ρ^0(760)			770 (h)	140 (h)	0.593 ±.108	$\eta\pi^\pm$	< 0.8	71 135
						e^+e^-	.0065 +.011 -.005	759 380
						$\mu^+\mu^-$	.0033 +.0016 -.0007	549 365
δ(965)	?( )	1⁻( )	963.1 ±4.2	<5	0.927 <.005	$\delta^\pm \to$ 1 charged+neutral(s)	≈ 60	
						$\delta^\pm \to \geq$3 charged+neutral(s)	≈ 40	
π_V(1003)	π(0⁺)	1⁻(0⁺)+	1003	70 ±15	1.006 ±.057	$K^\pm K^0$	large	11 75
						$\eta\pi$ see note in data listings		315 333
→ KK̄ may also be interpreted as due to large scattering length								
A1(1080)	π(1⁺)	1⁻(1⁺)+	1079 ±8	130 ±40	1.16 ±.14	ρπ	≈100	181 245
						$K\bar{K}$	< 0.25, $G=(-1)^{\ell+I}$ forbids this (Eq. 5)	
	unresolved mixture of resonance and "Deck effect"					$\eta\pi$	< 1.5	391 385
						$\eta'\pi$	< 1.5	-19
B(1210)	ρ(A) ?	1⁺(1⁺)- ??-	1208 ±12	119 ±24 S=1.6*	1.46 ±.14	$\omega\pi$	≈100	297 339
						ππ	< 30	941 594
						$K\bar{K}$	< 2	232 358
						4π	< 50	662 528
						$\phi\pi$	< 1.5	66 137
A2(1300)	π(2⁺)	1⁻(2⁺)+ (d)	1306 ±8* S=2.6*	81 ±8 S=1.4*	1.70 ±.11	$\rho\pi$	91 ±8	408 417
						$K\bar{K}$	3.8±1.3	314 425
						$\eta\pi$	5 ±8 S=2.9*	618 527
						$\eta'\pi$	< 1.5	208 276
						$\pi^+\pi^-\pi^0$(excl. $\rho\pi$)	< 17	892 616
π(1640) → 3π	π (A) ?	≥1⁻(A)+ ⊢?	1640 ±20	100 ±20	2.69 ±.16	3π	appears dominant	1235 792
						ρπ	< 40	746 636
						fπ	?]	251 319
						$K\bar{K}$	< 40	644 652
ρ(1650) g→2π	ρ(V)	1⁺(V)- S=1.4* → ±23	1637	150 ±50	2.68 ±.24	2π	observed	1358 807
						4π }	probably observed	1079 758
	$R_1R_2R_3$ bumps suggest more structure in this peak					ρππ		599 605
$R_1R_2R_3$ §								
S(1930)	?(V)	≥1⁺( )	1929	≤35	3.72	1 charged } +neutral(s)	6(+15/-6)	
X^-	? (e)	?	±14		≤.07	3 charged } +neutral(s)	92(+ 8/-20)	
						>3 charged } +neutral(s)	2(+13/-2)	
T(2200)	?( )	≥1	2195 ±15	≤13	4.82 ≤.03	1 charged } +neutral(s)	4(+11/-4)	
X^-						3 charged } +neutral(s)	94(+ 6/-19)	
						>3 charged } +neutral(s)	2(+13/-2)	
U(2380)	?( )	≥1	2382 ±24	≤30	5.67 ≤.07	1 charged } +neutral(s)	30 ±10	
X^-						3 charged } +neutral(s)	45 ±15	
						>3 charged } +neutral(s)	25 ±10	
K^+(494)	K(0⁻)	1/2(0⁻)	493.78		0.244	See Table S		
K^0(498)			497.7		0.248			
K^*(890)	K(1⁻)	1/2(1⁻)	892.4 ±0.8	49.8 ±1.7* S=1.1*	0.796 ±.044	Kπ	≈100	259 288
						Kππ	< 0.2	119 216
κ(725) §	$m_0-m_\pm = 3.5\pm1.8$ S=1.2*							
K_V(1080) §								
K_c(1215) §	K(A)	1/2(A)	1320 ±10	80 ± 20	1.742 ±.106	$K^*\pi$ } overlap	large	288 338
K_A(1320)	?	?				Kρ }		63 198
	m and Γ values taken from Shen+. Appreciable discrepancies with other experiments. See note in data listings.					Kω probably seen.	< 10	39 155
						Kπ	< 30	687 558
						Kη	< 10	278 405
K_V(1420)	K(2⁺)	1/2(2⁺)	1411 ±5 S=1.8*	92 ±7 S=1.2*	1.991 ±.130	$K\pi$	52 ± 5 } S 2.2*!	778 610
						$K^*\pi$	36 ± 6	379 407
						Kρ	9 ± 5	158 319
						Kω	1.0±1.7	134 293
						Kη	2.1±3.0	368 475
K_A(1800)	K(A)	1/2(A)	1789 ±10	80 ±20	3.20 ±.14	$K\pi$	< 10	1156 819
						$K^*\pi$	35 ±12	762 664
						$K_V(1420)\pi$	8 ± 5	243 315
						Kρ	7 ± 5	532 630
						Remaining Kππ	40 ±15	1021 801
						Kω	10 ± 3	508 616
$K^*_{3/2}(1175)$ §								
$K^*_2(1270)$ §								

§ The following bumps, excluded above, are listed among the data cards: σ(410), ε(700), H(975), K_SK_S(1440) and ρρ(1410), R_1, R_2, R_3(≈1700), κ(725) K_V(1080), K_c(1215), $K^*_{3/2}$(1175), K^*_2(1270).

* Quoted error includes scale factor $S=\sqrt{\chi^2/(N-1)}$. See footnote to Table S.

Footnotes continued in right margin.

N o n e t s

	CP=-1	CP=+1			
	(0⁻)	(0⁺)	(1⁻)	(1⁺)	(2⁺)
	η	η_V	ω	D	f
	η'	φ	ρ	E?	f'
	π	π_V		A_1	A_2
	K	tentative	K^*	K_A	K_V
		tentative			

$m_8=\sqrt{K^2+\frac{K^2-\pi^2}{3}}$	= 566.8 ±0.2	928.4 (i)±3.0	1391. ±13.	1444.3 ±6.9
$\sin^2\theta=\frac{\eta^2-m_8^2}{\eta^2-\eta'^2}$	= 0.033 ±0.001	0.414 (i)±0.013	0.25 ±0.10	0.29 ±0.06
θ =	10.4°	40.1°	29.7°	32.4°

(a) Γ M is the half-width of the resonance when plotted against M^2.

(b) For decay modes into ≥ 3 particles p_{max} is the maximum momentum that any of the particles in the final state can have. The momenta have been calculated using the averaged central mass values, without taking into account the widths of the resonances.

(c) Reported values range between 1% and 10%, and depend on assumptions on ρ-ω interference.

(d) If A2 → both ρπ and KK̄, then $J^P=2^+$.

(e) S is ρ(V) if identified with $\pi^+\pi^-$ bump at 1910 MeV. See note on mesons.

(f) Empirical limits on fractions for other decay modes of η'(958): $\pi^+\pi^-$ < 7%, 3π < 7%, 4π < 1%, 6π < 1%, $\pi^+\pi^-e^+e^-$ < 0.6%, $\pi^0e^+e^-$ < 1.3%, ηe^+e^- < 1.1%, $\pi^0\rho^0$ < 4%, $\pi^0\omega$ < 8%.

(g) Empirical limits on fractions for other decay modes of φ(1019): $\pi^+\pi^-$ < 20%, ηγ < 8%, η + neutrals < 13%, $\pi^+\pi^-\gamma$ < 4%, e^+e^- < 0.2% $\mu^+\mu^-$ < 0.5%, ωγ < 5%, ργ < 2% from p-wave fit to compiled spectrum of 2-4 GeV/c $\pi^+p \to \Delta^{++}p$, $|t|<10$ m_π^2, and comparison of $\rho^\pm-\rho^0$ in similar reactions. Results depend on background and t-cut; hence real errors unknown, but larger than statistical errors ~ 5 MeV. (See Matts Roos, Phys. Letters, to be publ.) Note contrast between Roos' p-wave fit vs. weighted average of published results (see listings). m(±) 778 vs. 757; m(0) 770 vs. 760, Γ(±) 160 vs. 132, Γ(0) 140 vs. 116. This demonstrates present uncertainty.

(h) m_ρ, Γ_ρ taken to be 10 MeV.

(i) Error on m_ρ